TECHNOLOGY DEP

JOURNAL OF APPLIED PHYSICS

PUBLIC LIBRARY
JUN 10 1941
DETROIT

JUNE
1941
Vol. 12 No. 6

Tomato Plant Makes Its Own Autograph by Radioactivity

JOURNAL
OF
APPLIED PHYSICS

JUNE, 1941 Vol. 12, No. 6

In This Issue

Page

The Defense Program and University Difficulties 439

Applications of Radioactive Tracers to Biology and Medicine JOSEPH G. HAMILTON 440

Explorations toward the Limit of Utilizable Pressures P. W. BRIDGMAN 461

Theory of the Plastic Properties of Solids. III. FREDERICK SEITZ AND T. A. READ 470

Résumé of Recent Research 487

Contributed Original Research

Temperature Distribution in Vacuum Tube Coolers with Forced Air Cooling I. E. MOUROMTSEFF 491

Method of Measuring the Thermal Conductivity of Rock Cores J. B. HERSEY 498

Preliminary X-Ray Study of Binary Alloys of Platinum with Cobalt, Molybdenum, and Tungsten RALPH HULTGREN AND ROBERT I. JAFFEE 501

Further Study of the Flow of Air Through Porous Media R. R. SULLIVAN 503

In Every Issue

Here and There 488

Calendar of Meetings 489

New Books 490

Innovations in Instruments 509

Instrument Booklets 510

Index to Advertisers viii

BOARD OF EDITORS

ELMER HUTCHISSON, *Editor*

Associate Editors

FRANCIS BITTER
W. F. BUSSE
ROBLEY D. EVANS
MORRIS MUSKAT
B. E. WARREN
J. B. WHITEHEAD

Publication of the American Institute of Physics

ADMINISTRATIVE STAFF

HENRY A. BARTON, *Director*

MADELINE M. MITCHELL, *Publications Manager*

JOHN T. TATE, *Adviser on Publications*

GOVERNING BOARD

PAUL E. KLOPSTEG, *Chairman*
GEORGE B. PEGRAM, *Secretary*
KARL T. COMPTON
WHEELER P. DAVEY
FLOYD A. FIRESTONE
HARVEY FLETCHER
R. C. GIBBS
ARTHUR C. HARDY
GEORGE R. HARRISON
A. STUART HUNTER
H. R. LILLIE
A. G. WORTHING
W. B. RAYTON
JOHN T. TATE
WALLACE WATERFALL

The JOURNAL OF APPLIED PHYSICS, published monthly at Prince and Lemon Sts., Lancaster, Pa., is devoted to physics in its role as the science basic to other natural sciences and to the arts and industries. Previous to 1937 this publication was known as PHYSICS. It aims to be of service not only in physical laboratories, but also in the laboratories of industrial, chemical, geological, geophysical, meteorological, radio, and similar concerns. The JOURNAL OF APPLIED PHYSICS publishes editorials, news of physicists and reviews, as well as technical papers of applied physics.

Manuscripts should be submitted to Elmer Hutchisson, Editor, University of Pittsburgh, Pittsburgh, Pennsylvania.

Subscriptions and orders for back numbers should be addressed to Prince and Lemon Streets, Lancaster, Pa. or to the American Institute of Physics, 175 Fifth Avenue, New York, N. Y.

SUBSCRIPTION PRICE

	U. S. AND CANADA	ELSEWHERE
To members of scientific societies	$5.00	$5.70
To all others	7.00	7.70

Single copies are $.70 each.

Changes of address and proofs should be addressed to the Publications Manager.

Advertising rates supplied on request. Orders, advertising copy and cuts should be sent to the American Institute of Physics.

Entered as second class matter at the Post Office at Lancaster, Pennsylvania, under the Act of March 3, 1897. Accepted for mailing at the special rate of postage provided for in the Act of February 28, 1925, authorized May 2, 1932.

Copyright 1941, by the American Institute of Physics.

One Ohm Standard

A-C Resistance Box

Brooks Inductometer

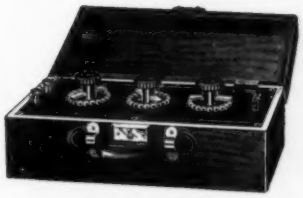
Mica Capacitor

Eppley Standard Cell

L&N STANDARDS OF RESISTANCE, INDUCTANCE, CAPACITANCE AND POTENTIAL

D-C RESISTORS

4210 ONE-OHM STANDARD RESISTOR—Adjusted to approx. value of Absolute Ohm. N.B.S. will certify to ±0.0001% in terms of the Washington Ohm, $100.00, plus N.B.S. certif.

N.B.S. TYPE RESISTORS—Limit of error: ±0.01% up to 0.1 watt; ±0.04% up to 1 watt. 4020, 1 ohm, $20.00; 4025, 10 ohms, $20.00; 4030, 100 ohms, $20.00; 4035, 1000 ohms, $20.00; 4040, 10,000 ohms, $25.00.

REICHSANSTALT TYPE RESISTORS—Limit of error, cooled in oil: ±0.02% up to 1 watt; ±0.05% up to 10 watts. 4221, 0.1 ohm, $50.00; 4222, 0.01 ohm, $55.00; 4223, 0.001 ohm, $120.00.

RESISTORS (SHUNTS) FOR LARGE CURRENTS—Limit of error, air cooling, ±0.04%.

	Ohm	Amps.	Volts Drop	
4360	0.1	15	1.5	$ 55.00
4361	0.01	100	1.0	100.00
4363	0.001	300	0.3	90.00
4364	0.001	500	0.5	175.00
4369	0.00004	1,500	0.06	187.00
4372	0.00002	2,000	0.04	187.00
4375	0.00001	3,000	0.03	300.00

SECONDARY-STANDARD RESISTORS—Limit of error ±0.1%. 4205, 1 ohm, $10.00; 4206, 10 ohms, $10.00; 4207, 100 ohms, $10.00; 4208, 1000 ohms, $10.00; 4209, 10,000 ohms, $10.00.

4245 TENTH-MEGOHM RESISTOR — 100,000 ohms. Limit of error ±0.1%, $50.00.

OPEN-DIAL-SWITCH RESISTANCE BOXES *††

No.	Ohms	Dials	Decade Steps	Price
4710	100	3	10x0.1+9(1+10)	$75.00
4711	1000	3	10x1+9(10+100)	70.00
4712	10000	3	10x10+9 (100+1000)	80.00
4715	1000	4	10x0.1+9 (1+10+100)	95.00
4716	10000	4	10x1+9(10+ 100+1000)	100.00
4720	10000	5	10x0.1+9(1+10+ 100+1000)	125.00

ENCLOSED-SWITCH RESISTANCE BOXES—For commercial-power frequency a-c as well as d-c.*†

No.	Ohms	Dials	Decade Steps	Price
4770	99	2	9(1+10)	$21.00
4771	990	2	9(10+100)	21.00
4772	9900	2	9(100+1000)	21.00
4773	999	3	9(1+10+100)	28.00
4774	9990	3	9(10+100+1000)	29.00
4775	9999	4	9(1+10+100+ 1000)	35.00
4776	999.9	4	9(0.1+1+10+100)	35.00

4452 PLUG-DECADE RESISTANCE BOX — 19,999.9 ohms. 9(0.1+1+10+100+1000)+10,000,*†† $110.00.

4252 POST-OFFICE PATTERN RESISTANCE BOX—11,110 ohms in steps of 1 ohm. Adjusted by removing plugs. Resistors 1, 2, 3, 4, 10, 20, 30, 40, 100, 200, 300, 400, 1000, 2000, 3000, 4000 ohms,*† $36.00.

4254 POST-OFFICE PATTERN RESISTANCE BOX—Similar to 4252, but 1,110 ohms. Resistors 1, 2, 3, 4, 10, 20, 30, 40, 100, 200, 300, 400 ohms, $30.00.

4244 MEGOHM RESISTANCE BOX — 1,000,000 ohms (4x200,000+2x100,000). Limit of error in resistors ±0.1%, $200.00.

4246 TENTH-MEGOHM RESISTANCE BOX—100,000ohms (10,000+20,000+30,000+40,000). Limit of error in resistors ±0.1%. Binding posts on ring mounted on insulating pillars, $90.00.

4247 TENTH-MEGOHM RESISTANCE BOX—Same as 4246 except, binding posts equipped with link connectors, $65.00.

A-C RESISTORS

SECONDARY-STANDARD A-C RESISTORS—Limit of error in d-c res. ±0.1%. Difference between a-c and d-c res. less than ±0.001% at 1 kc, less than ±0.01% up to 50 kc. 4631, 1,000 d-c ohms, $13.00; 4632, 2,000 d-c ohms, $13.00; 4633, 3,000 d-c ohms, $14.00; 4634, 4,000 d-c ohms, $14.00; 4640, 10,000 d-c ohms, $15.00; 4642, 20,000 d-c ohms, $17.00.

A-C RESISTANCE BOXES — Total 11,111.1 ohms, 10(0.01+0.1+1+10+100+1000), 6 dials, shielded. Differ principally in A-C characteristics. 4764*††, $300.00; 4765*††, $270.00; 4750**††, $100.00; 4749*†, $90.00.

A-C RESISTANCE BOXES—Total 11,110 ohms, 10(1+10+100+1000), 4 dials. 4748*††, shielded, $65.00; 4747*†, shielded, $55.00; 4746*††, unshielded, $60.00; 4745*†, unshielded, $50.00.

ATTENUATORS—Information on request.

INDUCTORS

STANDARDS OF SELF INDUCTANCE — Time const. approx. $1x10^{-3}$. Limits of error: 1530, ± 1%; 1531, 1532, 1533, ±0.2%; 1530, 1 mh, 1 amp., $30.00; 1531, 10 mh, 0.5 amp., $30.00; 1532, 100 mh, 0.15 amp., $30.00; 1533, 1,000 mh, 0.05 amp., $30.00.

1540 STANDARD OF MUTUAL INDUCTANCE—50 mh. Continuous current capacity 0.15 amp. Time const. approx. $5x10^{-4}$. Limit of error ±0.5% for freqs. up to 1000 cy., $40.00.

1520-A BROOKS INDUCTOMETER—Self-inductance range 1.5 to 12 mh. Continuous current capacity 1 amp. Time const. for max. setting, approx. $2x10^{-3}$. Limit of error ±0.3% of max. inductance for freqs. up to 1000 cy, $150.00.

1520-B BROOKS INDUCTOMETER—Self-inductance range 12 to 100 mh. Continuous current capacity 0.35 amp. Otherwise same as 1520-A, $150.00.

1520-C BROOKS INDUCTOMETER—Self-inductance range 100 to 800 mh. Continuous current capacity 0.1 amp. Time const. for max. setting, approx. $2x10^{-3}$. Scale calibrated at 1000 cy; correction data furnished for 60 cy. Limit of error ±0.3% of max. inductance at each of these freqs., $150.00.

1520-D BROOKS INDUCTOMETER—Self-inductance range 0.8 to 6 henrys. Continuous current capacity 0.03 amp. Limit of error ±0.9%. Otherwise same as 1520-C, $150.00.

CAPACITORS

1056 FIXED MICA CAPACITOR—0.5 mf. Limit of error ±0.25%, $30.00.

1061 ADJUSTABLE MICA CAPACITOR—1 mf, in 8 sections: 0.5, 0.2, 0.1, 0.1, 0.05, 0.02, 0.02, 0.01 mf. Limit of error for each, ±0.25%, $200.00.

1058 ADJUSTABLE MICA CAPACITOR—1 mf in 5 sections: 0.5, 0.2, 0.2, 0.05, 0.05 mf. Limit of error ±0.25%, $65.00.

1071 THREE-DIAL SHIELDED MICA CAPACITOR—1.11 mf in steps of 0.001 mf. 10(0.1+0.01+0.001). At 1,000 cy, capacitance diff. between each dial setting and its zero setting (other dials on zero) agrees with nominal ±(0.1%+0.5mmf), $325.00.

1070 THREE-DIAL MICA CAPACITOR—1 mf in steps of 0.001 mf. 9(0.1+0.01+0.001)+0.001. Limit of error 0.1 dial, ±0.25%; 0.01 dial, ±0.5%; 0.001 dial, ±2%, $175.00.

1188 ADJUSTABLE AIR CAPACITOR — Minimum, 50 mmf. Range 50 to 1,300 mmf on 2 dials: one reads up to 1,200 mmf in 100 mmf steps; other, 0 to 100 mmf, continuously adjustable. Quartz insulators, $170.00.

1187 ADJUSTABLE AIR CAPACITOR — Same as 1188, but has isolantite insulators, $150.00.

1185 ADJUSTABLE AIR CAPACITOR — Range approx. 40 to 1,100 mmf. Scale 0 to 100 div. Limit of error ±5 mmf, $30.00.

1170 HIGH-VOLTAGE ZERO-LOSS AIR CAPACITOR—For use up to 100,000 volts. Capacitance (adjustable) approx. 100 mmf at 12-inch (100-kv) spacing. Has guard circuit. Approx. 12'x7'x10'. Price on request.

1160 10-KILOVOLT CYLINDRICAL TYPE AIR CAPACITOR—Approx. 100 mmf. Max. continuous potential rating 10,000 volts at 60 cy. Electrostatically shielded. Low-voltage electrode guarded, $575.00.

1161 25-KILOVOLT CYLINDRICAL TYPE AIR CAPACITOR—Same as 1160, except: max. continuous potential rating 25,000 volts at 60 cy, $775.00.

STANDARD (POTENTIAL) CELLS

7308 EPPLEY STANDARD CELL—Not over 500 ohms. Emf guaranteed within ±0.01% of certified value, $20.00.

7309 EPPLEY STANDARD CELL — Same as 7308, except internal res. not over 100 ohms, $25.00.

7310 EPPLEY STANDARD CELL—Not over 500 ohms. Emf 1.018 volts, within ±0.1% at 20 C, $12.00.

*D-C res., with all dials or plugs at zero, does not exceed 0.03 ohm.

**D-C res., with all dials at zero, does not exceed 0.04 ohm.

†D-C res. change from zero setting, measured across binding posts, equals the readings of the dials ±(0.1%+0.01 ohm).

††D-C res. change from zero setting, measured across binding posts, equals the readings of the dials ±(0.05%+0.005 ohm).

LEEDS & NORTHRUP COMPANY, 4978 STENTON AVE., PHILA., PA.
LEEDS & NORTHRUP
Measuring Instruments · Telemeters · Automatic Controls · Heat Treating Furnaces

ALWAYS SET UP TO MEASURE

. . . . INDUCTANCE

. . . . RESISTANCE

. . . CAPACITANCE

A UNIVERSAL BRIDGE INEXPENSIVE AND COMPLETE

SINCE its introduction several years ago this general-purpose bridge has proven to be one of the most popular instruments in the General Radio line. In any laboratory where *any* electrical measurements are being made, this bridge is used as often as a voltmeter. One of its principal features is that it is completely self-contained and always set up for rapid measurements with good accuracy. Other features include:

- **DIRECT READING**—over very wide ranges:
  Resistance: 1 milliohm to 1 megohm
  Inductance: 1 micromicrofarad to 100 microfarads
  Capacitance: 1 microhenry to 100 henrys
- **A-C OR D-C MEASUREMENTS**—with built-in 1,000 cycle a-c hummer driven by four dry-cells, telephone headset being used for the a-c null indicator. The same dry-cells and a zero-center galvanometer are used for d-c measurements
- **GOOD ACCURACY**—over major portion of above ranges the capacitance and d-c resistance accuracies are good to 1%; inductance good to 2%
- **PORTABLE**—weighs only 30½ pounds with batteries
- **NO EXTERNAL STANDARDS**—the necessary standards are built into the instrument

The Type 650-A Impedance Bridge is moderately priced at only $175.00 complete except for 4 dry cells and headset.

• WRITE FOR BULLETIN 709 FOR COMPLETE DATA

GENERAL RADIO COMPANY, Cambridge, Massachusetts

BRANCHES: New York and Los Angeles

MANUFACTURERS of PRECISION LABORATORY APPARATUS

Journal
of
Applied Physics

Volume 12 June, 1941 Number 6

The Defense Program and University Difficulties

CONSIDERING the technical nature of modern warfare it is not difficult to understand the growing shortage of physicists in this country. In Great Britain the shortage is already extremely acute. The story of the part which British physicists have played in this war cannot yet be told but we have it on good authority that if it had not been for the superb work of physicists and other scientists the British would not have been able to hold out during the past year. In this country the increasing shortage of physicists has brought with it a difficult problem for our universities and colleges.

This problem is the maintenance of adequate scientific staffs to take care of the normal teaching load plus the rather large additional load brought about by the defense training program. In England most of the regular functions of the universities have had to be abandoned because of the urgency of a "fight for life." Since our situation is not quite so critical, it would be a mistake not to try to devise some method whereby the defense program could be carried on without completely disrupting the normal functions of the university.

Our responsibilities in the present emergency seem rather clear. First, we must see that every useful item of present-day scientific practice is applied to our military operations. Included, of course, is all the scientific information that we can obtain from Great Britain or from Germany. Second, we must push forward fundamental research programs which offer hope of military advantage. Presumably neither Great Britain nor Germany is able to do much fundamental research in the present emergency. In fact, one of the most effective ways in which America can take the offensive is to put a large part of its effort into developing fundamentally new techniques which may make many of the present military applications obsolete. We have however a further obligation. It will do little good to perfect new highly technical equipment if we do not have an abundant supply of well trained personnel to operate the equipment. Thus we are brought back to the problem of adequate staffs in the universities.

How can physics departments be kept operating and maintain training programs in view of the great demand for physicists in the defense research programs and in industrial laboratories? This question requires serious thought. Perhaps the best solution so far suggested is to divide large research programs into small units distributed geographically so that the part-time services of those most suited for defense training can be used in universities in all parts of the country. By a provision of sufficient clerical and technical help the training program could be carried forward without impairing too much the research program. A coordinator going from one district to another and frequent group meetings could keep each unit informed of what the others are doing and would provide a substitute for the stimulation of a large group organization. Unless a scheme of this general nature is used, we will find ourselves in a short time in as desperate a situation as Great Britain is at present as far as scientific personnel is concerned.

The Applications of Radioactive Tracers to Biology and Medicine

BY JOSEPH G. HAMILTON

Radiation Laboratory, University of California, and the Division of Medicine, University of California Medical School, San Francisco, California

A VERY large share of investigative work in the biological sciences has been devoted to the study of the metabolism of organisms ranging in complexity from bacteria to man and embracing the more important members of the plant and animal kingdoms. Until the discovery of artificial radioactivity by Curie and Joliot in 1934[1] the only method for studying the mechanisms whereby the various elements and compounds essential for life are assimilated, distributed throughout the tissues, converted into other compounds, and finally eliminated, was by a direct chemical approach to these problems. This mode of attack, although very productive of information, suffers from several serious limitations. First, in order to observe the manner by which a living organism metabolizes an element, as for example potassium, it is necessary to administer a sufficient amount so that a detectable increase in the amount of potassium in the body will be produced. This axiom applies to most of the elements and compounds that are normal constituents of biological systems. Normally, the content of these substances in most instances is kept within relatively narrow limits by the body and for this reason it is necessary to administer a sufficient quantity of the element or compound to disturb this carefully regulated balance to produce fluctuations that are large enough to be accurately determined by analytical chemical techniques. It is obvious that such procedures will frequently disturb the normal chemical and physiological processes of the organism, and the experimental data thus obtained may not present a true picture of the normal metabolism of the substances that are being studied. Second, it is not possible by chemical procedures to differentiate between the atoms or molecules of the administered material and those that are already present in the tissues of the plant or animal. For example, the increase in excretion of phosphorus by an animal following the administration of this element is made up in part by the phosphorus atoms already in the body, which were displaced by the administered element, and in part by a portion of the phosphorus given to the animal. The classical procedures of chemistry and physics do not permit the investigator to determine what proportion of the phosphorus atoms in the excreta came from the administered material and the fraction that were displaced from the pre-existing phosphorus in the tissues. This limitation applies to all metabolic investigations in which the elements or compounds are constituents of the organism that is being studied.

The first attempt to circumvent these limitations was made by Hevesy in 1923[2] when he employed a radioactive isotope of lead (radium D) to investigate the metabolism of that element in plants. His procedure made it possible to measure quantitatively the uptake and distribution of the administered lead by determining the radioactivity of the different portions of the plant. Due to the fact that the detection of radiolead by its radioactivity is more than a million times more sensitive than the ordinary chemical and physical methods, it was possible to study the metabolism of this element in such minute quantities that the toxic effects of the administered lead were avoided. Later, similar studies were undertaken with radio-bismuth (radium E). The applications of this technique were of limited value at that time, since lead and bismuth are not normal constituents of biological systems. The discovery of artificial radioactivity by Curie and Joliot[1] and the development of the cyclotron by Lawrence and his associates[3] has resulted in the preparation and identification of radioactive isotopes of all of the stable elements. These momentous developments have given the biologist probably the most useful tool for research since the discovery of the microscope, because almost all of the elements and compounds present

in biological systems can be "tagged" with the aid of artificial radio-elements and their course in living structures directly studied.

Chiewitz and Hevesy were the first investigators to employ the new tool of artificial radioactivity for biological research[4] and their initial studies were devoted to the investigation of the metabolism of phosphorus in rats with the aid of a radioactive isotope of that element. Although less than six years have elapsed since their first experiments with radio-phosphorus, artificial radioactivity has been applied as a tool in practically all of the biological sciences and the radioactive isotopes of twenty-one elements have already been employed in these various fields of investigation as tracers for metabolic studies. The amount of new and significant information which has been secured from the applications of this new technique to biological research is too extensive to be encompassed in a single article. Instead, an attempt will be made to describe the different techniques that are used and a few examples of the biological applications will be presented.

The fundamental postulate upon which rests the value of the artificial radio-elements as tracers is the fact that the radioactive isotope of a stable element differs only in its property of radioactivity and the chemical and physiological properties of the two forms of the element are identical so long as the radiations from the radioactive isotope are not sufficiently intense to produce physiological changes. This limiting factor is not of consequence in tracer studies since the amounts of radioactive material needed for this type of investigation are far too minute to produce any chemical or physiological changes by the action of their radiations.

The most simple and direct use of a radio-element as a tracer is accomplished by its administration as a simple inorganic compound, and the distribution of the tagged element in the various structures of the plant or animal determined by measuring the radioactivity of the samples of tissues and body fluids. For example, Chiewitz and Hevesy in their initial experiments administered radio-phosphorus as di-sodium phosphate to rats and at varying intervals of time sacrificed the animals and measured the radioactivity of the tissues as well as the content of the radio-phosphorus in the excreta eliminated during the experiments. This procedure enabled them to determine accurately the manner in which the animals metabolized a single known dose of phosphate. This general technique can also be employed to determine the rate of synthesis by the body of the administered radio-element into complex organic compounds. In such an instance the radio-element is given, and subsequently the labeled compound produced by the body and containing the radio-element is isolated and its radioactivity determined. For example, Miller and Hahn[5] have observed the rate of synthesis of hemoglobin, which is an iron-containing protein found in the red cells of the blood, from inorganic iron. They administered radio-iron as ferric salts to anemic dogs and subsequently removed part of the blood from the animals, obtained the hemoglobin in the pure state by chemical extraction and measured its radioactivity. Thus they were able to determine the proportion of the administered radio-iron which had undergone synthesis to form hemoglobin during the experiment. When it is desired to follow the metabolism of compounds that are taken into the body it is only necessary to incorporate into the substance by chemical synthesis the radioactive isotope of an element that is a normal constituent of the compound. For example, Borsook and his coworkers[6] have tagged vitamin B_1 (thiamin), which is a sulfur-containing complex organic compound, by preparing it synthetically from radio-sulfur. They have employed this radioactive vitamin to study certain phases of the metabolism of thiamin in normal and vitamin-deficient human subjects.

The property of gamma-ray radioactivity of many of the artificial radio-elements has made it possible in certain instances to follow the course of the tagged element or compound in the body of the intact animal. This is accomplished by placing a suitable measuring device, such as a Geiger counter, over the region of the body where it is desired to detect the accumulation of the tagged element or compound. This approach has two very definite advantages. First, it is possible to follow the ebb and flow of the metabolism of the tagged substance; second, it is not necessary to remove the tissues and organs of the body in order to ascertain their content of the adminis-

tered radioactive material. The second point is of particular importance when studies are to be conducted upon human subjects since it is often not feasible to secure samples of tissues and organs, particularly when normal individuals are being employed as controls. An example of this technique is its application for the investigation of iodine metabolism of the thyroid gland in normal and goiterous human subjects. The metabolism of the administered radio-iodine by the thyroid is determined by placing a Geiger counter tube over the neck and thereby measuring the gamma-rays of the radio-iodine accumulated by the thyroid.

The photographic action of the radiations from the artificial radio-elements has been employed to investigate the distribution of the administered radio-element in the tissues of plants and animals. Following the administration of the radio-element, thin slices of tissue are prepared, placed against a photographic film, and after a suitable period of time for adequate exposure the film is removed and developed. The section is then stained with various dyes which make it possible to see clearly the histological structure of the tissue under the microscope. The developed film and the slice of stained tissue are examined under the microscope and thus a correlation between the microscopic anatomy of the tissue and the deposition of the radio-element can be established since the areas of darkening on the film correspond to the regions of the tissue where greatest accumulation of the radio-element had taken place. This type of procedure is applicable to plant and animal tissues and in the case of small organisms, such as insects, it is a very useful method of investigating their metabolic characteristics since their organs are frequently too minute to be separated by dissection.

Phosphorus

Radio-phosphorus has been the most widely used of all of the artificially prepared radio-elements as tracers for metabolic studies in biological systems. Phosphorus is present in relatively large quantities in the tissues of all living organisms in both organic and inorganic chemical compounds. Over three-fourths of the total phosphorus in man and most animals is contained in the bony skeleton and is in the form of inorganic salts of calcium and magnesium. Small quantities of the phosphorus in the tissues and body fluids is present as ionic phosphate, but most of it is held in organic combination with a large variety of complex compounds. These organic phosphorus compounds can be divided into three general classifications: phospholipids, acid-soluble organic phosphates and protein phosphates. The phospholipids are organic compounds of fats with phosphoric acid. The acid-soluble organic phosphates embrace a large group of substances; notably carbohydrates, vitamin B_1, and certain enzymes, to which the phosphorus is presumably bound as an ester of phosphoric acid. The protein phosphates are complex nucleo-proteins which contain the phosphorus in firm chemical combination. The nucleo-proteins are present chiefly in the nuclei of cells and for this reason these substances are probably intimately related to cell growth and multiplication. The distribution of phosphorus in plants is somewhat similar except for the fact that the supportive structure in most plants is made up largely of cellulose which, of course, contains relatively little phosphorus.

The absorption and excretion of phosphorus in experimental animals and in man has been studied with the aid of radio-phosphorus by Hevesy and his co-workers,[4, 7, 8] Lawrence and his associates[9, 10] and by Greenberg and Cohn.[11] These investigators found that inorganic phosphates were efficiently absorbed from the digestive tract in animals and in man. Usually less than thirty percent of the administered phosphate escaped assimilation in the digestive tract when the labeled phosphorus was given by mouth to the animals and human subjects in the fasting state. In experimental animals the administration of either glucose or neutral fat with the phosphate enhanced the efficiency of absorption of the latter. The intravenous administration to normal human subjects of di-sodium phosphate which had been tagged with radio-phosphorus was followed by the elimination in the urine and feces of from four to twenty-three percent of the radio-phosphorus during the first twenty-four hours of the experiments. Thereafter, the rate of excretion rapidly fell and after the third day its daily value was less than one percent. The chief channel of elimination was by way of the kidneys, the

digestive tract accounted for approximately ten percent of tagged phosphorus that left the body. When the radio-phosphorus was given by mouth to human subjects and to experimental animals it was observed that from ten to forty percent of the administered material escaped assimilation and was eliminated in the feces. The excretory pattern of the assimilated radio-phosphorus was essentially the same as that which was observed when the phosphorus was administered by vein. The chief difference between the two channels of administration was that when the tagged phosphorus was given orally, approximately a quarter of it was lost because of the failure of the body to assimilate it completely.

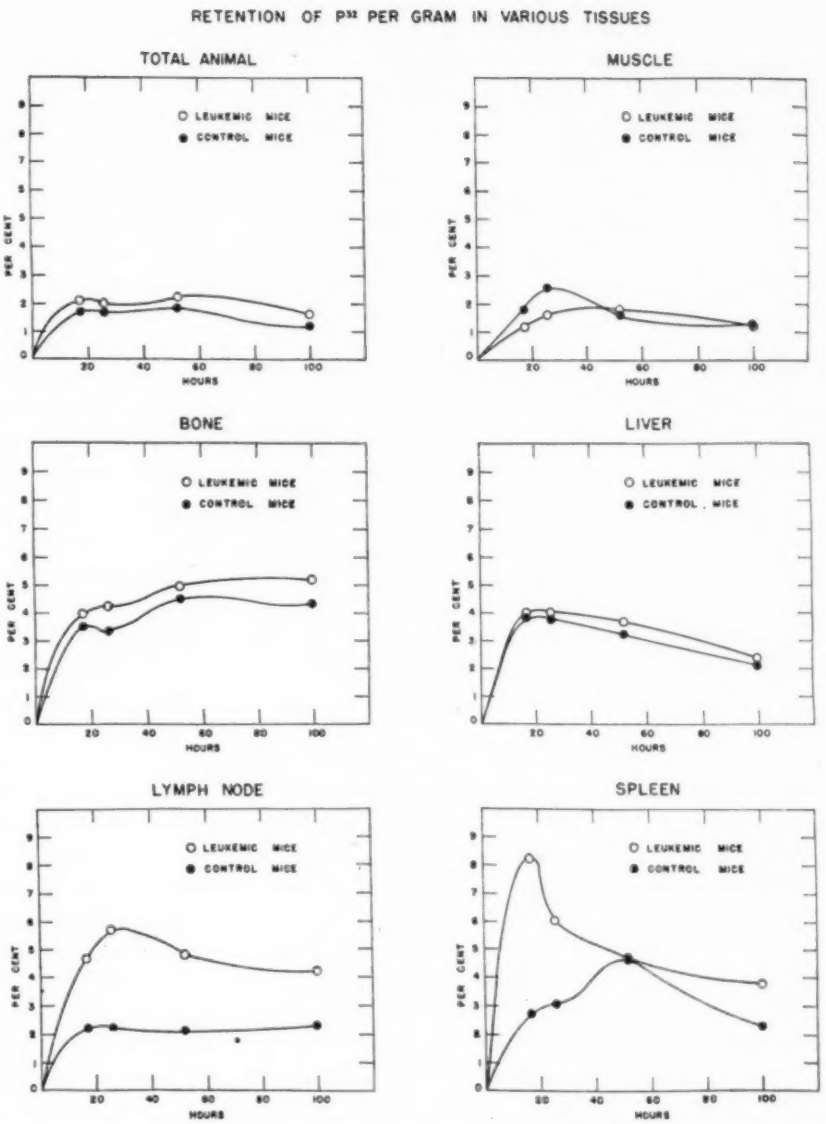

FIG. 1. The distribution of radio-phosphorus in the tissues of normal and leukemic mice.

The distribution of phosphorus in animal tissues has been extensively studied by the workers listed in the preceding paragraph as well as by many other investigators. It has been observed that the retention of a single dose of di-sodium phosphate which has been tagged with radio-phosphorus varied in different tissues in the following decreasing order: bone, muscle, liver, stomach plus small intestine, blood, kidneys, heart, lungs and brain. All of the above tissues, with the exception of brain, showed a rapid uptake during the first ten hours after the administration of the radio-phosphorus which was followed by a prolonged and steadily diminishing loss. In the case of brain tissue there was a very gradual and prolonged uptake of the phosphorus which was followed by a very gradual release of the accumulated element. This finding was interpreted to indicate that the turnover of phosphorus in the brain is very much slower than it is in other tissues. The retention of the radio-phosphorus per unit of fresh weight of tissue assumed the following order: bone, liver, stomach plus small intestine, heart, kidneys, lungs, blood, muscle, skin and brain. These studies suggested that the greater deposition of the labeled phosphorus in certain tissues, notably bone, would result in the selective irradiation of such structures by the beta-rays from the radio-phosphorus. Scott and Cook[12] first investigated the

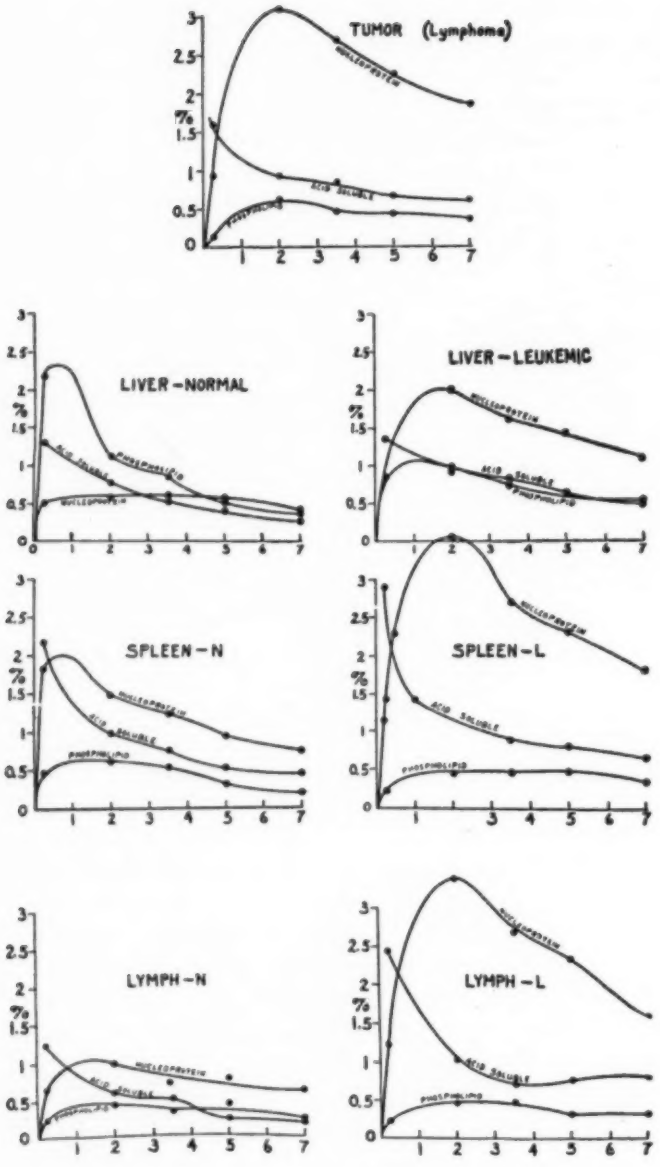

FIG. 2. A comparison of the rates of formation and distribution of the different organic phosphorus fractions in tumor tissue, and in normal and leukemic tissues. The ordinates indicate the percent of the administered labeled di-sodium phosphate per gram of tissue which was converted into phospholipids, nucleo-proteins, and the acid soluble fraction. The abcissa represents the time in days following the administration of the radio-phosphorus.

action of large doses of radio-phosphorus upon the cells in the circulating blood, using chicks as the experimental animals, and observed a slight but definite decrease of the polymorphonuclear leukocytes of the blood. Since these white blood cells are produced in the bone marrow their results indicated that there had been a selective irradiation of the marrow due to relatively large accumulation of the administered phosphorus in the bones. This work was repeated with mice by Scott and Lawrence[13] and similar results were observed. These observations led Lawrence and his group[14,15] to compare the phosphorus metabolism of normal and leukemic mice. Mouse leukemia is a rapidly progressive and fatal disease which is characterized by the excessively rapid multiplication of the white blood cells. The abnormal proliferation of these multiplying cells results in the infiltration of the soft tissues, notably the bone marrow, lymph nodes, spleen and liver, by the leukemic cells. A single dose of radio-phosphorus was given each one of a large group of normal and leukemic mice and then at varying intervals the animals were sacrificed and both the radio-phosphorus and total phosphorus content of the tissues assayed. Figure 1 indicates the retention of radio-phosphorus per gram of tissue, and it can be seen that there is striking difference between the normal and leukemic lymph nodes and spleens. The apparent slight difference of radio-phosphorus content in normal and leukemic bone was interpreted as being due to the fact that the phosphorus metabolism of the marrow was masked by that of the bone which has normally a very high content of phosphorus. The total phosphorus content of the normal and leukemic lymph nodes, spleen and liver were approximately the same. The greater accumulation of the single dose of tagged phosphate in the leukemic lymph nodes and spleen, although their total phosphorus contents were similar, was interpreted as an indication of the building of new tissue and a greater rate of metabolism of those tissues. This selective accumulation of radio-phosphorus in the leukemic tissues indicated that these regions would be subjected to a greater degree of irradiation from the beta-rays from the radio-phosphorus than would the normal tissues. The close resemblance of animal leukemia to the human form of this disease led these

investigators to employ radio-phosphorus in the treatment of the leukemias. This is the first instance in which tracer studies with artificial radioactivity has led to the application of an artificial radio-element as a direct and potentially valuable therapeutic agent in clinical medicine.

The conversion of inorganic phosphorus into organic phosphorus compounds by the body was first studied with the aid of radio-phosphorus by Hevesy and his associates[16] and by Artom and his co-workers.[17] These workers demonstrated that phospholipids are rapidly formed in the body from administered inorganic phosphates. Artom and his group extracted the phospholipids from the different organs of rats after the animals had received radio-phosphorus in the form of disodium phosphate and found that the phospholipids from the liver, kidney and intestine had the maximum radioactivity with medium values in the heart, lungs, spleen, pancreas, adrenals and testes, and lower values in the muscle and brain. These observations were interpreted to signify that the rates of synthesis of phospholipids from the administered phosphate varied in the different organs. Chaikoff and his colleagues[18] have not only confirmed these results using different experimental animals, but also have demonstrated that phospholipid synthesis takes place in excised slices of liver, kidney and intestine *in vitro*.[19] Later, they studied the phospholipid turnover of different types of malignant tumors in animals and found that each type of tumor had a characteristic pattern of phospholipid metabolism which was not related to cell type.[20] However, in each instance the rate of synthesis of the labeled phospholipid was rapid and in this respect resembled the phospholipid turnover of rapidly metabolizing tissues such as liver, small intestine and kidney. In other experiments[21] they implanted three different types of tumors in each of a large group of animals and found that the characteristic phospholipid metabolic pattern of each type was maintained. This series of observations, they concluded, indicated that the phospholipid turnover of the tumor cells remained independent of the host.

Lawrence and his group[22] have compared the distribution of phosphorus in the acid-soluble, phospholipid, and nucleo-protein fractions of normal and leukemic animal tissues. At varying times after the administration of labeled disodium phosphate the tissues were removed and the different organic phosphorus fractions extracted and their radio-phosphorus content determined. The results of some of these investi-

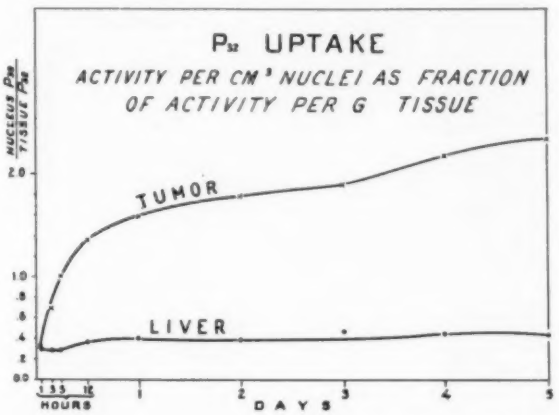

FIG. 3. The relative accumulation of radio-phosphorus by the nuclei of liver cells from normal rats and the nuclei from tumor (lymphoma) cells in mice.

gations are shown in part in Fig. 2, and it can be seen that the nucleo-protein fraction containing the labeled phosphorus was much greater in the tumor cells and in the leukemic tissues. This is interpreted to indicate that the nucleo-proteins were being synthesized by the leukemic and tumor cells at a much greater rate than in the normal tissues. Marshak[23] has devised a technique for the separation of cell nuclei from the cytoplasm and has employed this procedure to determine the relative uptake of the administered phosphorus in the nuclei and cytoplasm of normal and malignant cells. He observed that the nuclei of the malignant cells not only accumulated more labeled phosphorus than the normal cell nuclei but also the relative proportion of the administered phosphorus in the nuclei as compared to that in the cytoplasm was much greater in the malignant cells than in normal cells (Fig. 3). This metabolic pattern of the nuclei of malignant cells was found to be not restricted to neoplastic tissue, but a characteristic, as well, of rapidly multiplying normal cells. A comparison of the uptake of phosphorus in the nuclei of malignant cells and the nuclei of rapidly regenerating liver cells from animals in which a large part of the liver had been previously removed revealed that the phos-

FIG. 4a. Radio-autograph of the distribution of radio-phosphorus in the leaves of the tomato plant. The light areas are, of course, the regions where the greatest accumulation of radio-phosphorus took place. The leaves were removed from the plant 36 hours after the introduction of the labeled phosphate into the nutrient solution.

phorus uptake of the nuclei of these two very different types of cells was essentially the same. From these observations the author concluded that variations in phosphorus metabolism of cell nuclei are dependent in part upon the rate of cell multiplication and not a peculiarity of malignancy *per se*.

Stout and his co-workers[24] have followed the metabolism of inorganic phosphates in the leaves and fruit of the tomato plant by the use of radio-phosphorus and the technique of radio-autography. They administered the radio-phosphorus to roots of the plants as di-sodium phosphate and after a period of several days removed the leaves and fruit. The leaves and thin slices of the fruit were placed on photographic films and left together for a sufficient interval of time to allow the radio-phosphorus beta-rays to leave images of the distribution of the accumulated labeled phosphorus in the specimens. The radio-autographs shown in Fig. 4 indicated that the assimilated phosphorus was accumulated in the conduction system of the leaves and in the seeds of the green fruit. The ripe fruit can be seen to have accumulated small traces of the administered phosphate, but in this instance no detectable storage took place in the seeds which suggests that in the ripe fruit the development of the seeds had been completed before the radio-phosphorus was given.

These workers have employed radio-phosphorus to study the mechanism of the upward movement of inorganic ions in cotton, willow and geranium plants.[25] Following the administration of the labeled phosphate to the roots of the plants the bark was carefully detached from the wood and held away from it with the aid of small strips of waxed paper. When it had been demonstrated that a considerable fraction of the radio-phos-

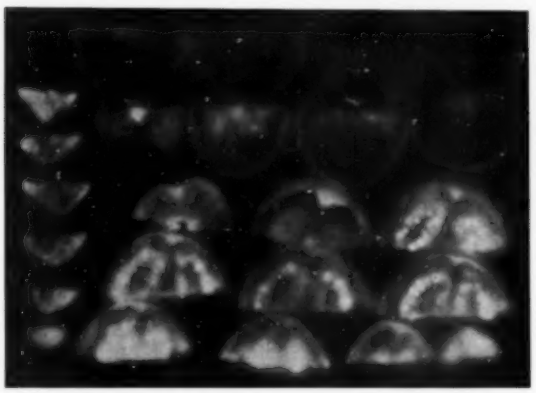

FIG. 4b. Radio-autograph of the distribution of radio-phosphorus in the fruit of the tomato plant, the light areas being the regions where the greatest accumulation of radio-phosphorus took place in the fruit. The fruit at various stages of development were removed from a plant, other than the one whose leaves are shown in Fig. 4a, 9 days after the administration of radio-phosphorus. The vertical column at the left represents the radio-autographs from small green fruit, the lower three horizontal rows were taken from sections of a large green fruit, and the upper two rows represent sections from a fully ripe tomato fruit. The intensity of the images are proportional to the concentration of the radio-phosphorus accumulated in the different samples of fruit since the fruit were taken from the same plant at the same time.

phorus had moved from the roots to the aerial parts of the plant above the region where the bark had been detached, the plants were harvested and the stripped section of bark and underlying wood examined for radioactivity. It was found that there was very little radio-phosphorus in the detached portions of the bark while the wood directly beneath had as much as two thousand times more radio-phosphorus. The bark nearby which had not been separated from the wood had about the same content of the labeled phosphorus as did the wood. Similar results were observed when radioactive isotopes of sodium, potassium and bromine were employed in these studies. The results of these investigations indicate that both the anions and cations of salts assimilated by plant roots are normally transported to the aerial portions of the plants by way of the wood. Furthermore, such studies have demonstrated that the cells of the bark draw their mineral nutrients from the conducting vessels in the wood.

These investigators[26] have conclusively demonstrated that assimilated phosphorus can move downward as well as upward in the aerial portion of the tomato plant. This was shown by growing roots on the aerial portion of the stem midway between the top of the plant and the normal root structure. These side roots were introduced into a nutrient solution containing radio-phosphorus as di-sodium phosphate and after several hours the side roots were excised. The various portions of the plant above and below the side roots were examined for radio-phosphorus and it was found that a small but readily measurable portion of the assimilated phosphate had moved in the downward direction and had even entered the normal root structure and the nutrient solution at the base of the plant. This phenomena of downward movement of minerals in plants was also demonstrated by these workers in another experiment.[27] In this instance a few drops of di-sodium phosphate solution containing radio-phosphorus was painted on the surface of a willow leaf. After several days the leaf and those adjacent to it were removed from the plant and the distribution of the labeled phosphorus demonstrated by radio-autographic technique (Fig. 5). The white area to the left was due to the large content of radio-phosphorus at the point where the solution was painted on the leaf. The dotted lines indicate the outlines of the leaves and the light streaks passing through the central axis of the leaves represent the tagged phosphorus which had been absorbed through the intact surface of the leaf and had spread to all directions from that point.

FIG. 5. A radio-autograph showing the capacity of the intact leaf to absorb labeled di-sodium phosphate and the circulation of the absorbed phosphate into adjacent leaves. The dotted lines indicate the outlines of the leaves and white area at the left is the region where the solution containing the radio-phosphorus was painted on the leaf. The light streaks passing down the central axis of the leaves represent the path of circulation of the absorbed phosphate.

The metabolic processes of insects has been poorly understood because of the minute size of the various organs which has made it very difficult to study their functions by direct biochemical methods. Radioactive tracers can be employed as an approach to this problem since the tracer techniques are so much more sensitive than any of the classical chemical analytic procedures. In many instances the complete and quantitative collection of the excretory products

and the dissection of the organs in the smaller insects is very difficult. For this reason the application of the technique of radio-autography appears to be a very promising investigative method in this field. The tagged element or compound can be administered either orally or parenterally and subsequently the insects sacrificed and sections of the tissues prepared from which radio-autographs are made. Craig[28] was the

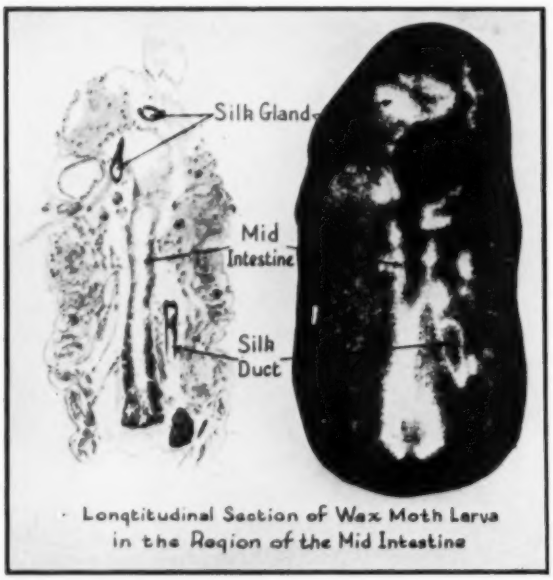

FIG. 6. A photomicrograph of a section and its corresponding radio-autograph from a wax moth larva showing the distribution of labeled phosphorus in the tissues of the insect (×10).

first investigator in the field to employ this technic and Fig. 6 will serve as an example of the type of results which can be secured from this method of approach to problems of insect metabolism. In this particular experiment radio-phosphorus was administered two weeks before the insects were sacrificed and then the sections and radio-autographs were prepared. The insects used in these experiments were the larvae of a small silk-producing moth and the longitudinal section shown in Fig. 6 was taken from the central portion of the larva, which is about three millimeters in diameter. The corresponding radio-autograph indicates that the phosphorus was selectively accumulated in the walls of the digestive tract, silk glands, and the ducts of the silk glands. The selective deposition of the labeled phosphorus in these areas indicated that these organs were developing rapidly and hence had a greater demand for the administered phosphate. The applications of tracer technique with the aid of artificial radioactivity to the problem of development of more effective insecticides is of considerable importance since it will be possible to tag various compounds employed in pest control and directly observe the localization of these substances in insect tissues.

Iodine

Iodine is an essential element for the higher animals. It is used in the synthesis of the hormone thyroxine, an organic iodine compound which serves as a regulatory agent for certain oxidative processes in the body. If it is absent or present in insufficient quantities the oxygen consumption of the animal decreases and the general level of metabolism is lowered. If the rate of formation of thyroxine is increased above normal requirements the rate of oxygen consumption is elevated and as a result the substances that are normally burned in the body will be consumed more rapidly than they can be replaced by the intake of food. The thyroid gland is the organ which presumably conducts the synthesis of thyroxine and controls the release of this hormone into the rest of the body. The thyroid also contains a relatively large amount of iodine, most of which is held in organic combination. The normal human thyroid weighs approximately twenty grams and contains from five to twenty milligrams of iodine. The content of iodine in other tissues of the body is very small and averages, per gram of wet weight of tissue, less than one five-thousandth the amount in the thyroid. This remarkable concentration of iodine by the thyroid is unique since no other structure in the body is known to possess the ability to selectively accumulate any element to such a high degree.

In the initial studies with radio-iodine[29] the rate of absorption of iodine from the digestive tract in normal human subjects was compared with that of four other radio-elements: sodium, potassium, chlorine and bromine. A solution containing the radio-element was administered by mouth to each subject and the rate of uptake from the digestive tract into the rest of the body was determined by measuring the gamma-ray

radioactivity of the subject's hand. This was accomplished by having the subject grasp the counter tube of a Geiger counter and hold it inside of a large lead box which served to shield the counter tube from the radiations from the rest of the body (Fig. 7). The rate of change of the radioactivity of the hand was measured for a period of several hours after the ingestion of the solution. The radio-sodium and radio-potassium were administered as their chlorides, the radio-chlorine as lithium chloride, the radio-bromine as potassium bromide, and the radio-iodine as sodium iodide. Eight normal human subjects were employed for each of the five radio-elements, and composite curves were prepared which are shown in Fig. 8. All of the five radio-elements were absorbed very rapidly, so that the radio-active atoms were detectable in the hand within a very few minutes after ingestion of the solutions. There were no significant differences between the rates of absorption of the tagged sodium, chlorine, bromine and iodine. The labeled potassium, however, was found to be taken up more slowly by the body in all of the subjects receiving the radioactive isotope of this element.

Radio-iodine was first employed by Hertz and his group[30] to demonstrate the rapidity of accumulation of iodine by the thyroid gland. They used rabbits in their experiments and observed that an appreciable fraction of the administered radio-iodine could be detected in the thyroid within a few minutes after the material had been given. They also noted that the uptake of the labeled iodine by the thyroid was much greater in the animals with hyperplastic thyroids. Later[31] they studied the effect of the administration of varying amounts of inert iodine together with the radio-iodine and observed that the proportion of the administered iodine accumulated in the thyroid glands of rabbits diminished with the total weight of iodine given to the animals. This phenomenon was due to the fact that the thyroid can store only a limited quantity of iodine and hence with large doses of iodine the thyroid was able to take up only a small fraction of the administered material.

FIG. 7. A method for the measurement of the radioactivity of the hand with the aid of a Geiger counter. The lead case served to shield the counter tube from the radiations from the rest of the body. This procedure was employed to determine the rates of absorption from the digestive tract of the radioactive isotopes of sodium, potassium, chlorine, bromine and iodine.

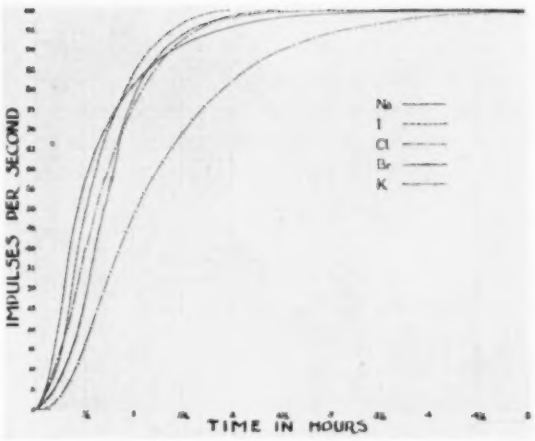

FIG. 8. The rates of absorption from the digestive tract of the radioactive isotopes of sodium, potassium, chlorine, bromine and iodine in normal human subjects.

The excretion of iodine following oral administration of a solution of sodium iodide containing fourteen milligrams of iodine and a known quantity of radio-iodine (10–50 μC) was studied by Hamilton and Soley[32] in a group of normal human subjects and patients with several types of thyroid disorders. The urine and feces were collected for five days after the administration of the labeled iodide and the proportion that was excreted by these channels of elimination was determined by measuring the radio-iodine content in the excreta. The rates of excretion in both the patients and the normal controls were found to be quite rapid and the kidneys served as the principal path of elimination (Fig. 9). These rates of excretion by the kidneys were found to be exponential in character and were similar in the normal controls and patients with goiters. The rates of urinary elimination by the two patients with spontaneous myxoedema were less rapid but retained an exponential pattern. Myxoedema is characterized either by a total atrophy of the

gland and a resultant lack of production of the thyroid hormone, or by failure of existing thyroid tissue to function normally. The absence of thyroid hormone in the body under these circumstances causes a marked retardation of metabolic processes and the reduced rate of elimination of

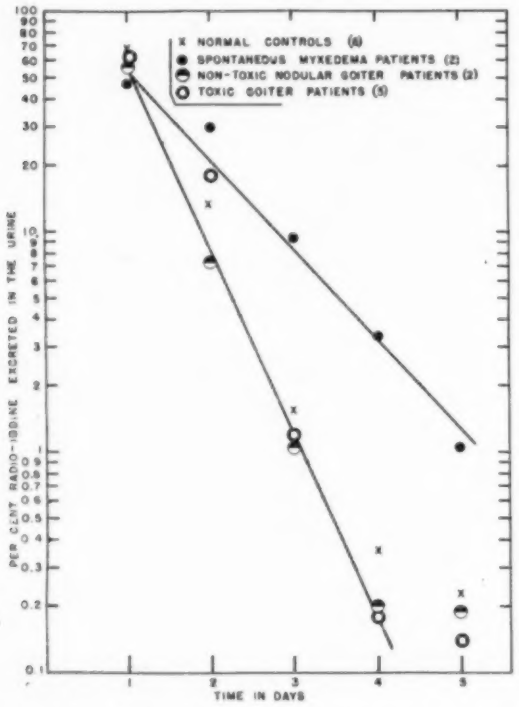
X NORMAL CONTROLS (6)
SPONTANEOUS MYXEDEMA PATIENTS (2)
NON-TOXIC NODULAR GOITER PATIENTS (2)
TOXIC GOITER PATIENTS (5)
PER CENT RADIO-IODINE EXCRETED IN THE URINE
TIME IN DAYS

FIG. 9. The rates of urinary excretion per day of iodine in a group of patients with different types of thyroid disorders and normal controls following the administration of 14 milligrams of iodine as sodium iodide and containing radio-iodine.

the administered iodine was an expression of the general slowing down of physiological functions. The thyroid glands of the goitrous patients were subtotally removed two days after administration of the radio-iodine and the total iodine and radio-iodine content of the thyroids was determined. These experiments revealed that from one to thirty percent of the administered iodine was accumulated in the thyroid glands in the group of forty patients studied by this procedure. This technique was employed in two patients with cancer of the thyroid and after the tissue had been removed the cancerous portion of the gland was dissected from the remaining normal thyroid tissue. The uptake of the administered labeled iodine was determined in the two types of tissue and it was found in both patients that the remaining normal tissue had a relatively large uptake of radio-iodine, but the cancerous portion in each instance took up only very small traces of radio-iodine. On the basis of radio-iodine uptake per gram of tissue the cancerous portion accumulated approximately one one-hundredth the amount that was taken up by the remaining normal thyroid tissue.

The interpretation of the data secured from the determinations of the iodine uptake by the thyroids of the goitrous patients was made very difficult because in many of the patients it was necessary to treat these individuals with relatively large quantities of iodine for a prolonged interval of time to diminish the hazards of the surgical removal of the thyroids. Moreover, only one determination of the uptake of iodine by the gland was possible since each patient was operated upon but once; and, of course, no information concerning the uptake of iodine by the thyroids of normal human subjects could be obtained by this method of approach.

The next step in the study of iodine metabolism was made by measuring the uptake of the administered radio-iodine by the intact thyroid glands of normal controls and patients suffering from various types of thyroid disorders.[33] Radio-iodine was administered orally to the subjects in the same manner as in the preceding experiments, but none of the individuals had received iodine before the radio-iodine was given and no additional iodine was given until the experiments were concluded. The uptake of the administered labeled radio-iodine was quantitatively determined by measuring the gamma-ray radioactivity of the gland with the aid of a Geiger counter. The counter tube was placed against the neck directly over the thyroid as is shown in Fig. 10. A large number of determinations of the radio-iodine content of each thyroid was made over a period of time ranging from four days to a month. Composite curves for each clinical type of thyroid disorder studied by this procedure and for the normal controls are shown in Fig. 11. The ordinate indicates the percentage uptake of the administered iodine by the thyroids and the abscissa represents the period of time in days after the labeled iodine had been given. The patients with hypothyroidism had a type of

thyroid disorder which is characterized by the failure of the thyroid gland to synthesize sufficient thyroxine to meet the normal metabolic demands of the body and as a result the general metabolic level of such individuals was greatly lowered. The very small uptake of the administered radio-iodine by the thyroids of these patients suggested that the inability of the gland to synthesize the thyroid hormone was related to the inability of their thyroid glands to accumulate the labeled iodine. The patients with nontoxic goiters probably developed this particular type of thyroid disorder because the amount of iodine taken into the body from food, water, etc., was not sufficient to meet the normal requirements of the body and as a result the thyroid increased in size as a result of its attempt to maintain a normal output of thyroxine. The

FIG. 10. The technique employed for the measurement of the uptake of radio-iodine by the thyroid gland *in situ*. The counter tube was placed against the thyroid gland to determine the gamma-radiation from the accumulated radio-iodine.

relatively larger uptake of the administered iodine by the thyroids in this instance can be attributed in part to the apparent need for iodine by goiters of this type. The similar form of the uptake curves for the normal controls and the patients with nontoxic goiters suggested that the mechanism of iodine accumulation and storage

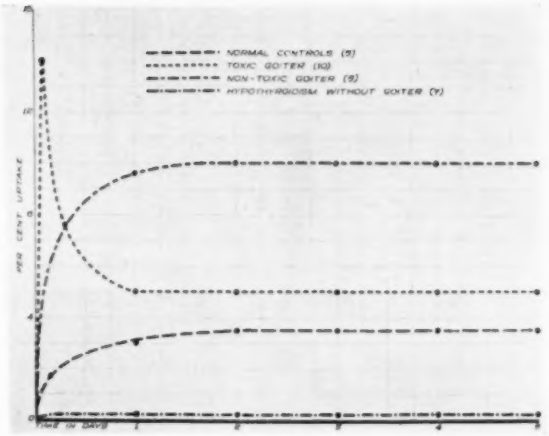

FIG. 11. The uptake of radio-iodine by the intact thyroid glands of normal human subjects and of patients with different types of thyroid disorders.

was similar in these two types of individuals. The thyroid glands of the patients with toxic goiters had spontaneously developed the capacity to produce and discharge into the rest of the body a quantity of the thyroid hormone which was far in excess of their normal metabolic requirements. This situation implied a greater need of the thyroid tissue for iodine since the thyroid hormone contains considerable iodine and this material was being synthesized and discharged into the blood stream at an excessively rapid rate. The thyroids of these patients with hyperthyroidism (toxic goiter) have been shown to accumulate the administered iodine at a remarkably rapid rate. The time required for the maximum uptake in the thyroid after the labeled iodine had been given to these patients ranged from one to four hours while in the case of the normal controls and patients with nontoxic goiters, it required two days for the maximum accumulation of iodine by the thyroid. The rapid uptake of iodine by the thyroids of the patients with toxic goiters was followed by the rapid loss of from one-half to four-fifths of the radio-iodine which had accumulated during the first few hours of the experiments. These results are interpreted as indicating that the over-active thyroid cells not only had a marked avidity for the accumulation of iodine but also that the mechanism for retention of the recently stored iodine had been altered. This technique may be of diagnostic value in the study of diseases of the thyroid. However, at the

present time, only typical cases suffering from thyroid disorders have been investigated by this procedure. Borderline types of thyroid disorders must be investigated before this approach can be evaluated as a diagnostic test, since it is in this region of clinical doubt that a new method of diagnosis must operate if it is to be superior to pre-existing methods.

The technique of radio-autography, which was first devised by Lacassagne and Lattes,[34] has been found to be very well adapted to the study of the relationship between the deposition of iodine in the thyroid and the microscopic anatomy of the tissue.[35] The anatomical unit of the thyroid gland is the acinus which consists of a spherical envelope made up of a single layer of cells which enclose a clear noncellular material that is termed colloid. The acinus can be compared to a grape, the skin corresponds to a single layer of thyroid cells and the pulp is analogous to the inclosed colloid. Each acinus in the normal human thyroid gland ranges from fifty to two hundred microns in diameter. The acini are richly supplied with blood vessels which serve as their main channel of contact with the rest of the body since the thyroid is a ductless gland. The thyroid is made up of a large number of these acini and can be compared to a bunch of grapes, except for the fact that the acini are "bound together" by numerous strands of connective tissue which makes it almost impossible to dissect out the individual acini. The thyroid cells presumably act to abstract the iodine from the blood stream and convert it into thyroglobulin, which is stored in the colloid of the acini for future use by the body. Very little is known definitely about the actual mechanisms of iodine metabolism of the different components of the thyroid and the preceding description merely gives some of the more salient points of the most widely accepted theory of thyroid physiology.

The distribution of the accumulated radio-iodine in the thyroid tissue was studied in the following manner. A solution of from 100 to 1000 μC of radio-iodine containing fourteen milligrams of iodine as sodium iodide was administered by mouth to the patients and two days later the thyroid glands were removed. The thyroid tissue was "fixed" in a ten-percent solution of formaldehyde for twenty-four hours and then embedded in paraffin. Thin sections of the impregnated thyroid tissue were cut with the aid of a microtome and the cut sections, which ranged from three to five microns in thickness, were mounted upon large glass slides. The mounted sections were washed in xylene to dissolve out the paraffin and then were dipped in a dilute solution of collodion and set on edge to dry. This technique served to remove all of the paraffin and left the sections protected by a film of collodion of approximately one micron in thickness. The prepared sections were then placed on Agfa No-Screen X-Ray film and placed in a small press to hold the films in close contact

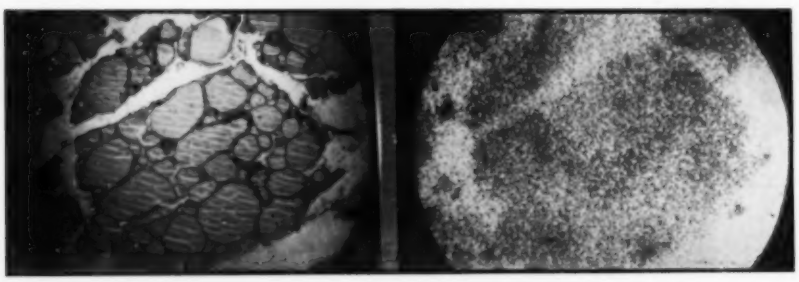

FIG. 12. Photomicrograph of a section of normal thyroid tissue and its radio-autograph (×60). Here, as in Figs. 13, 14, and 15, the areas of darkening of the radio-autograph represent the regions of greatest accumulation of radio-iodine in the accompanying section of thyroid tissue.

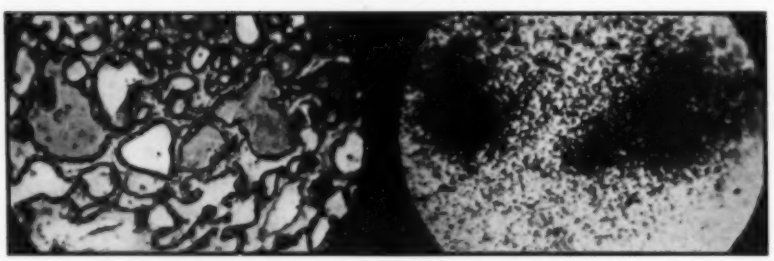

FIG. 13. Photomicrograph from a section of hyperplastic thyroid tissue and its radio-autograph (×120). The large grayish areas in the section on the left represent colloid, the remaining acini are devoid of colloid. The radio-autograph indicates that most of the accumulated radio-iodine was stored in the colloid.

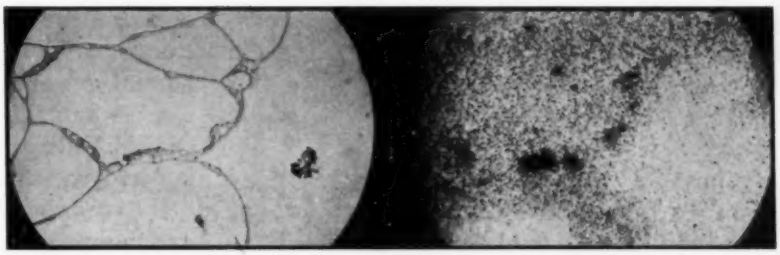

FIG. 14. Photomicrograph of a section of thyroid tissue and its radio-autograph from a patient with a nontoxic goiter (×60). Here the acini are enlarged and distended with colloid which had accumulated very little of the administered radio-iodine. The cells and small acini surrounding the large colloid deposits had a much greater ability to store the labeled iodine.

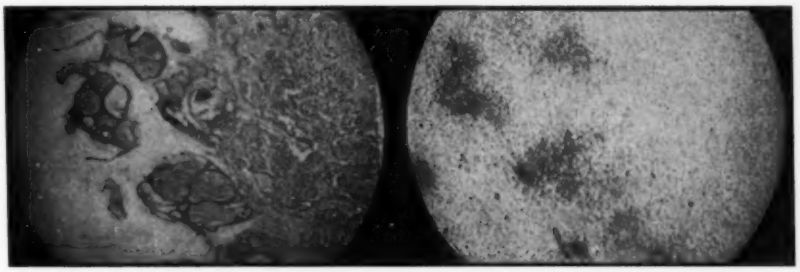

FIG. 15. Photomicrograph of a section and its corresponding radio-autograph from a patient with a cancer of the thyroid (×60). The diffuse cellular area covering the right half of the section is made up of cancerous thyroid tissue. To the left are three small islands of uninvaded thyroid tissue which accumulated most of the radio-iodine.

with the sections. After a suitable period of exposure* the films were removed and developed, and the sections were stained with hemotoxlyn and eosin. The histological structure of each section and its corresponding radio-autograph were compared under a microscope. The areas of darkening on the radio-autographs represent the regions in the sections where the greatest accumulation of the labeled iodine had taken place. Typical sections of normal thyroid tissue, nontoxic goiter, thyroid hyperplasia, and cancer of the thyroid, are shown in the following figures. Figure 12 was secured from a sample of normal thyroid tissue and the radio-autograph indicates that the accumulated radio-iodine was quite evenly distributed throughout the section. The degree of resolution of the radio-autograph was not sufficient to distinguish the cells individually but it appears that there was no great difference between the amount of tagged iodine in the cells and in the colloid. The section shown in Fig. 13 was obtained from a patient with a cancer of the thyroid. The cancer had destroyed most of the gland and as a result the small amount of remaining normal thyroid tissue had become hyperplastic in order to supply an adequate amount of the thyroid hormone to meet the patient's metabolic requirements. The section reveals a marked degree of cellular activity of the noncancerous thyroid tissue with little colloid present. The radio-autograph indicates that the small amount of remaining colloid had a much higher proportion of the accumulated radio-iodine than the cells of the adjacent acini. This suggests that when a marked degree of thyroid hyperplasia takes place there is rapid movement of part of the iodine accumulated in the thyroid cells into the colloid while the remainder is returned by the cells into the blood stream. The next section and radio-autograph, Fig. 14, was from a patient with a nontoxic goiter. The accumulated radio-iodine in this instance is predominantly stored in the cells and small acini which surround the larger acini. The section in Fig. 15 shows the difference between the deposition of iodine in relatively normal thyroid tissue and in cancerous tissue. The obvious absence of appreciable radio-iodine in the neoplastic areas indicates that in this instance the thyroid cells, which had undergone malignant changes, had lost their ability to accumulate iodine.

Element 85

One of the procedures employed for confirming the identification of the recently discovered

* Satisfactory radio-autographs can usually be obtained from sections of plant and animal tissue which contain a sufficient number of radioactive atoms to give a total of 2×10^6 beta-particles per square centimeter striking the film during the exposure. This value is for radio-elements which emit beta-particles with an average energy in excess of 150 kev. The period of exposure, of course, depends upon the strength of the sample which, in turn, determines how long an interval of time is required to obtain the necessary number of beta-particles.

halogen,[36,37] eka-iodine (element 85), demonstrated that this new element is accumulated in the thyroid gland and excreted in a manner similar to iodine. Element 85 is the heavy homolog of iodine and is radioactive with a half-life of seven and a half hours. It decays directly by the emission of energetic alpha-particles as well as by K capture and the result of the latter type of disintegration is, of course, the emission of the K x-rays of the adjoining element, polonium (actinium C′) followed by the almost immediate decay of this very short-lived natural radio-element by the emission of an alpha-particle. Element 85 is prepared by the alpha-particle bombardment of metallic bismuth with 32-Mev alpha-particles and the radio-element can be separated from the bismuth by distillation in vacuum.

The periodical character of the physical and chemical properties of the elements is paralleled to a considerable degree by their physiological action and for this reason it was felt that further proof of the identity of element 85 could be secured by a comparison of its biological properties with those of iodine. The radio-iodine was prepared by the deuteron bombardment of metallic tellurium and separated without carrier, since element 85 was also separated from the irradiated bismuth without carrier, and in order to secure a valid comparison of the metabolism of these two halogens it was desirable to administer both elements in approximately equivalent quantities. It was estimated that approximately 10^{-13} gram of element 85 and 10^{-12} gram of radio-iodine were prepared for each experimental animal.

A group of normal and thyrotoxic guinea pigs received by injection a solution containing both radio-iodine and element 85. The excretion of these two radio-halogens in both the urine and feces was quantitatively determined and at varying intervals of time the animals were sacrificed and the content of both radio-iodine and element 85 in the tissues were measured. The thyrotoxic animals were prepared by the previous administration of the thyrotropic hormone from the anterior portion of the pituitary gland. This substance stimulates the thyroid gland and its administration induces an excessive elaboration of the thyroid hormone by increasing the functional activity of the thyroid gland. The thyroids of thyrotoxic animals have a greater capacity for the accumulation of iodine as compared with normal animals and the general metabolism of the thyrotoxic animals is analogous to the clinical findings that are encountered in human hyperthyrodism.

A comparison between the metabolism of these two radio-halogens is shown in Fig. 16 and it can be seen that they are accumulated in the thyroid in a similar manner, although the proportion of element 85 taken up by the thyroid was consistently less. The rates of excretion of radio-iodine and element 85 were almost identical and the kidneys acted as the chief channel of elimination for both substances. The content of radio-iodine and element 85 in the other tissues examined was found to be less than one percent of their concentration in the thyroid gland. The prolonged retention of element 85 in the thyroid suggests that it is probably bound firmly as an organic compound and possibly is attached to benzene rings in a manner similar to iodine. A

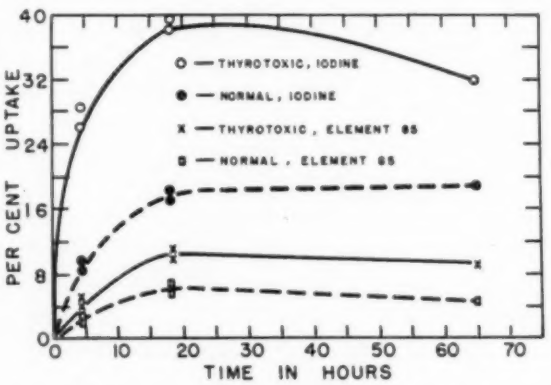

FIG. 16. A comparison of the uptake of radio-iodine and element 85 by the thyroid glands of normal and thyrotoxic guinea pigs.

sample of element 85 was administered to a patient with a nontoxic goiter and the uptake by the thyroid gland of the halogen was determined[38] by measuring the radioactivity of the gland *in situ* as has been described in similar studies with radio-iodine. In the case of element 85 its content in the thyroid was followed by the measurement of the x-radiation. The uptake curve was found to resemble those obtained with radio-iodine in this type of thyroid disorder, and at the end of twenty-four hours approximately ten percent of the administered element 85 was accumulated in

the thyroid. Due to the short half-life of element 85 it was not possible to continue the experiment for a longer period of time.

Iron

Whipple and his associates have employed radio-iron as a tracer for the study of iron metabolism and, in particular, the various factors relating to the conversion of inorganic iron to the hemoglobin of the red blood cells. Until these studies with radio-iron were possible it had been generally assumed that the iron taken into the body in the food, water, etc., was absorbed in the stomach and small intestines and the amounts of this element which were thus absorbed but were in excess of the normal requirements of the body were then re-excreted in the lower portions of the digestive tract. In other words, content of iron in the body was regulated by excretion.

Dogs were employed as the experimental animals for the studies with radio-iron and in the initial experiments Whipple and his group[39] compared the uptake of radio-iron in normal animals, and in dogs which had been previously rendered anemic by repeated bleeding and were maintained on a diet which was deficient in iron. Both groups of animals received the labeled iron orally as inorganic ferric salts. The animals were sacrificed at varying intervals of time after the administration of the radio-iron and the radioactivities of the tissues determined with the aid of a Geiger counter. These experiments revealed that the uptake of the tagged iron was from 4.1 to 12.7 percent in the anemic animals and in the normal controls the uptake was very much less, ranging from 0.08 to 0.24 percent. The bulk of the absorbed radio-iron in the anemic dogs was incorporated into the red cells of the blood while in the control group a much smaller fraction of the absorbed iron was in the red cells. These studies indicated that the uptake of the administered radio-iron was determined by the need of the body for iron and that in the anemic (iron deficient) animals not only was the total absorption of the labeled iron much greater; but also the relative proportion of the absorbed radio-iron in the blood was larger in this group than in the control animals. In later experiments[40] these investigators studied the metabolism of tagged iron following its intravenous administration in

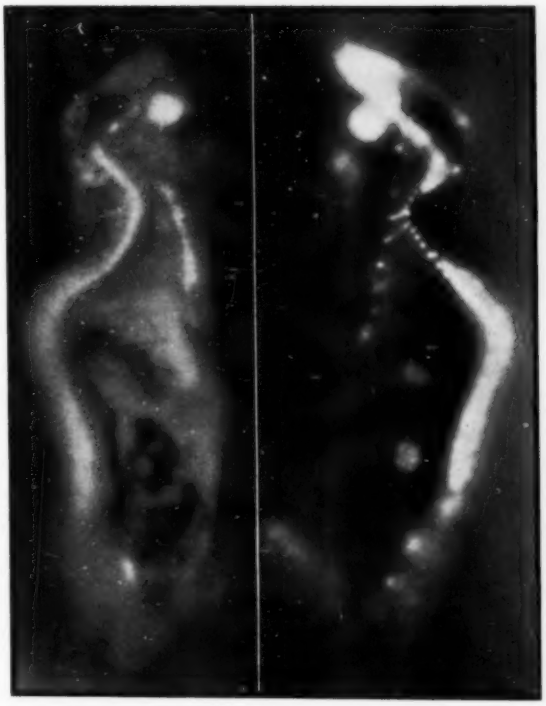

$_{15}P^{32}$ $_{82}Sr^{89}$

FIG. 17. The difference in distribution of recently absorbed radio-phosphorus and radio-strontium in rats as shown by the technique of radio-autography.

normal and anemic dogs. They observed that the rates of elimination of the radio-iron were very slow in both groups of animals and no significant differences in rates of excretion were noted between the normal and anemic dogs. From these observations the authors concluded that the body controls the level of its iron stores by regulating the quantity of iron absorbed from the digestive tract rather than by its capacity to eliminate the assimilated iron. It was shown in other studies by Whipple and his co-workers[5, 41] that the absorbed radio-iron in the blood was almost entirely converted into the iron-containing protein, hemoglobin. Moreover, they observed that the radio-iron was more efficiently converted into hemoglobin when the total amount of iron administered was very small. In a recent experiment these investigators[42] determined the iron uptake of a normal dog following the oral administration of radio-iron and found that 1.3 percent was assimilated. The animal was then rendered acutely anemic by the removal of approximately two-thirds of its total circulating blood and

TABLE I. *Distribution in the tissues of radioactive calcium, strontium and phosphorus 24 hours after an intravenous injection of radio-calcium lactate, Radio-strontium lactate or sodium radio-phosphate.*

	PERCENT OF DOSE PER GRAM WET WEIGHT					
	BONE	MUSCLE	SKIN AND HAIR	DIG. TRACT	LIVER	OTHER VISCERA
Ca^{45}	22	0.33	0.20	0.36	0.12	0.23
Sr^{89}	12	0.17	0.15	0.23	0.07	0.13
P^{32}	5.2	1.4	0.75	1.3	3.0	2.1

twenty-four hours later the same amount of radio-iron was given to the animal by mouth. The uptake of this second dose of radio-iron was approximately the same as it had been before the animal had been bled. Sufficient time was then allowed to permit the hemoglobin level of the circulating blood to be replenished to a nearly normal value at the expense of the body stores of iron. A third sample of radio-iron of approximately the same degree of radioactivity and containing the same amount of total iron was administered by mouth at the end of this last period of the experiment. This time the uptake was ten percent as compared to the two preceding experiments in which the uptake in both instances was less than two percent. The authors suggest that the absorption of iron is not influenced by the presence of anemia *per se* but is controlled by degree of depletion of the tissue iron and in particular by the amount of iron present in the cells lining the digestive tract.

Austoni and Greenberg[43] investigated—with the aid of radio-iron—the absorption, excretion and distribution of iron in rats which had been maintained on normal and iron-deficient diets. The animals received the iron in the form of ferric chloride and it was administered by stomach tube in doses of from two to eight milligrams. At varying intervals of time the animals were viviperfused to free all of the tissues from blood and the content of radio-iron in the blood, tissues and excreta determined. These studies revealed that for the normal animals it required about twelve hours for a single dose of labeled iron to pass through the stomach and small intestine. The passage of the radio-iron through the digestive tract was significantly slower in the animals which were maintained on the iron-deficient diet. The uptake of the administered iron by the blood and tissues was greater in the anemic animals and the specific accumulation of absorbed iron per gram of tissue was highest in the bone marrow, blood, spleen, liver and heart. The total accumulation was greatest in muscle and blood and at the end of ten days in the anemic animals 25 percent of the administered radio-iron was stored in the muscle and 14 percent remained in the blood. At the end of this interval the corresponding tissues of the normal animals only contained small traces of radio-iron. This work confirms the observation of Hahn and his co-workers that the absorption of iron by the body is increased if the tissues have been previously depleted of their stores of this element. The studies of Austoni and Greenberg have demonstrated the significant fact that muscle tissue apparently acts as the chief storage depot for iron in anemia.

Calcium and Strontium

The bony skeleton of animals is composed largely of calcium and phosphorus in the form of tri-calcium phosphate and for this reason the considerable interest in the metabolism of calcium has stimulated investigators to apply radio-calcium to metabolic problems which concern this element. Campbell and Greenberg,[44] and later Pecher,[45] demonstrated with the aid of labeled calcium that this element is almost entirely stored in the bones, with but small traces being distributed in the soft tissues of the body. This selective deposition of radio-calcium in the bony structures suggested that this radio-element might be of therapeutic value in the treatment of malignant conditions which involve these portions of the body. The very long half-life of radio-calcium (180 days) and weak activities that are available definitely precluded the application of this radio-element to therapeutic purposes. Pecher predicted,[45] and subsequently demonstrated, that strontium, which is in the same group in the periodic system, is handled in the body in a manner similar to calcium. Radio-strontium has a half-life of 55 days, can be readily prepared in relatively large amounts, and emits very energetic beta-particles. Table I indicates the distribution of phosphorus, calcium, and strontium in the tissues of mice when these substances

were administered as organic salts. Although the proportion of strontium taken up in the body is lower than that of calcium it will be noted that the selectivity of deposition of these two elements in bone is almost the same. In Fig. 17 a comparison between the distribution of strontium and phosphorus is shown by the use of the technique of radio-autography. In this experiment one animal received radio-phosphorus and the other was given radio-strontium. Two and a half days later the animals were sacrificed and sections of the entire animals were prepared and these sections placed upon films in order to secure the radio-autographs. It will be seen in Fig. 17 that in the case of phosphorus there was a moderate degree of accumulation of that element in the skeleton together with considerable quantities throughout the soft tissues, while with strontium almost all of this substance that had been assimilated by the animal was in the bony structures.

These studies indicate that since radio-strontium is so selectively deposited in bone and possesses desirable radioactive properties (half-life, beta-ray energy, and availability) it may prove useful in clinical therapy and at the present time this phase of the problem is under investigation.

Carbon and Nitrogen

One of the outstanding examples of the application of a radioactive isotope as an indicator for fundamental research in the metabolic processes of biological systems has been the use of radiocarbon by Ruben, Kamen, and their co-workers to study the metabolism of carbon dioxide in a wide variety of organisms. These investigators[46] demonstrated that plants and algae containing chlorophyll had the ability to assimilate a small but measurable proportion of tagged carbon dioxide from the air in the complete absence of light. An extensive study of this phenomenon of "dark reduction" in the green algae, *Chlorella Pyrenoidosa*, was carried out. The results of these studies indicated that the assimilated carbon dioxide was reduced to a carboxylic acid which was attached to a large complex molecule. This reaction in the dark was found to be reversible in character and can be represented by the following equation: $RH+CO_2 \rightleftharpoons RCOOH$. It was suggested by them that this reaction represented the first step in the long and complicated series of chemical reactions which finally result in the formation of sugars, starches, etc., by green plants. The chemical identity of the molecule "R" to which the labeled carbon dioxide is bound as a carboxylic acid is not known. However, the authors[47] observed with the aid of the ultracentrifuge and diffusion measurements that the RCOOH molecule has a molecular weight of approximately 1000 when it is extracted from the algae by the use of boiling water. In the absence of light all of the labeled carbon appeared to be in the carboxyl group, which suggests that under these conditions no further reduction of the assimilated carbon dioxide takes place. The "dark uptake" of the tagged carbon dioxide was very rapid when it was first introduced into the vessel containing the plants; but the rate of uptake diminished while the plants were maintained in the atmosphere containing radioactive carbon dioxide, and at the end of an hour very little additional carbon dioxide was accumulated. This was interpreted to indicate that the "dark uptake" of carbon dioxide was a reversible chemical reaction and at the end of an hour equilibrium had been established with as many tagged molecules leaving the plant as new molecules of the gas from the surrounding atmosphere entered the leaves. When the experiment was conducted in the presence of light the uptake of carbon dioxide continued very rapidly and at the same rate from the time when the material was administered until the end of the experiment several hours later. Thus it was apparent that the assimilation of the labeled carbon dioxide in the light was not a reversible reaction. Moreover, in the presence of light only a small fraction of the accumulated labeled carbon was found in the carboxylic radical, apparently most of the radiocarbon was converted to a more highly reduced state. In some plants, as for example barley, approximately twenty percent of the assimilated carbon dioxide was synthesized into sugar within two hours when the experiment was conducted in the presence of light. From these observations and the results of other experiments the authors suggest the following type of reaction for the "light reduction" of carbon in the presence of chlorophyll, $RCOOH+H_2O+h\nu \rightarrow RCH_2OH+O_2$.

The RCH_2OH molecule may take up carbon dioxide as did the original RH molecule, thus providing the mechanism for a cyclical process leading to the eventual synthesis of typical photosynthetic carbon compounds by the step by step addition of assimilated carbon dioxide onto the enzyme molecule "R." This mechanism implies that simple sugars are not synthesized directly in the plant but that they are split off from large polyhydric molecules which are built up on the enzyme "R." In each step, however, the initial reaction involving each assimilated carbon dioxide molecule is its reduction to a carboxylic acid group which is a nonphotochemical reaction. The further reduction of the carboxylic radical involves photochemical reactions and requires the participation of both chlorophyll and light.

The mechanism for photosynthesis which these authors have developed from their work with radio-carbon is in considerable variance with the classical theory of photosynthesis which has been accepted by most investigators in this field. The latter concept postulated the following type of reaction in the leaves of the plant: $H_2O+CO_2+h\nu \rightarrow HCHO+O_2$, and the subsequent polymerization of the formaldehyde to form more complex carbon compounds. A careful search was made for the presence of carbon compounds of low molecular weight, including formaldehyde, in *Chlorella* exposed to the tagged carbon dioxide and none was found within the range of sensitivity of the method which would have detected less than one part in a million of these substances had they been present.

These investigators observed with the aid of radioactive carbon dioxide that nonphotosynthetic organisms (cells which do not contain chlorophyll and do not utilize light in their metabolic processes) had the capacity to reduce carbon dioxide.[48] They employed many different types of microorganisms, including yeast cells, *B. coli*, and rat liver cells, in their experiments and found that when these organisms carried out their metabolic activities in media to which labeled carbon dioxide had been added a significant portion of the carbon dioxide was reduced and converted into organic compounds such as acetic acid, propionic acid, etc. In some cases a portion of the labeled carbon dioxide was found to have been incorporated into the cellular material which is made up of large and complex molecules. These observations are most striking since these organisms secure their energy by the oxidation of carbohydrates, fats, proteins, etc.; and as a result carbon dioxide is one of their chief metabolic end products. Obviously, since such organisms excrete carbon dioxide, the classical chemical and physical methods could never have demonstrated that a small but finite proportion of the carbon dioxide molecules in their tissues are reduced. Furthermore, these workers have shown that in some instances for every twenty-five to fifty carbon dioxide molecules produced by oxidation one molecule was reduced. The evidence thus far obtained has led to the suggestion that all living organisms have the capacity to reduce carbon dioxide.

Many organic compounds, such as sugars, acetic acid, propionic acid, lactic acid, etc., are quite difficult to tag directly with radio-carbon by synthesizing them in the test tube. However, these substances can be readily prepared by administering radioactive carbon dioxide to suitable organisms and after a period of an hour or so the labeled compounds may be separated from the biological material.[49]

Mention should be made in this section of the experiments by this group of workers[50] who found that if barley plants are exposed to radio-nitrogen a small quantity of labeled nitrogen compounds are formed in the tissues of the plants. The authors point out that this may be due to an exchange of the labeled nitrogen with the nitrogen compounds in the plants. On the other hand, their observations may indicate that barley plants can utilize small amounts of atmospheric nitrogen for nutrition. The results of these experiments are of considerable interest since there is considerable controversy concerning the fixation of nitrogen by non-leguminous plants.

Conclusion

This report has attempted to describe the experimental techniques employed in the applications of radioactive tracers to metabolic studies in biology and medicine. A few examples of the results secured with radioactive tracers have been presented in order to illustrate the wide diversity of applicability of this new tool of research to the

TABLE II.

Radio-Element	Type of Radiation	Half-Life	Energy of Radiation in Mev: Particles	Energy of Radiation in Mev: Rays	Yield in Microcuries per Microampere Hour	Produced by
$_1H^3$	B^-	20 yr.	0.013		0.1	Be-*d*-$_1H^3$
$_6C^{11}$	B^+	21 min.	0.95		500*	B-*d*-*n*
$_6C^{14}$	B^-	>1000 yr.	0.150		0.00005	N-*n*-*p* (Be-*d*-*n*)**
$_7N^{13}$	B^+, γ	9.93 min.	1.2, 0.92	0.28	500*	C-*d*-*n*
$_{11}Na^{22}$	B^+, γ	3.0 yr.	0.58	1.3	3*	Mg-*d*-α
$_{11}Na^{24}$	B^-, γ	14.8 hr.	1.4	1.46, 2.0, 3.03	10,000	Na-*d*-*p*
$_{12}Mg^{27}$	B^-, γ	10.2 min.	1.8	0.9	500*	Mg-*d*-*p*
$_{15}P^{32}$	B^-	14.30 days	1.69	No γ	200	P-*d*-*p*
$_{16}S^{35}$	B^-	88 days	0.107		0.1	S-*d*-*p*
$_{17}Cl^{38}$	B^-, γ	37 min.	1.1, 5.0	1.65, 2.15	1000*	Cl-*d*-*p*
$_{19}K^{42}$	B^-, γ	12.4 hr.	3.5		50	K-*d*-*p*
$_{20}Ca^{45}$	B^-, γ	180 days	0.2, 0.9	0.7	0.01	Ca-*d*-*p*
$_{25}Mn^{54}$	K, γ	310 days		0.85	1	Fe-*d*-α
$_{26}Fe^{59}$	B^-, γ	47 days	0.4, 0.9	1.0	0.03	Fe-*d*-*p*
$_{27}Co^{56}$	K, γ, e^-, B^+	270 days	0.4(B^+)		1	Fe-*d*-2*n*
$_{29}Cu^{64}$	B^-, B^+, K	12.8 hr.	0.58(B^-) 0.66(B^+)	No γ	3000	Cu-*d*-*p*
$_{30}Zn^{65}$	B^+, K, γ, e^-	250 days	0.4(B^+)	0.45, 0.65, 1.0	0.5	Cu-*d*-2*n*
$_{33}As^{76}$	B^-, B^+, K, γ	26.8 hr.	1.1, 1.7, 2.7(B^-), 0.7, 2.6(B^+)	1.5, 2.2, 3.2	10	As-*n*-γ (Be-*d*-*n*)**
$_{33}As^{74}$	B^-, B^+, γ	16 days	1.3(B^-), 0.9(B^+)		2	Ge-*d*-2*n*
$_{35}Br^{82}$	B^-, γ	34 hr.	0.7	0.65	10	Br-*n*-γ (Be-*d*-*p*)**
$_{37}Rb^{86,88}$	B^-, γ	18 days			10	Rb-*d*-*p*
$_{38}Sr^{89}$	B^-	55 days	1.50	No γ	7	Sr-*d*-*p*
$_{53}I^{131}$	B^-, γ	8.0 days	0.687	0.4	20	Te-*d*-*n*
$_{85}?^{211}$	K, α, γ	7.5 hr.	6.0		1	Bi-α-2*n* (32 Mev αs

biological sciences. It should be pointed out that radioactive tracers have been thus far employed chiefly by the biologists and the workers in these fields have developed techniques such as the labeling of compounds, radio-autography, etc., to meet their research problems. These different methods are applicable to research problems in other scientific fields and to industry.

The appendix included in this paper gives the pertinent physical data including yields for the radio-elements which have been employed as tracers in biology and medicine.

Appendix

Table II, with the exception of the yield data, was obtained from the tables given by Livingood and Seaborg in *Reviews of Modern Physics*[51] and later by Seaborg in *Chemical Reviews*.[52]

All of the yields are given as microcuries per microampere hour. The term "microcurie" refers to the absolute number of disintegrations per second of the artificially prepared radio-element; namely, 3.7×10^4 disintegrations per second. All yields given which have a single asterisk placed beside them refer to data obtained from the 37" Berkeley cyclotron which produces 8,000,000-volt deuterons. The remaining yields, with the exception of element 85 and the radio-elements produced by neutrons, refer to direct bombardment with 16,000,000-volt deuterons from the 60" Berkeley cyclotron. The 32,000,000-volt alpha-particles employed for the production of element 85 were obtained from the 60" cyclotron. The data given in the last column on the right refers to the nuclear reactions which result in the yields shown in the adjoining column. The double asterisks refer to the production of the radio-elements by neutrons resulting from the bombardment of beryllium by 16,000,000-volt deuterons. These yields from neutrons, which are expressed as microampere-hours of deuterons, were estimated on the basis of the following quantities of material irradiated by the neutrons: $_6C^{14}$ from 25 kilograms of ammonium nitrate, $_{33}As^{76}$ from 500 grams of cacodylic acid, and $_{35}Br^{82}$ from 2000 cc of brombenzene.

The values given for the yields are in many instances approximations and are subject to considerable error. The data for the yields of $_{11}Na^{24}$, $_{15}P^{32}$, $_{26}Fe^{59}$, $_{38}Sr^{89}$ and $_{53}I^{131}$ are estimated to be accurate to approximately 50 percent. The remaining yield data are much less exact and are subject to considerably larger fluctuations in accuracy.

Bibliography

1. I. Curie and F. Joliot, Nature **133**, 201 (1934).
2. G. Hevesy, Biochem. J. **17**, 439 (1923).
3. (a) E. O. Lawrence and D. Cooksey, Phys. Rev. **50**, 1131 (1936). (b) E. O. Lawrence *et al.*, Phys. Rev. **56**, 124 (1939). (c) E. O. Lawrence, Science **90**, 407 (1939).
4. O. Chiewitz and G. Hevesy, Nature **136**, 754 (1935).
5. L. L. Miller and P. F. Hahn, J. Biol. Chem. **134**, 585 (1940).
6. H. Borsook, J. B. Hatcher and D. M. Yost, J. App. Phys. **12**, 325A (1941).
7. O. Chiewitz and G. Hevesy, Kgl. Danske Vidensk. Selsk. Biol. Medd. **13**, 9 (1937).
8. G. Hevesy, L. Hahn and O. Rebbe, Kgl. Danske Vidensk. Selsk. Biol. Medd. **14**, 3 (1939).
9. J. H. Lawrence, K. G. Scott and L. W. Tuttle, New International Clinics **3**, 33 (1939).
10. L. A. Erf, L. W. Tuttle and K. G. Scott, Proc. Soc. Exp. Biol. Med. **45**, 652 (1940).
11. W. E. Cohn and D. M. Greenberg, J. Biol. Chem. **123**, 185 (1938).
12. K. G. Scott and S. F. Cook, Proc. Nat. Acad. Sci. **23**, 265 (1937).
13. K. G. Scott and J. H. Lawrence, personal communication.
14. J. H. Lawrence and K. G. Scott, Proc. Soc. Exp. Biol. Med. **40**, 694 (1939).
15. J. H. Lawrence, L. W. Tuttle, K. G. Scott and C. L. Conner, J. Clin. Invest. **19**, 267 (1940).
16. G. Hevesy and E. Lundsgaard, Nature **140**, 275 (1937).

17. C. Artom, G. Sarzana, C. Perrier, M. Santangelo and E. Segrè, Nature, **139**, 836 (1937).
18. (a) I. Perlman, S. Ruben and I. L. Chaikoff, J. Biol. Chem. **122**, 169 (1937). (b) B. A. Fries, S. Ruben, I. Perlman and I. L. Chaikoff, J. Biol. Chem. **123**, 587 (1938). (c) C. Entenman, S. Ruben, I. Perlman, F. W. Lorenz and I. L. Chaikoff, J. Biol. Chem. **124**, 795 (1938).
19. A. Robinson, I. Perlman, S. Ruben and I. L. Chaikoff, Nature **141**, 119 (1938).
20. H. B. Jones, I. L. Chaikoff and J. H. Lawrence, J. Biol. Chem. **128**, 631 (1939).
21. H. B. Jones, I. L. Chaikoff and J. H. Lawrence, J. Biol. Chem. **133**, 319 (1940).
22. L. W. Tuttle, L. A. Erf and J. H. Lawrence, J. Clin. Invest. **20**, 57 (1941).
23. A. Marshak, Science **92**, 460 (1940).
24. D. I. Arnon, P. R. Stout and F. Sipos, Am. J. Bot. **27**, 791 (1940).
25. P. R. Stout and D. R. Hoagland, Am. J. Bot. **26**, 320 (1939).
26. P. R. Stout, J. App. Phys. **12**, 327A (1941).
27. P. R. Stout, personal communication.
28. E. Lindsey and R. Craig, Ann. Ent. Soc. Am., in press, (1941).
29. J. G. Hamilton, Am. J. Physiol. **124**, 667 (1938).
30. S. Hertz, A. Roberts and R. D. Evans, Proc. Soc. Exp. Biol. Med. **38**, 510 (1938).
31. S. Hertz, A. Roberts, J. H. Means and R. D. Evans, Am. J. Physiol. **128**, 565 (1940).
32. J. G. Hamilton and M. H. Soley, Am. J. Physiol. **127**, 557 (1939).
33. J. G. Hamilton and M. H. Soley, Am. J. Physiol. **131**, 135 (1940).
34. A. Lacassagne and J. Lattes, Comptes rendus soc. de biol. **90**, 352 (1924).
35. J. G. Hamilton, M. H. Soley and K. B. Eichorn, University of California Publications in Pharmacology **1**, No. 28, 339 (1940).
36. D. R. Corson, K. R. MacKenzie and E. Segrè, Phys. Rev. **58**, 672 (1940).
37. J. G. Hamilton and M. H. Soley, Proc. Nat. Acad. Sci. **26**, 483 (1940).
38. J. G. Hamilton and M. H. Soley, unpublished data.
39. (a) P. F. Hahn, W. F. Bale, E. O. Lawrence and G. H. Whipple, J. Am. Med. Assn. **111**, 2285 (1938). (b) P. F. Hahn, W. F. Bale, E. O. Lawrence and G. H. Whipple, J. Exp. Med. **69**, 739 (1939).
40. P. F. Hahn, W. F. Bale, R. A. Hettig, M. D. Kamen and G. H. Whipple, J. Exp. Med. **70**, 443 (1939).
41. P. F. Hahn, J. F. Ross, W. F. Bale and G. H. Whipple, J. Exp. Med. **71**, 731 (1940).
42. P. F. Hahn, and G. H. Whipple, J. App. Phys. **12**, 314A (1941).
43. M. E. Austoni and D. M. Greenberg, J. Biol. Chem. **134**, 27 (1940).
44. W. W. Campbell and D. M. Greenberg, Proc. Nat. Acad. Sci. **26**, 176 (1940).
45. C. Pecher, Proc. Soc. Exp. Biol. Med. **46**, 86 (1941).
46. (a) S. Ruben, W. Z. Hassid and M. D. Kamen, J. Am. Chem. Soc. **61**, 661 (1939). (b) S. Ruben, W. Z. Hassid and M. D. Kamen, J. Am. Chem. Soc. **62**, 3443 (1940).
47. (a) S. Ruben, M. D. Kamen and L. H. Perry, J. Am. Chem. Soc. **62**, 3450 (1940). (b) S. Ruben and M. D. Kamen, J. Am. Chem. Soc. **62**, 3451 (1940).
48. (a) S. Ruben and M. D. Kamen, Proc. Nat. Acad. Sci. **26**, 418 (1940). (b) S. F. Carson, J. W. Foster, S. Ruben and M. D. Kamen, Science **92**, 433 (1940).
49. M. D. Kamen and S. Ruben, J. App. Phys. **12**, 310A (1941).
50. S. Ruben, W. Z. Hassid and M. D. Kamen, Science **91**, 578 (1940).
51. J. J. Livingood and G. T. Seaborg, Rev. Mod. Phys. **12**, 30 (1940).
52. G. T. Seaborg, Chem. Rev. **27**, 199 (1940).

Explorations toward the Limit of Utilizable Pressures

By P. W. Bridgman

Harvard University, Cambridge, Massachusetts

THERE is no sharply defined limit to attainable pressures. On a microscopic scale, as when two crossed knife edges are pressed together, or for an infinitesimal interval of time, as when a projectile wedges itself into a suitably constricted massive target, pressures may be obtained which everyone must concede are very high, but which cannot be precisely evaluated because of the indefiniteness of the conditions. There is no profit from the point of view of physics in trying for "records" in the attainment of high pressures, and little physical interest unless it is possible to do something with the pressure in the way of finding the properties of matter under new conditions. It has been evident for some little time that physical measurements could be made at pressures higher than those usually employed hitherto; a year or more ago[1] I published some results obtained with pressures well above 100,000 kg/cm², and a little later Goranson and Johnson[2] at the Geophysical Laboratory announced some results in essentially the same range. The next thing is obviously to do something with the pressures which have thus been made available. The answer to this problem involves a good deal of preliminary exploration, as does always the opening of a new field. I have already in my own work been through two such stages of exploration, initially in extending the useful range to 12,000 kg/cm², and then later in extending it to 50,000.

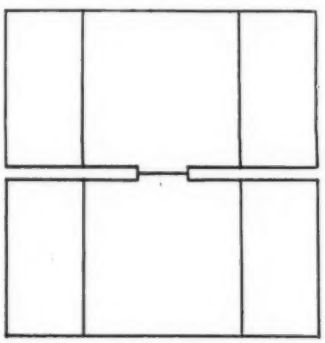

Fig. 1. General disposition of short Carboloy bosses on massive blocks with shrunk-on steel retaining rings.

Since my report of a year ago, I have been further appraising the possibilities and have obtained results of some intrinsic interest which I report here. The highest pressures which are measurable with fair accuracy and at the same time offer any possibility of use as a tool in determining the properties of matter appear to be attainable by a combination of "short pistons" with high confining pressures. By the use of short pistons, which are nothing but low bosses on massive blocks, I obtained a number of years ago[3] results up to 50,000 kg/cm² equivalent hydrostatic pressure combined with shearing stresses up to the plastic flow point. This apparatus was of steel; the compressive stresses obtainable in the best steels with ordinarily constructed pistons are roughly of the order of 30,000. The higher figure reached with the short pistons is made possible by the effective support afforded by the surrounding massive parts. If the short pistons are made of Carboloy, higher figures can naturally be reached. I have recently attained on the face of a Carboloy boss, pressed in the atmosphere of the room against a similar boss, as indicated in Fig. 1, an average intensity of 154,000 kg/cm² without destructive rupture. The height of the bosses was 0.005 inch and the diameter of the faces 0.130 inch. The Carboloy blocks in this experiment received partial support from shrunk-on steel rings, as indicated. The manner of rupture was complicated; many fine radial cracks surrounded the bosses, and at the periphery of the blocks near the steel retaining rings thin laminae flaked off parallel to the free face. It is difficult to explain the formation of these laminae except on the heuristic principle that under such high stresses rupture has to occur somewhere, and that it occurs as best it can on the only free faces.

If the arrangement of Fig. 1 is immersed in a fluid in which there is a high hydrostatic pressure, the stress may be increased because of the increase of strength produced by high confining pressure, as already described in my previous

note. A number of variations of the device of Fig. 1 were tried, but it was first necessary to develop some satisfactory device for measuring the thrust while immersed in the liquid under pressure. The experiments were all set up in my apparatus for 30,000 kg/cm², in which pressure is produced in a true liquid, isopentane, and in which electrically insulated leads can be taken into the pressure chamber and accurate measurements made.[4] In most of the experiments the pressure was controlled by a block of bismuth within the apparatus. Bismuth undergoes a transition with marked volume change at 25,430 kg/cm². By suitably choosing the amount of liquid which initially fills the apparatus it is possible to have the piston make up on the Carboloy pieces in the range within which the transition runs, so that the surrounding hydrostatic pressure remains constant. The force pushing one Carboloy piece against the other may be found from the force on the piston of the main apparatus in excess of that required to make the transition run in the absence of the Carboloy. The excess pressure on the piston is comparatively small, and its precise measurement is obscured by friction, so that some more accurate method of obtaining the thrust is desirable. The use of the bismuth control is not a necessity but only a convenience; in some cases it was dispensed with and replaced with a solid block of steel. This is necessary if the effect of other confining pressures than those of the transitions is to be studied.

Various devices were tried for measuring the thrust inside the pressure chamber. For example, a grid of manganin wire wound over mica and compressed between flat steel plates, which has been satisfactorily used under other conditions, proved to have so much hysteresis because of friction that it was not suitable. The arrangement finally adopted was to transmit the compressive force through a thin sleeve of hardened steel, which was cut into a longitudinal grid as indicated in Fig. 2. In this way a fairly long path is provided for an electric current without greatly diminishing the compressive strength of the uncut sleeve. Under compressive stress the electrical resistance diminishes. The change of resistance is measured by a potentiometer method through two current leads (one grounded) and two potential leads. Insulation from the rest of the apparatus is provided by thin mica washers under each end of the grid. This type of compressometer functions without appreciable hysteresis from friction or other causes, and without appreciable yielding under the compressive force, two important advantages. It doubtless could be used for other purposes than that for which it was designed.

In use, the resistance of the grid changes first because of the hydrostatic pressure in the surrounding liquid, and secondly, after the piston makes up, because of the additional compressive stress. If the resistance of the grid is plotted against the hydrostatic pressure in the fluid as given by a manganin pressure gauge immersed in it, the instant when the piston makes up is shown by a discontinuity in the direction of the line, and the amount of compressive stress by the difference between the prolonged line and the actual change of resistance. The compression coefficient of the grid is determined by independent experiment, which may be arranged with such dimensions and with sufficient repetitions to effectively eliminate uncertainty from friction. The effect of hydrostatic pressure on the compression coefficient must be allowed for; at 25,000 the compression coefficient was found to be about 17 percent less than at atmospheric pressure. The

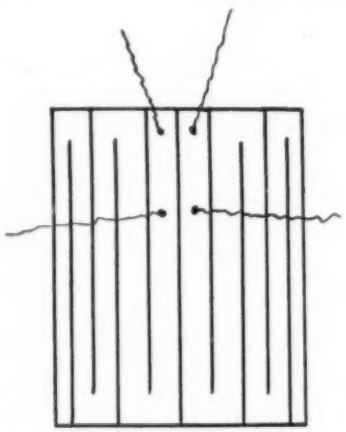

FIG. 2. The steel grid for measurement of compressive force with current and potential leads.

compressometer was constructed from "Teton" steel from the Ludlum Steel Company; it was heat treated to maximum hardness and drawn back to 200°C. In this condition the compression coefficient is such that the resistance decreases by something of the order of 2.5 percent under a

stress comfortably below the elastic limit. Subject to this limitation, the grid may be designed by change of dimensions to give any desired sensitivity for any desired load. With the particular set-up used in these experiments the sensitiveness of the readings was about $\frac{1}{4}$ percent on the maximum compressive force, and the force itself could be taken from the plot with an uncertainty less than one percent. In all the work reported here the compressive force was checked from the total thrust on the piston; the discrepancy between the two measurements was seldom as much as ten percent; the grid measurement was, of course, much preferable, and is the measurement reported here.

Having now a suitable device for measuring compressive force within the confining liquid, we may return to our short pistons. An arrangement essentially like that of Fig. 1 was carried under the confining pressure afforded by the second bismuth transition (27,000) to a differential pressure on the face of the bosses of 264,000 kg/cm², making a total pressure of 291,000, without correction for elastic distortion. Under this stress there was only partial failure of the specimens; there were many fine radial cracks around the bosses and many fine circumferential slip bands in the faces of the bosses around the outer edges. The symmetry of the bosses enforces the condition that the face of each boss remains plane at every stress, without dishing. Under these conditions, the height of the boss being such a small fraction of its diameter, one may expect a qualitatively good enough solution to the problem of the elastic distortion to be afforded by the known solution for the distortion of a semi-infinite solid subject to a specified force or displacement over a circular area on its plane face, as given, for example, on page 190 of the third edition of Love. The mathematical solution gives the at first surprising result that the boss contracts in the plane of its face toward its own center, instead of expanding as would at first appear more natural. The reason for this is that the entire region under the face of the boss is a region of such high average volume compression that the effect of this volume compression prevails against the expanding tendencies. Assuming this correction, and taking the known elastic constants for the particular grade of Carboloy used, No. 905, the figure 291,000 above corrects to 300,000. The correction for elastic distortion is thus so small that it was not applied in the rest of this work.

The confining stress on the lateral faces of the Carboloy blocks in the arrangement above was somewhat greater than that of the surrounding liquid because of the shrunk-on steel sleeve. This additional stress was the maximum allowed by the tensile strength of the steel and may have amounted at atmospheric pressure to perhaps 5000 kg/cm². Under the confining pressure of the liquid this is further increased because of the differential compressibility of steel and Carboloy by one or two thousand more, not a particularly important effect.

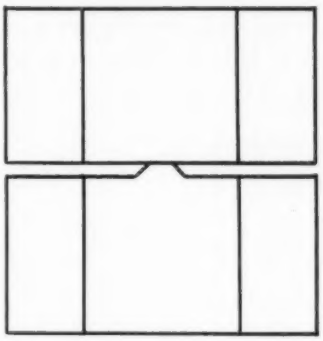

FIG. 3. Conical truncated Carboloy boss against a flat anvil for reaching higher pressures than possible with the arrangement of Fig. 1.

If one gives up the condition of symmetry, one can get considerably higher with these bosses. If the sides of the boss are made conical instead of cylindrical the tendency to fail at the edge by slipping is much decreased. The angle used was 45°. If such a boss is pushed against a plane surface, as in Fig. 3, it receives further support from the surface as it penetrates it. It is with this sort of an arrangement that I have reached the highest pressures. The boss leaves in the face of the opposing anvil a permanent impression with tapering walls, seen under a measuring microscope as two concentric circles. The smaller circle at the bottom of the impression marks the edge of the face of the boss, and the larger circle the limitation of penetration with plastic flow by the conical sides of the boss. The reality of the support afforded to the boss by penetration into the flat face of the anvil is shown by the fact that nearly always the diameter of the face of the boss was permanently decreased after exposure to pressure. The average stress on the area of

contact was calculated as that given by the total thrust measured with the compressometer acting over the area of the larger circle. The average stress on the originally plane face of the boss is of course larger than this, but by an amount which it would be difficult to calculate. There is an effect tending to reduce this estimate of the average stress, namely the effect of the region of elastic contact beyond the edge of the plastic zone which is marked by the limits of the permanent impression. The width of this elastic zone is

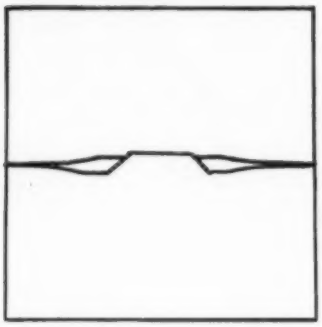

FIG. 4. If the boss is short, the distortion may be such as to allow support by the edges beyond a certain pressure.

doubtless small and its effect is partially neutralized by the elastic contraction toward the center already mentioned; no correction for it was attempted.

If the boss is too short, the elastic distortion of the rest of the Carboloy may be so great as to allow contact at the edges of the blocks, as suggested in Fig. 4. With blocks of the dimensions indicated and a height of the boss of 0.005 inch, support around the edges begins at an average pressure on the boss of something over 300,000 kg/cm². Whether such contact has occurred or not is easily established by inserting a disk of tin foil between the Carboloy pieces. To avoid such support around the edges it suffices to make the height of the boss greater. With a boss height of three times as much, that is 0.015 inch, and with a confining pressure of 26,000, a one-sided compression of 360,000 was obtained, making a total average hydrostatic pressure over the area of contact of 386,000. The limit was imposed by fear of exceeding the elastic limit of the compressometer, not by behavior of the Carboloy. A photograph of the two Carboloy pieces is shown in Fig. 5. There was no destructive rupture, but the pressure between the opposing pieces increased smoothly up to the maximum. Both pieces had many fine radial cracks, and there was a deep circumferential crack running around the boss near its upper edge. This circumferential crack did not appear immediately after release of pressure, but developed spontaneously on standing several days. The same is often true of the radial cracks. The boss was shortened, that is, pushed into its surroundings, by 0.005 inch; the depth of the impression in the anvil was something more than 0.003 inch.

Somewhat higher stresses are realizable if the geometry is so arranged as to permit destructive rupture. This may be done by turning the boss into a cone slightly truncated at the point. Such a conical boss, 0.009 inch across the flat face and 0.035 inch high, was pushed to destructive rupture against a flat anvil under a confining pressure of 26,500. The cone was reduced to a highly burnished stump 0.016 inch high, flanked by slip planes on angles greater than 45°, and with highly developed cleavages on the basal plane. There were no radial cracks in either piece. The impression in the anvil was somewhat obscured by the impact of the irregular stump after rupture, but a conservative estimate of the area gave for the average one-sided compressive force on the area of contact just before rupture 400,000,

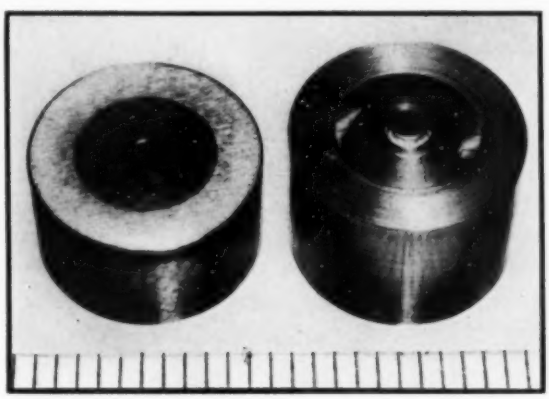

FIG. 5(a). Appearance of boss and anvil after exposure to 386,000 kg/cm². The scale is in millimeters.

making the total stress roughly 425,000 kg/cm², of the same order as that described in the last paragraph with a different arrangement. There is no reason to think that these were the optimum conditions, and one would expect by changing the angle of the cone and the ratio of face to

height to be able to improve these figures somewhat, but I do not believe that any very great improvement is to be expected. The maximum pressure possible between Carboloy pieces of this particular grade and with confining pressures of the order of 25,000 is thus probably somewhere between 400,000 and 500,000 kg/cm².

The very high stresses which are thus attainable under confining pressure are, I believe, made possible by a mechanism which is not altogether simple. The effect is not to be described simply as an increase of strength under confining pressure. Normally Carboloy is highly brittle and breaks with little plastic flow. The main effect of the confining pressure is, I think, to remove this brittleness and permit reaching the region of appreciable plastic flow, within which cold working effects of various sorts occur. The simultaneous changes produced by the hydrostatic pressure in the intrinsic properties of the undistorted lattices of the several components are, I think, less important. Carboloy is remarkable for the extent of the plastic region within which progressively increasing cold working occurs; this is doubtless closely connected with the complicated structure of Carboloy to be expected from its manner of formation. The fact that plastic flow occurs in Carboloy was already mentioned in my first note in connection with experiments on the strength of pistons; it is now dramatically shown by the permanent depressions in the Carboloy anvils, which give the impression of having been formed in a die, like a copper coin.

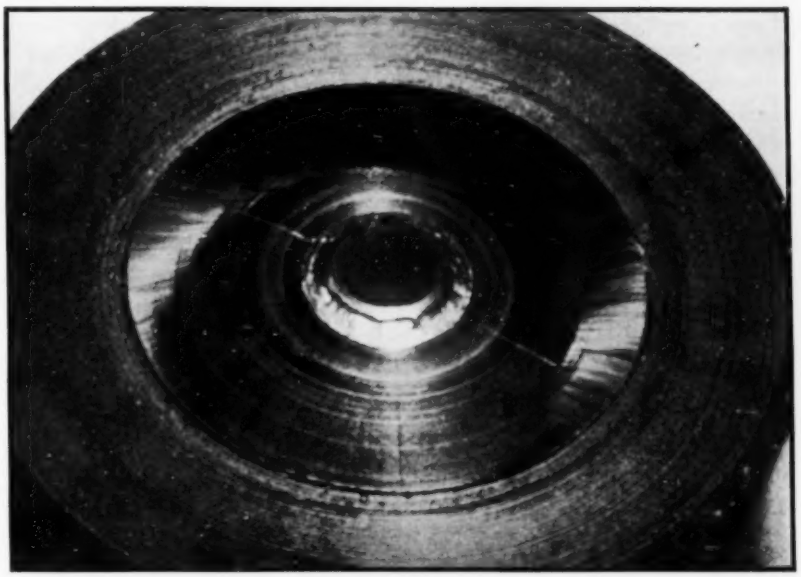

FIG. 5(b). Enlarged details of boss shown in Fig. 5(a).

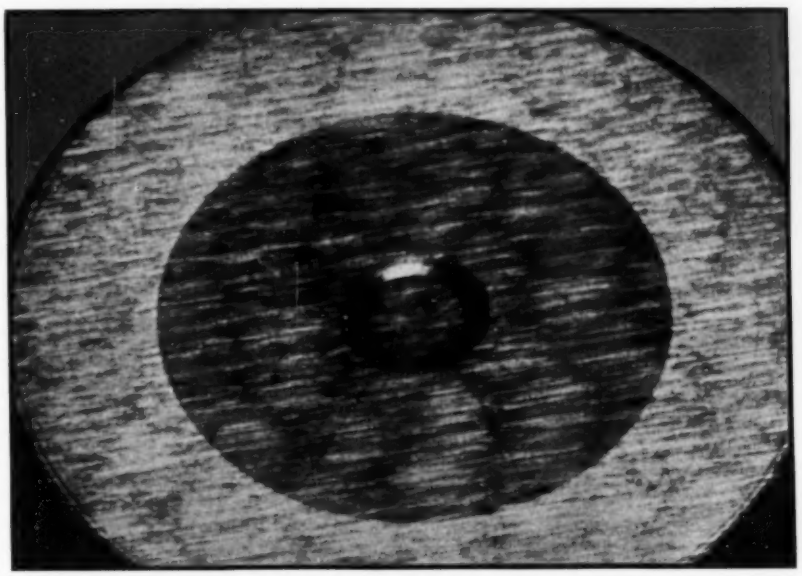

FIG. 5(c). Enlarged details of anvil shown in Fig. 5(a).

The radial cracks I believe are almost certainly formed on release of pressure. Cracks will be found in Carboloy after exposure to a maximum of only 200,000. If the cracks were formed under pressure it is difficult to visualize how crack formation could start at 200,000 and continue all the way up to nearly 400,000 without destructive rupture. The production of the cracks is doubtless

brought about in some such way as follows: With increasing pressure the boss is pushed without rupture more or less bodily into its surroundings because of their plasticity, where it remains on release of pressure in a medium which now has become brittle again and which has to crack because of the elastic expansion of a too large intruded foreign body. The same applies to the anvil. The complicated plastic flow pattern in the block under the region of contact is suggested by the photograph of the ruptured block in Fig. 6.

Having now attained such high pressures, the problem is to find what can be done with them. It must be confessed that it is not possible to do very much beyond a study of the manner of fracture under such extreme conditions; it seems that the higher the pressure the less one can do. However, it is possible to place thin sheets of any solid material between the boss and the anvil. The first effect of squeezing the Carboloy pieces together is to extrude the sheet laterally until it reaches an equilibrium thinness set by its coefficient of friction and plastic flow strength. If anvil and boss remain perfectly flat, and if the material has a low plastic flow strength like lead or tin, the final equilibrium thickness at 400,000 is pretty small, as a simple calculation shows, but fortunately the anvil and boss dish a little at their centers so that the material is sealed in between them even before the boss begins to penetrate plastically into the anvil. The stress within the trapped wafer is a hydrostatic pressure, except for a comparatively small superposed shearing stress which is limited by the plastic flow strength of the wafer. It is thus possible to produce very small and thin wafers of various solids that have been subjected to pressures up to nearly 400,000. These wafers contain enough material so that it is possible, by using recent improvements in technique, to make an x-ray analysis of their structure to find whether there has been any permanent alteration. Two examples of such permanent alteration were already known, black phosphorus and a permanent solid form of CS_2 which I have recently produced at pressures around 40,000 and temperatures around 150°C. Diamond, if it had not been capriciously formed in nature, would have been another example. The question is whether there may not be many other substances which are permanently transformed after they have been once subjected to very high pressures.

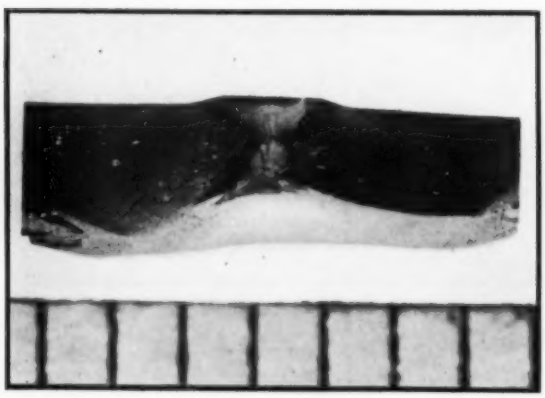

FIG. 6. Section through a ruptured boss showing the flow pattern. The scale is in millimeters.

Dr. A. B. Greninger, fortunately, has developed the difficult technique, and Mr. L. A. Carapella, under Dr. Greninger's direction, has examined with great skill samples of seven different elements which have been exposed to pressures varying between 300,000 to nearly 400,000. These were average pressures calculated as described; the actual pressures were higher because the wafer was compressed only by the flat face of the boss. The results, unpleasantly, were negative, except perhaps in one case. The x-ray pictures were not particularly easy of interpretation, because of the indefiniteness of the lines to be expected from the smallness of the sample and the fineness of grain due to the exceedingly severe mechanical working, but in all cases, except two, lines were found which coincided sufficiently well with lines of the original material. The materials examined were: graphite, sulfur, selenium, black phosphorus, thallium, indium, and tin. Indium showed no lines at all, apparently having been made amorphous by the very severe working. Tin, on the other hand, gave all the lines of the original sample; without doubt it recrystallized at room temperature after exposure to pressure. The only possible positive result was given by sulfur; the lines of the original material entirely disappeared, and a few broad lines replaced them. Either sulfur was rendered amorphous like

indium and the lines were due to some accidental impurity or else there was a permanent change.*

There is little in the way of theoretical guide as to the best materials to try for such possible transformations. Graphite was tried for obvious reasons, the next three because of their position in the periodic table, and the last three because their crystal system is different from the ordinary run of metals. However, it was recognized that with low melting metals the chances of permanent transformations are comparatively small, but thermodynamically reversible transformations are rather to be expected, and these of course could not be detected by the method used. It may perhaps be anticipated that in general the chances of finding irreversible transformations would be greater among compounds, and that the chances of success would be greater at higher temperatures. When theory has advanced sufficiently to indicate where are the most likely places to look for permanent transformations, it will be profitable to resume this exploration. The possibility of new chemical compounds is to be kept in mind, with geophysical applications.

Mention may be made of an unsuccessful attempt to produce the graphite-diamond transition at higher temperature. At 600°C, by means of a Carboloy boss and flat anvil and with no confining pressure I have applied a pressure of 75,000 kg/cm² to a wafer of single crystal graphite with no alteration.

It does not appear to me that it is possible at present to do very much else with such high pressures. Of course it would be possible to make a much more elaborate study of rupture under such extreme conditions, and this would doubtless be rewarding, although not of the most fundamental physical interest. It might also conceivably be possible to get some information about the electrical resistance of thin wafers while under pressure, but the technical difficulties are obviously great. It seems hopeless, however, to try for such other properties as compressibility on such minute quantities of material.

At lower pressures however, between 100,000 and 150,000, it appears possible to handle sufficient quantities of material to permit measurements of at least compressibility, which is possibly the most important information required at high pressures. I have made preliminary studies of the possibility of compressibility measurements in the apparatus indicated in Fig. 7. The material, confined in a cylinder small enough to enter the cylinder of the 30,000 apparatus, is subject to a confining pressure exerted by a surrounding liquid

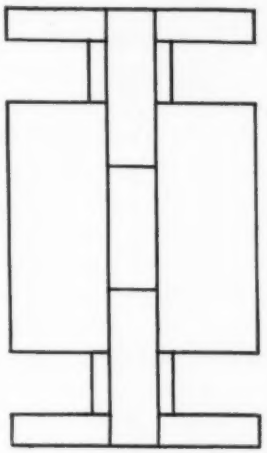

FIG. 7. Apparatus for measuring compressibilities under confining pressure.

and is further compressed by the two pistons indicated, the force on which is measured with the compressometer already described. The maximum displacement is given by the permanent distortion of lead sleeves surrounding the pistons. One of the limitations of this method is set by the strength of the pistons. The strength of the pistons is increased by the confining pressure; the amount of such increase of strength is different for different materials, so that a material not suitable for the piston under ordinary conditions might conceivably become advantageous at high confining pressure. Since there is no adequate theory, the only recourse is to an experimental examination; I report here the results of an examination of the strength of various possible materials under confining pressure, usually of about 25,000.

In my previous note I had reported compressive strengths of Carboloy pistons under 25,000 confining pressure of 200,000 or more. It now appears that this figure was much too high. The confining pressure was there exerted entirely by metallic bismuth with no true liquid, and the apparatus was very small. The result was that friction was high and the interpretation of the results difficult.

* The experiment with sulfur has been repeated; on the repetition, no lines at all could be found.

When I now look back over these original experiments with the hindsight afforded by my recent work it appears that none of the original results were inconsistent with those now obtained with the improved apparatus; it is merely that the significant discontinuity in the early curves was not the one which at that time appeared to me as most probably significant, but another one. I have now made eleven new measurements of the compressive strength of Carboloy pistons under a confining pressure of about 25,000 exerted in a true liquid, the compressive force being measured with the compressometer described above. The pistons were all of grade No. 905 Carboloy; the dimensions varied from 0.06 to 0.09 inch diameter and the length from 0.10 to 0.20 inch. Under these conditions compressive fracture occurred at one-sided compressive stresses distributed in the range between 100,000 and 125,000, making the total hydrostatic pressure attainable with such pistons between 125,000 and 150,000. All these pistons showed some plastic deformation at fracture; the maximum was a decrease of length of about 9 percent. At first I thought that the low figure compared with the first measurements might be some effect of the liquid penetrating the pores, an effect which Birch and Bancroft[5] have found is important for most rocks, and which might possibly be feared here because of the manner of formation of Carboloy by the sintering of a fine powder. To clear up this point measurements were made with the piston sealed into a metal jacket to prevent access of liquid; the jacket was thin enough not to interfere with the measurements of stress. Once a jacket of lead was used, once one of copper, and once one of bismuth; no effect was found, but the results were distributed in the same range as for the unjacketed material. I believe that there is no reason to question the essential correctness of the figure 100,000 to 125,000 for the compressive strength of this grade of Carboloy under a confining pressure of 25,000. The increase of strength over the normal figure is of the order of magnitude of the confining pressure itself; the strength apparently does not run away exponentially as has been suggested.

Steel was naturally investigated first of all for piston material. There is an increase of strength, but not by enough to give any promise. Thus a piston of glass-hard "Teton" steel was upset and permanently shortened by 9.2 percent under 48,000 one-sided compressive stress with a confining pressure of 25,000, against a normal strength of around 30,000. The increase is less than the confining pressure. The possibility of plastic deformation is noticeably enhanced by the confining pressure, but under normal conditions this steel even in the glass-hard condition will take a permanent shortening of from two to three percent. Another grade of steel gave on a single test figures perhaps 10,000 higher than the Teton steel, but there were experimental uncertainties. Other arrangements were used with short bosses on steel, but there was never sufficient increase of strength to suggest that any steel would become a serious competitor of Carboloy.

Quartz was naturally tried because of the great increase of strength under confining pressure first found by Griggs[6] and stated in my first note to have been verified by me. Measurements under improved conditions do not give nearly as high figures as at first reported. In explanation of the original high values it is to be remarked that the experiments of Griggs were made under the same conditions as mine, that is, with a small apparatus in which stress was exerted entirely by a soft metal with no true liquid. Six new tests were now made on quartz confined with a true liquid; in four of these the stress was measured with the compressometer. Specimens of single crystal quartz, cut parallel to the "c" axis gave for the compressive strength 40,000 with 25,000 confining pressure, 39,000 with 23,000 confining, and 33,000 with 16,000 confining. The fracture in all cases was complete, with reduction to a fine powder and no evidence of plastic deformation. Sosman[7] reports the strength at atmospheric pressure to be 24,000. Again it is evident that there is no such exponential increase of strength with confining pressure as has been suggested; in fact the increase appears to be linear within the error of the measurements.

Quartz glass does not behave markedly differently from the single crystal; the compressive strength of one sample under 25,000 confining pressure was 39,600.

Other minerals are known to be considerably stronger than quartz under normal conditions, and accordingly small cylinders of the most

promising of these were tested to destruction. Under a confining pressure of 25,000 the compressive strength of a spinel was found to be 62,000, of sapphire 72,000, and of tourmaline 89,000. In all cases fracture was complete, to a fine powder. Thus none of these minerals is the equal of Carboloy.

Finally, in order to proceed to the logical conclusion and be sure that nothing was missed, a small cylinder of clear diamond, 0.060 inch diameter and 0.090 inch long was fractured. The crushing strength under a confining pressure of 23,000 was 129,000. Failure was complete, to a fine powder. The Carboloy anvils by which the compressive stress was transmitted to the diamond were marked with fine lines indicating cracks in the diamond just before rupture, but there was no appreciable general indentation, showing that the plastic flow of the Carboloy produced in the experiments with Carboloy bosses does not begin noticeably at pressures below 130,000. It would thus appear that diamond may be superior to Carboloy as a piston material under confining pressure, but the superiority is too slight to justify the expense except perhaps for very special purposes. It is not so clear whether diamond would be superior in the form of bosses. Certainly no large scale single crystalline material originally brittle like the minerals tested above would be expected to permit a plastic deformation as great as that shown by Carboloy under the confining pressures reached here, and the great strength of the Carboloy bosses depends on the great range of plastic deformation. At much higher confining pressures minerals and in particular diamond may perhaps become superior. A consideration on the other side of the argument is that already at atmospheric pressure something roughly equivalent to a diamond boss is known to be very strong; if one calculates by ordinary elasticity theory the stresses in the apex of a diamond penetrator indicating a hardness of C 79 when pressed against a piece of Carboloy in a Rockwell testing machine a figure of 250,000 kg/cm^2 will be found.

Doubtless very high figures could be obtained with a haphazardly oriented aggregate of microscopic diamond grains cemented with something analogous to the bonding material of Carboloy. Unfortunately the fine grained diamond aggregates which sometimes occur in nature have an open porous structure.

For financial assistance in this work I am indebted to the Milton Fund of Harvard University. I am also indebted to my assistant Mr. Charles Chase for the skillful performance of the difficult mechanical details. For the Carboloy I am indebted, as in all this work, to the generosity of the Carboloy Company.

Bibliography

1. P. W. Bridgman, Phys. Rev. **57**, 342 (1940).
2. R. W. Goranson and E. A. Johnson, Phys. Rev. **57**, 845 (1940).
3. P. W. Bridgman, Phys. Rev. **48**, 825 (1935); Proc. Am. Acad. **71**, 387 (1937).
4. P. W. Bridgman, Proc. Am. Acad. **72**, 157 (1938).
5. F. Birch and D. Bancroft, J. Geol. **46**, 59, 113 (1938).
6. D. Griggs and J. B. Bell, Bull. Geol. Soc. Am. **49**, 1723 (1938).
7. R. B. Sosman. *The Properties of Silica* (Chemical Catalogue Co., New York, 1927), p. 481.

Theory of the Plastic Properties of Solids. III[1]

BY FREDERICK SEITZ

Randal Morgan Laboratory of Physics, University of Pennsylvania, Philadelphia, Pennsylvania

AND

T. A. READ*

Westinghouse Research Laboratories, East Pittsburgh, Pennsylvania

Part A. Single Crystals (Concluded)

THE previous two installments of this series dealt principally with the topic of slip in single crystals. We shall discuss other phases of the plastic properties of single crystals in the present installment.

3. CREEP[2]

In the range of stress below the critical shearing stress for slip, as determined by a machine capable of measuring rates of elongation only relatively crudely, solids extend or contract slowly under load. This effect, known as creep, has been studied most extensively on commercially interesting material[3] since it is highly important when metals are stressed at elevated temperatures, as in turbines and boilers. Fortunately, there are a few enlightening experiments dealing with single crystals of pure materials. We shall discuss these categorically, as in the case of slip.

It should be emphasized that there is ample room for ambiguity in the definition of creep since the term is used loosely in the literature. Thus a flow that is regarded as slip by an investigator using a very precise technique would be called creep by a practical investigator making cruder measurements. This reflects the fact that there is an intimate connection between slip and creep.

a. The connection between slip and creep

The end results of creep in single crystals usually appear to be similar to those of slip in that the elongation occurs in a manner implying relative motion along definite crystallographic planes.

One of the distinguishing features of the process of slip is the production of slip bands, so that if the processes occurring during slip and creep were identical in any given case we might expect to establish this by observing slip bands in a specimen that has undergone creep. This phase of the topic has not been investigated as fully as it should be, for the only observation on the point seems to be that of Chalmers[4] who studied creep for very small loads in crystals of tin and found no slip bands. Actually, the processes of creep and slip seem to pass continuously from one to another as the stress is raised in this metal, so that it is highly unlikely that they are essentially different effects. For this reason it is most probable that slip bands occurred in Chalmers' creep experiments but were not resolvable in an optical microscope because of the small elongation.

In this connection, it should be mentioned that creep has been observed[5] in bismuth which apparently exhibits twinning and not slip when strained beyond the elastic limit rapidly, as in ordinary tensile tests. It is possible that in this metal the creep mechanism has a closer resemblance to twinning than to slip; however, it is also possible that slip occurs along with twinning but is responsible for only a small fraction of the elongation. In the second case, the creep at low stresses could be the residue of the slip occurring at high stresses. We shall

---

* Westinghouse Research Fellow.

[1] The previous two installments of this series appeared in the February and March issues of this journal.

[2] A treatment of the topic of creep along the general lines of this section, which is, however, based on the application of Eyring's rate theory to inelastic strain rates in solids, has been given by W. Kauzmann, A.I.M.E. Tech. Pub. No. 1301 (1941).

[3] The practical aspects of creep are discussed in the book *Creep* by H. J. Tapsell (Oxford Press, 1931), and in the review article by J. J. Kanter, *A.S.M. Handbook* (1939).

[4] B. Chalmers, Proc. Roy. Soc. **156**, 427 (1936); J. Inst. Metals **61**, 103 (1937).

[5] W. Boas and E. Schmid, Zeits. f. Physik **100**, 463 (1936).

return to this point in the next section after discussing some of the properties associated with twinning.

It has often been suggested that creep and diffusion are intimately connected. This proposal seems completely untenable at present, inasmuch as the passage through a lattice plane of the types of lattice imperfections responsible for diffusion cannot result in the displacement of the part of the crystal above the plane relative to that below the plane, but can only displace the material in the plane.

In any case, we shall proceed on the assumption that creep takes place by the motion of dislocations of the same type as those introduced in the discussion of slip, and shall attempt to correlate creep experiments with single crystals on this basis. With this assumption there are two possible simple equations for the rate of strain dS/dt at any instant during a creep test. In the first place, it is possible that dislocations move relatively slowly during creep and that the creep rate is given by

$$dS/dt = N\bar{v}\lambda \qquad (1a)$$

in which N is the density of dislocations cutting across a plane that is normal to the slip plane and extends in the slip direction, $\bar{v}$ is the mean velocity with which they move, and λ is the slip distance associated with the passage of one dislocation. Since λ is a constant, presumably equal to a fundamental lattice spacing in the slip plane, variations in the creep rate should imply variations in N and $\bar{v}$.

In the second place, it is possible that dislocations move a distance L almost instantaneously and then become stuck, so that their rate of motion is not actually detectable. In this case, their rate of generation rather than their rate of motion will determine the creep rate. In fact, the creep rate will be given by the equation[6]

$$dS/dt = L\lambda dN/dt. \qquad (1b)$$

If Eq. (1b) is valid, creep should be observable as a slow rate of flow only when dislocations can be generated, for otherwise the few dislocations present will move almost instantaneously and the corresponding elongation would be instantaneous. Now, as we shall see, a type of creep is observable at temperatures so low that dislocations should not be generated if our picture is correct. This indicates that Eq. (1a) is valid at least in these cases, and we shall begin our discussion by using it. On the other hand, as we shall see below, Eq. (1b) has certain advantages for correlating creep measurements at higher temperatures. Thus it is possible that Eq. (1a) is valid when dislocations cannot be generated, whereas Eq. (1b) is sometimes valid when they are. It is also possible, of course, that the processes should be combined in intermediate cases.

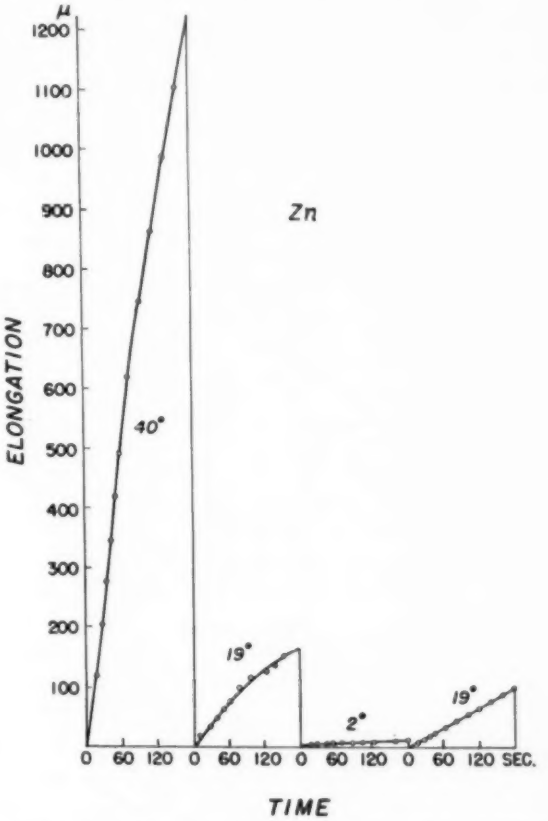

FIG. 38. The creep of zinc at constant load for temperatures near room temperature. It may be seen that the initial rate is more rapid than the steady-state one and that the latter decreases rapidly with temperature. (After Boas and Schmid.)

b. The two creep ranges

The process of creep usually may be divided into two ranges when regarded as a function of

[6] This equation was suggested first by Kochendörfer as we shall see later (cf. reference 12).

time. These ranges are clearly shown[7] in Fig. 38 for creep in single crystals of zinc and cadmium in the borderline region between slip and creep. In both of these cases, the elongation *versus* time curves are characterized by a rapid rise at short times for the virgin material and a steady flow at long times. This suggests the division shown

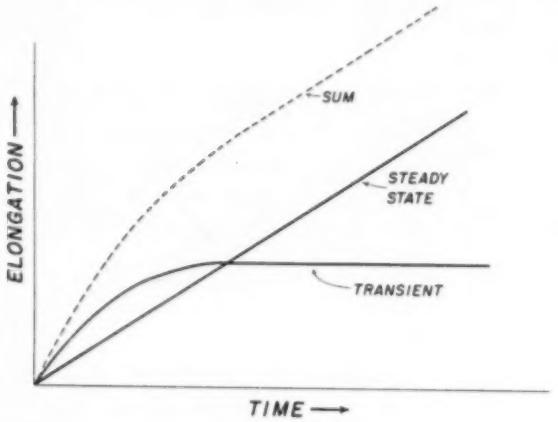

FIG. 39. Hypothetical division of the creep curve into transient and steady-state parts.

in Fig. 39 in which the strain *versus* time curve is resolved as the sum of a linear curve passing through the origin and a curve that starts linearly at the origin and asymptotically approaches a constant value. From the standpoint of velocity of flow, the second curve is analogous to a transient since its contribution to the velocity is negligible at long times. The existence of this transient is recognized in practical work by reference to the "short time creep rate" and the steady or "long time creep rate." We shall refer to the two components as the transient and steady-state parts.

Some investigators have obtained creep curves which cannot be analyzed in the manner of Fig. 39. Figure 40 shows a time *versus* strain curve obtained by Miller[7] on a zinc crystal at room temperature under the stress of 8 g/mm². It is to be noted that this stress is much smaller than those used by Boas and Schmid.[7] Miller's creep curve shows the normal behavior for the first 60 hours, that is, a gradually decreasing strain rate, but then the strain rate begins to *increase*. Somewhat similar results were found by Gensamer and Mehl[8] on iron crystals and by Burghoff and Mathewson[8] on α-brass crystals; however, the initial period of decreasing strain rate was absent in these materials. The elongation *versus* time curves obtained on these crystals are S-shaped, as shown in Fig. 41, which is taken from the paper by Burghoff and Mathewson. Before we discuss the S-shaped creep curve let us consider the more frequently encountered type of creep curve shown schematically in Fig. 39.

The steady-state creep rate is strongly dependent upon temperature, being greater at high temperatures than at low. It has been analyzed[5] carefully in several metals and generally appears to obey the law

$$\text{Rate} = A \exp(-\epsilon/kT) \qquad (2)$$

in which A is a constant, etc. Experimental values of ϵ are given in Table V. The universal

TABLE V. *Value of the activation energy ϵ for the steady-state creep rate. (Expressed in electron volts).*

	Zinc	Cadmium	Bismuth	Tin
ϵ	0.73	0.66	0.87	0.75

validity of this law has been questioned by Boas and Schmid who showed that the creep rate of zinc and cadmium is far larger at liquid-air

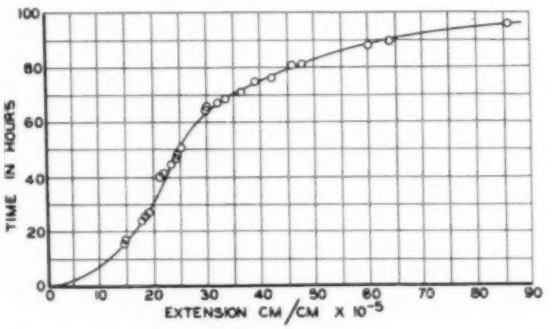

FIG. 40. The creep of a zinc single crystal at 25°C caused by a resolved shearing stress on the slip plane of 8.0 g/mm². (After Miller.)

temperature than is to be expected from Eq. (2) on the basis of room temperature measurements of the steady state. In the writers' opinion their conclusion is not justifiable, for a survey of their

[7] W. Boas and E. Schmid (reference 5). Creep curves at low stresses have been obtained by R. F. Miller, Trans. A.I.M.E. **122**, 176 (1936).

[8] M. Gensamer and R. Mehl, Trans. A.I.M.E. **131**, 372 (1938); H. Burghoff and C. Mathewson, A.I.M.E. Tech. Pub. No. 1288 (1941).

experimental results indicates that they probably measured only the transient at liquid-air temperatures and that the steady-state rate actually was zero (see Fig. 42). It should be added that these experiments indicate that the transient creep rate is much less sensitive to temperature than the steady-state rate.

Creep experiments in which the transient occurs have also been carried out by Chalmers.[4] He made very sensitive tests on single crystals of tin at room temperature and found curves of the type shown in Fig. 43, which seem to show that the steady-state rate becomes zero for sufficiently small stresses. The heavy curves show the fractional elongations as functions of time for two single crystals of tin, whereas the lighter lines show the ratio of the rate of elongation to the elongation in the two cases. The interesting features of the latter two curves are first that they are linear, at least near the origin, which implies an exponential slowing down of the rate of elongation with increasing time, and second that they approach zero, which shows that the elongation stops.

It is interesting to speculate on the origin of the two components of the creep curve. Let us begin by considering the creep at very low temperatures and low stresses where only the transient occurs. In this case, we cannot expect new dislocations to be generated if the picture of their formation developed in the previous section

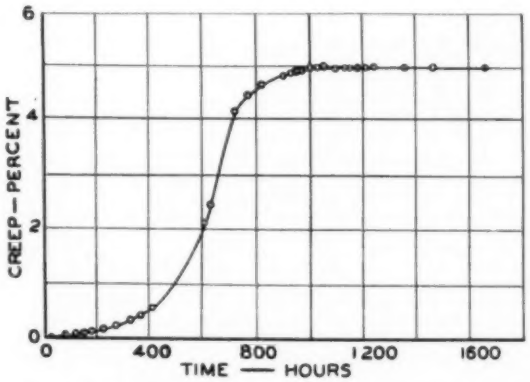

FIG. 41. The creep of a single crystal of 70–30 brass at 25°C under a maximum resolved shearing stress of 1100 g/mm². (After Burghoff and Mathewson.)

is correct, so that creep can occur only as a result of motion of dislocations already present. Under the action of the stress and what little

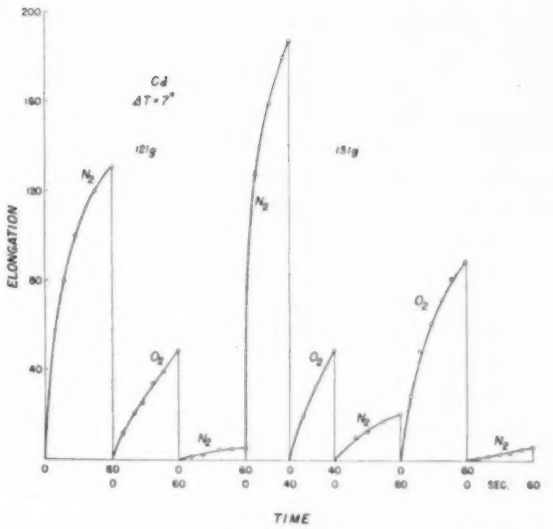

FIG. 42. The creep of two specimens of cadmium at temperatures near 90°K. The liquid-nitrogen bath was 7°K lower than the liquid-air bath. The ordinate is in microns. The elongation was carried out at a given temperature for one minute for three successive runs on the first specimen (load 121 g) and for five runs on the second (load 151 g). It may be seen that the rate of elongation decreases to practically zero at the end of several elongations.

thermal energy is available some of these dislocations will move until they meet an obstacle too large to be overcome and will then stick so that the creep eventually ceases. We may visualize this sticking process as occurring in stages, some of the dislocations moving larger distances than others. Viewing this mechanism from the standpoint of Eq. (1a), we may say that the average velocity $\bar{v}$ decreases to zero as creep proceeds. The initial rate of creep then measures the average velocity of flow of all of the dislocations that start moving.[9]

If the stress is raised higher and higher, a fraction of the dislocations may be assisted past regions where they were stuck and the motion of this fraction may impart an increased creep rate to the specimen. If the temperature is so low that no new dislocations can be formed, even these dislocations should eventually become

[9] Recent experiments (as yet unpublished) on internal friction in copper by A. W. Lawson indicate that the internal friction of plastic origin may be increased at low temperatures by applying static stresses no larger than those needed at room temperature. These results seem to indicate that the type of dislocation required to account for internal friction may be generated with comparative ease even at low temperatures. It is possible, in the case of copper, that these are short dislocation nuclei and not full-length dislocations of the type needed to account for slip or extensive creep.

stuck and the elongation should stop. The only really low temperature creep measurements are those of Boas and Schmid discussed above, and these correspond to a single transient for the range of stress investigated. Actually, more extensive flow should be possible at higher stresses in the metals they studied, for extensive slip can be induced in them, as we saw in Section 2. The creep observed in zinc and cadmium at room temperature undoubtedly is accompanied by the production of dislocations and will be discussed below.

The initial creep rate has been determined as a function of stress for several specimens of tin by Chalmers, the results being shown in Fig. 44. It may be seen that the rate increases linearly with stress for stresses below 100 g/mm², and then increases more rapidly. The more rapid rates measured by Chalmers are within a factor ten of the rates measured by apparatus designed for ordinary slip measurement, so that Fig. 44 covers practically the entire range of creep. In fact, the value of the critical shearing stress for tin listed in Table II (first installment), namely 130 g/mm² is indicated by the vertical arrow in the figure.

It should be mentioned at this point that the creep with limited extension is observed only for the range of stress of Fig. 44 in which the velocity varies linearly. This region has been designated as the α-range by Chalmers. Both of the curves shown in Fig. 43 correspond to this range. An interesting and important fact associated with this range is that the total extension appears to be practically independent of the load and is about 10^{-5}. In the region above the knee of the curves shown in Fig. 44, which Chalmers designates as the β-range, the steady-state rate is finite for given load. Measurements in this range were carried out for extensions as large as 10^{-3}, which is the limit that could be attained with Chalmers' apparatus.

The linear relation between creep rate and stress is readily explained qualitatively if we assume that in the α-range the barrier between two successive minima for motion of dislocations is lowered in the direction of the applied stress by an amount $-a\sigma$ and is raised in the opposite direction by an amount $a\sigma$, where a is a positive constant. With this assumption, the probability per unit time that a dislocation will jump in the direction of the field by a distance separating two successive minima of potential is

$$p_+ = \frac{1}{\tau} \exp\left(-(\epsilon_0 - a\sigma)/kT\right)$$

in which τ is the time required for the transition from one equilibrium position to the next in the event that the dislocation receives the required activation energy. Reasoning from our model, we might expect τ to be of the order of an atomic oscillation time, that is 10^{-13} sec. Similarly, the probability for a transition in the opposite direction is

$$p_- = \frac{1}{\tau} \exp\left(-(\epsilon_0 + a\sigma)/kT\right).$$

The mean velocity with which a dislocation drifts in the direction of the field then is

$$\bar{v} = \lambda(p_+ - p_-)$$

or

$$\bar{v} = \frac{\lambda}{\tau} \exp\left(-\epsilon_0/kT\right) \sinh\left(a\sigma/kT\right). \qquad (3)$$

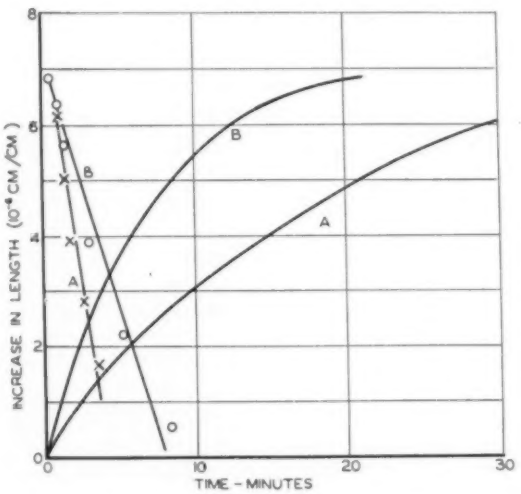

FIG. 43. The creep curves at low stress for two specimens of tin. (After Chalmers.) The applied shearing stress was 120 g/mm² in both cases. Curves *A* are for Chempur tin and curves *B* for Williams-Harvey tin. The heavier curves are the elongation *versus* time curves whereas the other curves are the logarithmic derivatives of these, that is $dl/dt/l$, where l is the elongation.

Substituting this in Eq. (1a), we obtain

$$\frac{dS}{dt} = \frac{N\lambda^2}{\tau} \exp\left(-\epsilon_0/kT\right) \sinh\left(a\sigma/kT\right).$$

For small values of $a\sigma/kT$ this equation reduces to

$$\frac{dS}{dt}=\sigma\frac{N\lambda^2 a}{kT\tau}\exp(-\epsilon_0/kT). \qquad (3a)$$

Possible origins of the deviations from this linear relation will be discussed later in the section.

The type of creep shown in Fig. 44 should be associated with an internal friction of the type discussed in part *d* of Section 2. Moreover, if the interpretation of the internal friction of pure single crystals given there is correct, it should be the main source of internal friction. The range of strain amplitude corresponding to the linear part of the curves in Fig. 44 extends from zero to 10^{-5}. This range is actually larger than that used by Read in the work described in Section 2. It may be shown that the decrement should be independent of amplitude for constant frequency in the α-region of Fig. 44, and an estimate of this decrement gives a value of about 10^{-9} for a frequency of ten thousand cycles/sec. This value is obtained in the following way. In the linear portion of the curve the creep rate r satisfies the equation

$$r=\alpha\sigma, \qquad (4)$$

where $\alpha\sim 5\cdot 10^{-16}$ cm²/dyne-sec. Thus the rate at which energy is dissipated is $\alpha\sigma^2$, or the energy dissipated per cycle per unit volume is

$$\alpha\sigma^2/2\nu,$$

where ν is the frequency and σ now denotes the stress amplitude. The ratio of this to the elastic energy is

$$\frac{\alpha\sigma^2}{2\nu}\Big/\frac{\sigma^2}{2E}=\frac{\alpha}{\nu}E, \qquad (5)$$

where E is Young's modulus, which is $5\cdot 10^{11}$ dynes/cm². Substitution of the appropriate quantities leads to values of the order of 10^{-9}. This result indicates that the internal friction of Chalmers specimens should be very low for the α-range of amplitude. Read found the internal friction of his own specimen to be several orders of magnitude larger ($6.9\cdot 10^{-5}$). The source of this discrepancy is hard to place on the basis of present information since both creep and decrement values are not available for the same specimen and range of amplitude. In the first place it is possible that the discrepancy implies

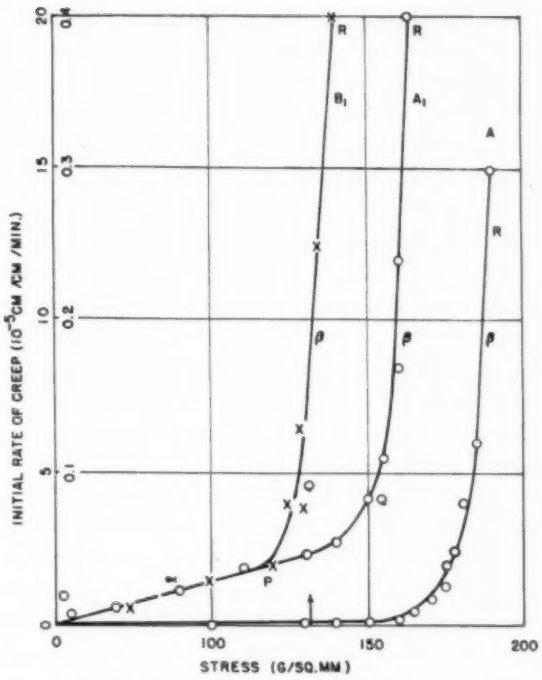

FIG. 44. The dependence of the initial creep rate upon stress for two specimens of tin. Curves A_1 and B_1 have the right-hand scale of ordinate, curve A has the left-hand one. A_1 and A were obtained for Chempur tin, curve B_1 for Williams-Harvey tin. The vertical arrow indicates the critical shearing stress as measured by other workers.

an error either in the suggested mechanism of internal friction or in the treatment of α-creep; in the second, it is possible that the tin single crystals on which Chalmers made his creep measurements had markedly different properties from those measured by Read. The first of these alternatives is probably the more important. This is indicated first by the fact that, according to Chalmers the amount and rate of creep in the α-range are not affected by the previous history of the specimen, whereas Read found that the internal friction is sensitive to annealing or, on the other hand, to slight amounts of cold work. Moreover, the linear dependence of creep rate on stress found by Chalmers should give rise to a decrement independent of the amplitude of vibration, as remarked above. Actually Read found a rapid increase of decrement with amplitude for stresses smaller than those used by Chalmers. We conclude, then, that the mechanisms responsible for α-creep and for internal friction must differ in some essential way (see footnote 9).

The constant α in Eq. (3) may also be determined from the creep data obtained by Miller[7] on single crystals of zinc. The average creep rate for the first 20 hours of the curve in Fig. 40 gives $\alpha = 8 \cdot 10^{-16}$ cm²/dyne-sec., a value only slightly different from the one we obtained above from Chalmers' data on tin. If we substitute this value of α in Eq. (5) we again obtain a value of the decrement of about 10^{-9}, which is, of course, much smaller than the observed internal friction (see for example, Figs. 16 and 18 in installment I). This large difference in inelastic strain rates in zinc, observed in creep tests on the one hand and internal friction measurements on the other, might arise because the rate determining process in the creep test is the formation of dislocations, whereas most of the energy dissipation in the vibrating crystal results from the irreversible motion of dislocations already present. One piece of evidence which supports this viewpoint is the fact that the creep of the zinc crystal does not stop but apparently continues indefinitely.

Boas' and Schmid's measurements show that the initial rates of creep in zinc and cadmium at liquid-air temperature are very nearly the same as those at room temperature, even though the steady-state value is nearly zero at low temperatures for the loads they employed. If this is true, it indicates, according to our picture, that v in Eq. (1a) is very nearly independent of temperature. It is also possible, of course, that the initial values of N were higher at low temperatures, but we shall not consider this possibility. We may note here that this result is in disagreement with Eq. (1b), for we should expect the rate of generation of dislocations to be very sensitive to temperature. According to Eq. (3a), we should conclude from the temperature independence of $\bar{v}$ that ϵ_0 is very small, of the order of 0.01 ev or less. This is in agreement with previous assumptions that the activation barrier for motion of dislocations is small.

Let us now make an estimate of τ, the time required for the transition of the dislocation from one equilibrium position to the next, on the basis of Chalmers' measurements of the creep of tin in the α-range. Combining (3a) and (4) on the assumption that ϵ_0 is small, we obtain

$$\alpha = N\lambda^2 a/kT\tau.$$

If we set $\alpha = 5 \cdot 10^{-16}$, as we obtained above, and set $\lambda^2 = 10^{-15}$ cm², we obtain

$$a/kT = 5 \cdot 10^{-1}\tau/N.$$

Now σa should be of the same order of magnitude as ϵ_0 when σ is near the critical shearing stress for very low temperatures since, by assumption, the applied stress is then large enough to make the dislocations move without the aid of temperature. Thus $\sigma_c a/kT$ should be near unity at liquid-air temperature. Since $\sigma_c \sim 10^7$ dynes/cm², we obtain from the last equation

$$5 \cdot 10^6 \frac{\tau}{N} \sim 1. \qquad (6)$$

The value of N is about 10^{12} cm^{-2} in the most work-hardened state since about one atom in a thousand is then near the center of a dislocation (see Section 2, Part *f*). We have no basis on which to make a really accurate estimate of this number in the carefully annealed state, but we can make a judicious guess. According to Taylor's theory, the critical shearing stress varies as N^2. Since this stress drops by at least a hundred during annealing from the most hardened state, we can set 10^{11} as an upper limit for N. This variation of σ_c is observed in aluminum, but not in zinc and cadmium, in which it appears to vary as N. Thus in these cases we should set the upper limit to N for the annealed state as 10^{10}. We shall tentatively take 10^8 as a plausible value. In this case, τ derived from Eq. (6) is 20 sec., which at first sight seems unreasonably large by a very large factor, for, as mentioned above, we might expect it to be nearer 10^{-13} sec. Moreover, we can satisfy Eq. (6) with a value of τ as small as 10^{-13}, only by assuming that N is much less than unity, which is far too small to account for the limiting value of extension of several microns observed in the experiments. We may see this from the fact that if each dislocation moves a distance L, the total strain is $N\lambda L$. Thus if L takes the maximum possible value of 1 cm for a specimen of ordinary size, N should be at least 10^5. On the other hand, if L is of the order of a micron, N should be at least 10^9.

These estimates indicate that the quantitative aspects of creep measurements may not be consistent with the picture of creep we have been

discussing.[10] Moreover, the situation is not saved by using the picture associated with Eq. (1b), for, as we mentioned above, the initial creep rate is not sufficiently temperature sensitive at liquid-air temperatures according to the measurements of Schmid and Boas. In spite of these difficulties we shall continue employing the theory of dislocations, since we cannot say with certainty that the theory is at fault. It is possible, for example, that the time needed for the motion of a dislocation from one equilibrium position to another is much longer than the atomic relaxation time because such motion requires the cooperative action of atoms along the entire dislocation line. A plausible method of testing this possibility is as follows: The internal friction should decrease more rapidly than $1/\nu$ with increasing frequency (the dependence given by Eq. (5)) for frequencies greater than $1/\tau$ since the dislocations then would not have sufficient time to jump from one equilibrium position to another in a single cycle. If the values of τ estimated from Eq. (6) are valid, this frequency should lie in the experimentally attainable range. Preliminary data on the frequency dependence of the internal friction of copper crystals over the range 30–100 kilocycles indicate that the frequency variation is slight and thus that τ must be considerably smaller than 10^{-5} sec. in this metal.

The deviation from linearity that occurs in the β-range of Fig. 44 cannot be fitted with a simple function of the form $\sinh(a\sigma/kT)$; however, this part of the curve could be fitted with the hyperbolic sine of a quadratic function of the type $(a\sigma+b\sigma^2)/kT$, in which both a and b are positive constants. At first sight, it would seem that this result could be obtained by taking into account the lowering of the activation barrier by powers higher than the first in σ. Unfortunately, it turns out that the sign of b derived by considering the lowering of a barrier that has the form of an inverted parabola near its top is opposite to that of a.

In searching for other explanations of the β-range the following possibilities occur:

1. This range may be connected with the onset of generation of dislocations. As we shall see below, this assumption would explain why a steady state with a finite rate of creep occurs in the β-range, but it does not explain the more rapid initial velocity of creep in tin unless we assume that the newly generated dislocations move an appreciable distance and become stuck in a very short time, so that there is an additional creep component of the type corresponding to Eq. (1b).

2. It is also possible that the β-rise in creep rate is connected with the release of dislocations which are already present in the crystal and are stuck. This type of explanation evidently faces a number of difficulties, for, in the first place, it is necessary to explain why all dislocations do not behave in a similar way, and, in the second, it is necessary to explain why the number released should vary in just such a way as to give the sharp rise of the β-part of the curve. We saw in Part *c* of Section 2 that the rise in internal friction of copper with amplitude could be explained by assuming that the number of mobile dislocations increases with increasing stress, but it seems unlikely that that effect and the present one can be connected, for the range of stress used in Read's work corresponds to the part of Fig. 44 in the immediate vicinity of the origin.

In any case, more extensive work of the type carried out by Chalmers should prove very valuable in clearing up fundamental questions of this type. It is interesting to note that if a sharply rising β-range of creep occurs in all metals, it should be possible to define an unambiguous critical shearing stress in terms of the knee of creep curves of the type of Fig. 44.

When the conditions of temperature and stress are such that dislocations can be formed, we may expect a steady-state creep rate in which dislocations are generated and annihilated at the same rate. If R_g is the rate at which they are formed and βN is the rate at which they are annihilated, the equilibrium density of dislocations may be determined from the condition

$$R_g=\beta N.$$

If β is independent of N, as it would be if the probability of annihilation were independent of

[10] An analysis of the creep rates of polycrystalline metals by W. J. Kauzmann, which was presented at the February 1941, meeting of the A.I.M.E., indicates that this difficulty with the characteristic jump time for the atomic systems whose motion gives rise to creep appears very generally.

the density of dislocations, N would be determined by the equation

$$N = R_a/\beta.$$

On the other hand, if β is dependent upon the density, as it would be if annihilation occurred by the union of pairs of dislocations of opposite sign, the equation for N would be more complicated. Thus if $\beta = bN$

$$N = (R_a/b)^{\frac{1}{2}}.$$

Since both N and $\bar{v}$ in Eq. (1a) could be dependent upon temperature through a Boltzmann type function in this steady-state case, it follows that ϵ in Eq. (2) should generally be a composite activation energy if Eq. (1a) is correct. On the other hand, if Eq. (1b) is correct in this range, the activation energy should be just that for generation of dislocations since dN/dt is the only temperature dependent quantity in (1b).

Now the experiments on internal friction indicate that dislocations in zinc are readily formed and destroyed at room temperature, and make it seem likely that the steady-state creep rate in zinc and cadmium is of the type considered here. Since tin will resoften at room temperature, the same conclusion seems probable in the case of this metal.

The transient creep component requires additional consideration in the case in which dislocations are formed. Let us suppose, first of all, that a certain number of dislocations are present initially and that the initial creep rate is the same as it would be if dislocations were not formed. In this event N in Eq. (1a) will increase with time and we should expect the creep rate to increase with time if $\bar{v}$ is unaffected by the rise in N, for the same reason that the internal friction increases with time in Read's experiments on the internal friction of zinc. When the density of dislocations becomes sufficiently high, dislocations will inhibit one another and v will decrease. If v decreases faster than $1/N$, the creep rate will slow down until the steady state described previously is reached, that is until dislocations are destroyed at the same rate as they are formed. Actually, we should expect v to decrease very rapidly when the density of dislocations is such that hardening occurs, for the interaction of dislocations will then affect the activation energy required for their motion. Now we saw above that the creep rate does not usually increase in the early stages of flow in zinc, cadmium and tin, but is instead, a continuously decreasing function (see Fig. 42). This may be explained by assuming that the initial density of dislocations in the specimens used was so high, as a result of previous handling, that $\bar{v}$ is a decreasing function of N at start of the experiments. This assumption does not lead us to contradictions with Read's results, for he worked in a far lower range of stress than was employed in the creep experiments. On the other hand, initially increasing creep rates are observed in some cases, an example of which is shown in Fig. 41. It may be that the explanation of this effect is that suggested above.

It is interesting to observe that if annihilation of dislocations does not occur, that is, if the material is not in the resoftening range of temperature, N will increase and the creep rate for constant load will approach zero because of the decrease in $\bar{v}$. In other words, the material will flow until the critical shearing stress reaches the applied stress.

On the other hand, if we assume that Eq. (1b) is valid, the initial creep rate is due to the generation of dislocations. Unless we assume either that dislocations already present influence the rate at which new ones are formed, or that L in Eq. (1b) decreases with increasing density of dislocations, it is difficult to understand why the creep rate should decrease with time.

The fact that the rate of flow is a function of stress in tin suggests that the stress-strain curve should usually be dependent upon the velocity with which the strain is induced in slip experiments that are carried on at a temperature where creep is important, that is, above the resoftening temperature. Such velocity dependence has been observed in zinc by Orowan[11] and in naphthalene by Kochendörfer.[12] The work of the latter is very interesting and important, for he carried out a complete set of room-temperature slip and creep experiments for stresses near and above the critical shearing stress. He found that glide and slip occur in the organic crystal in a manner resembling, in all essential respects, the

[11] E. Orowan, Zeits. f. Physik **89**, 605, 615, 634 (1934).
[12] A. Kochendörfer, Zeits. f. Krist. **97**, 263 (1937); Zeits. f. Physik **108**, 244 (1938).

behavior of metals and ionic crystals, the plastic flow being determined by the critical shearing stress in the slip planes. Average stress-strain curves for several velocities covering a 125-fold range are shown in Fig. 45. The curves are obtained by taking the mean of measurements on a number of crystals, the individual curves being less smooth. Although naphthalene resoftens at room temperature, the resoftening time was sufficiently long that extensive measurements could be carried out before appreciable resoftening would have taken place in an unstressed crystal. From this work Kochendörfer has drawn the following conclusions:

1. The dependence of the stress-strain curves on velocity is not directly related to the resoftening that ordinarily occurs during the extension, for the velocity dependence was found even when the resoftening in a hardened stress-free specimen was negligible in the time required for extension.

2. The velocity of flow cannot be represented as a single function of stress and strain for all experimental conditions, that is,

$$dS/dt \neq f(\sigma, S).$$

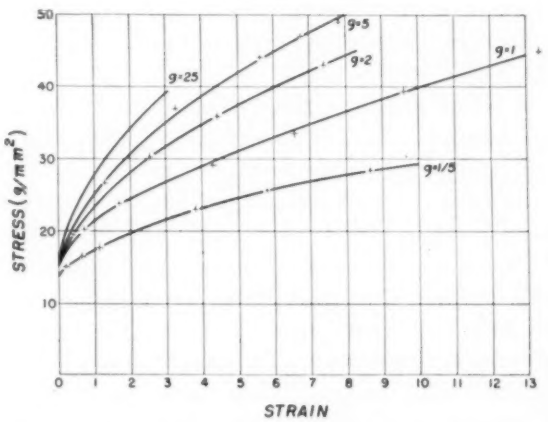

FIG. 45. Stress-strain curves in naphthalene for various velocities of flow. These curves are averages of somewhat less regular experimental curves. (The unit velocity of flow corresponding to $g=1$ is 3.1 per hour.)

From the standpoint of our Eq. (1), this is equivalent to the statement that $N\bar{v}$ is not a single-valued function of the stress and strain, but generally will depend upon the condition under which σ and S were attained. This observation does not necessarily disprove that N is a single-valued function of S, as postulated in Taylor's theory, for $\bar{v}$ may be the function "at fault." However, the results strongly suggest that the distribution of dislocations is very different depending upon whether the strain is achieved rapidly or slowly.

TABLE VI. *Increments of stress required to change the velocity of strain from u_1 to u_2. (The values are given in g/mm². The unit of u is a strain of 3.1 per hour.)*

u_1	5	1	$\frac{1}{5}$
u_2			
0	0.95	0.43	0.17
$\frac{1}{5}$	0.78	0.26	
1	0.52		

3. In addition to this purely negative conclusion, Kochendörfer found evidence for the following experimental law: When a specimen has reached a given state of elongation, the stress required to make it flow with velocity $u=dS/dt$ is given by an equation of the form

$$\sigma = \tau + \varphi(u),$$

where τ is dependent upon the specimen and its previous history and $\varphi(u)$ is a fixed function for all specimens. Or, expressed in another way, the change $\Delta\sigma$ in stress required to change the velocity of flow from u_1 to u_2 is independent of the state of the specimen. Table VI contains a list of values of $\Delta\sigma$ for several velocities.

Kochendörfer attempted to interpret these results in terms of dislocation theory on the basis of the following assumptions:

1. Dislocations generated at a boundary move almost instantaneously to an opposite boundary, where they become stuck. According to this picture, the rate of flow is determined almost entirely by the rate at which dislocations are generated, so that Eq. (1b) is valid.

As we mentioned in the introductory paragraphs, this assumption is not necessarily in complete contradiction with our Eq. (1) for it is possible that our equation is applicable for low stresses, below or near the critical shearing stress, whereas Eq. (1b) is valid at stresses well above the critical shearing stress, with which Kochendörfer is principally concerned. In fact we saw previously that the explanation of the facts surrounding the β-range of Chalmers' creep curves on tin may require a similar assumption. If our picture of formation of dislocations is correct, Eq. (1b) should not be applicable at low

temperatures where dislocations cannot be generated. Kochendörfer uses it even in this range for metals, however, making the assumption that, as a result of stress magnification, dislocations can be generated at any temperature by stresses considerably smaller than the shearing stress for an ideal lattice.

2. Dislocations influence the hardening of the material in the way postulated by Taylor.

3. In a work-hardened state of the crystal, the effective stress σ_e for producing dislocations, that is, for lowering the activation energy ϵ_1 for generating dislocations by an appreciable fraction, is less than the applied stress by an amount τ, where τ is related to the hardening influence of the dislocations present. In other words

$$\sigma_e = \sigma - \tau.$$

Since dN/dt is a function of σ_e and the temperature, it follows that for given τ, that is, for a given state of the specimen, dS/dt is determined by variations in σ_e, that is by variations in $(\sigma - \tau)$.

This assumption, that dislocations present influence the rate of production, is necessary if Eq. (1b) is to be used, as we have seen previously. Kochendörfer makes no attempt to explain the manner in which this influence occurs.

4. The annihilation of dislocations requires a large activation energy, of the order of 0.9 times ϵ_1. Moreover, this activation barrier may be decreased by stress in a manner analogous to the way in which the activation energy ϵ_1 is lowered, the stress effective for this being not the average stress σ but the reduced stress $(\sigma - \tau)$, as in the case of generation of dislocations. According to this assumption the rate at which dislocations are annihilated is not simply a function of temperature, but is a strongly increasing function of stress, for stresses larger than τ.

It is easy to see in a qualitative way from assumption (3) that the applied shearing stress should increase with increasing velocity of flow and with increasing hardness of the specimen. Moreover, it is easy to see from assumption (4) that the number of dislocations present at the end of a certain elongation will be dependent upon the stresses applied during the elongation. More quantitative application of this theory shows that it furnishes a good correlation of much of the available experimental material on rapid flow, not only for naphthalene, but for metals as well.

For reasons mentioned above, a picture built on these assumptions is not entirely consistent with the framework we have been constructing in this series of articles. It is possible, however, that the differences in viewpoint, particularly those concerning the generation of dislocations at low temperatures will be reconciled during the future development of the subject.

e. Discontinuities occurring during creep

Joffe[13] first observed that plastic flow in rock-salt occurs discontinuously at temperatures above 250°C, the individual extensions being of the order of microns. Generally speaking, the jumps decrease in size with decreasing temperatures and increase in frequency with increasing temperature, so that they are not observable over the entire range of temperature. The same effect has subsequently been observed in the metals aluminum,[14] α-brass,[14] and zinc.[15] In the case of zinc, Schmid and Valouch showed conclusively that the effect is associated with slip and not with twinning, which, as we shall see in the next section, gives rise to discontinuous flow of a different type.

It seems possible that this effect is related to the heating effects accompanying cold work, that is, that the heat generated during the motion of one dislocation furnishes part of the thermal energy required for the next, and so forth. Since the energy required to produce cold work is about ten times higher than the stored energy (cf. Section 2, Part *f*) it follows that the moving dislocation is the source of considerable thermal energy. This interpretation is in qualitative agreement with the fact that the effect is not observable at sufficiently low temperatures.

4. Twinning

If a number of neighboring equivalent atomic planes slip past one another by distances equal to an integer multiple of a lattice spacing, the

[13] A. Joffe, *The Physics of Crystals* (McGraw-Hill Book Company, Inc., New York, 1928).
[14] M. Classen-Nekludowa, Zeits. f. Physik **55**, 555 (1929).
[15] E. Schmid and N. A. Valouch, Zeits. f. Physik **75**, 531 (1932).

symmetry of the crystal is not altered and the specimen remains a single crystal. This type of change seems to occur during slip and creep. On the other hand, if a sequence of neighboring atomic planes move by one another by distances not equal to an integer multiple of a lattice spacing, the region in which the motion takes place will not retain its symmetry. This type of change occurs in the process of twinning. In this case the relative motion of planes is not random, however, but takes place in such a homogeneous fashion that the region in which the distortion occurs remains a single crystal even though it does not have the same orientation as the original crystal. Since the new orientation may be derived from the old by rotation or reflection, the new crystal is commonly called a twin.

In the simplest case of twinning, a sequence of parallel neighboring planes move past one another by the same relative distance. Thus in face-centered cubic metals twinning commonly occurs by the motion of a sequence of (111) planes through a relative distance equal to one-third of a translation (Fig. 46). In this case the new orientation may be derived from the old by

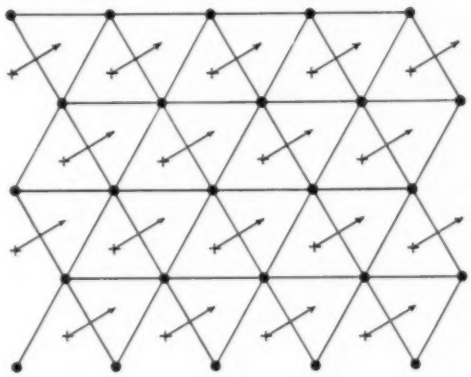

FIG. 46. The relative displacement of atoms in neighboring (111) planes of face-centered cubic crystals during twinning. The crosses and dots represent planes displaced from one another in the vertical direction.

reflecting in a plane parallel to the plane of motion. Twinning does not always occur in such a simple manner, however. For example, Chalmers[16] has shown that twinning in tin probably occurs by the motion of two different systems of planes through different distances.

When twinning is produced by the application

[16] B. Chalmers, Proc. Phys. Soc. **47**, 733 (1935).

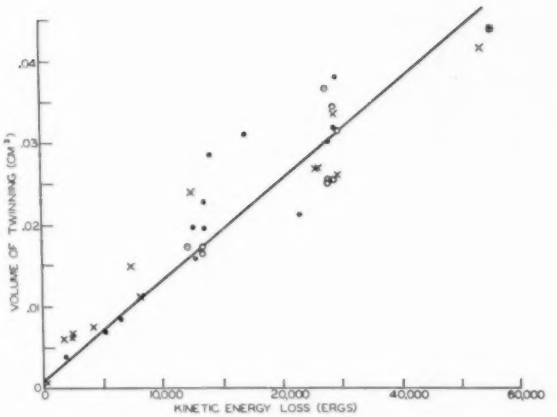

FIG. 47. Relation between the volume of twinned material (tin) and the kinetic energy transferred to the specimen during impact. Since the two are proportional, Chalmers concludes that a critical amount of elastic energy must be available to produce twinning.

of static load, which is possible only in a few substances, it seems to require[17] the application of a shearing stress of the order of 10^7 dynes/cm^2, although there is not the same amount of conclusive evidence for this point as in the case of slip.

Chalmers[16] has suggested, as a result of extensive work on twinning in tin by means of impact, that twinning requires the existence of a definite amount of available elastic energy per unit volume (Fig. 47). In the case he studied, it was found that this threshold energy is $8 \cdot 10^5$ ergs/cm^3, which would be attained by a stress of the order of magnitude 10^8 dynes/cm^2. Most of this elastic energy was converted into heat, within the error of Chalmers' measurements, but this accuracy was not sufficiently high to indicate what fraction, if any, was stored in the specimen.

It is found frequently that twinning occurs during the elongation or compression of specimens in slip experiments. In all of these cases the appearance of twinning is marked by a discontinuous jump in the shearing stress. Thus Fig. 48 shows[18] the form of the stress-strain curve of cadmium obtained under conditions in which twinning occurs most easily. The irregularities occurring for elongations greater than 20 are associated with twinning. Stress-strain curves for bismuth[19] are entirely irregular.

[17] This has been investigated in zinc, for example, by R. F. Miller (see reference 7).

[18] W. Boas and E. Schmid, Zeits. f. Physik **54**, 16 (1929).

[19] H. J. Gough and H. L. Cox, J. Inst. Metals **38**, 227 (1932).

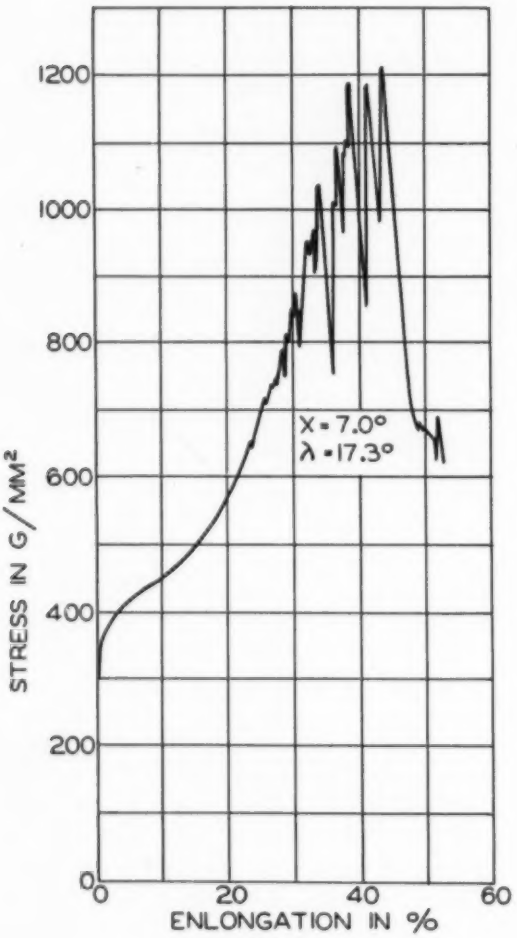

FIG. 48. The stress-strain curve for a specimen of cadmium. The irregularities occurring for elongations larger than 20 percent are associated with twinning. (After Boas and Schmid.)

The question of whether or not twinning may be produced by a gradual process analogous to creep has not been investigated. As we mentioned in the previous section, creep is observed in bismuth which apparently exhibits[19] only twinning when deformed extensively. Thus it is possible, in this case, that twinning may occur gradually, or that there is a comparatively small amount of slip accompanying twinning.

The mechanism of twinning has been subject to much less theoretical investigation than that of slip. There are many similarities between the problems, however, for in both cases inelastic flow is produced by stresses far less than the critical shearing stress for a perfect crystal. Frenkel and Kontorova[20] have suggested that twinning is caused by the passage of dislocations that are the same in principle as those responsible for slip. The case of twinning differs from that of slip, however, in that the plane neighboring a plane through which a twin dislocation has passed becomes relatively unstable if the crystal is under stress, so that a twin dislocation is readily generated in it. It is also possible that the thermal energy released by the passage of the first dislocation furnishes the activation energy for the next, so that an avalanche of twin dislocations pass through a long sequence of neighboring planes.

In any event it seems likely that the fundamental processes of twinning and slip are sufficiently alike that an understanding of the former will follow quite naturally when the theory of the latter is in more complete form.

5. Rupture

A crystal will rupture if placed under sufficiently high tensile stress. Careful work[21] shows that associated with each crystallographic plane of a specimen there is a characteristic normal stress at which the crystal will break on this plane. Since this normal stress is usually widely different for differently oriented planes, it can be measured for only one or two of the weakest planes. In the case of metals, the critical breaking stress is much less sensitive to the previous history of the specimen than is the critical shearing stress for slip. For example, Fig. 49 shows[22] the dependence on the previous shearing strain of the breaking stress for a number of specimens of zinc at liquid-air temperature. In all these cases the crystals broke on the basal plane. It may be seen that the spread in values is of the order three rather than of the order fifty as in the case of the critical shearing stress, and that any dependence on shearing strain lies nearly within the spread of values for given shear. However, there is a slight downward trend of the points, which Fahrenhorst and Schmid found to be more accentuated at liquid-hydrogen tempera-

[20] J. Frenkel and T. Kontorova, J. Phys. U.S.S.R. **2**, 137 (1939).

[21] See, for example, the discussions in the books by Schmid and Boas and by Elam.

[22] W. Fahrenhorst and E. Schmid, Zeits. f. Physik **64**, 845 (1930).

tures and less accentuated at room temperature. It should be added that the critical breaking stress appears to be practically independent of temperature in the range from room temperature to liquid-hydrogen temperature in both zinc and bismuth.

The breaking stresses of many salts are much more sensitive to previous treatment than those of metals. This effect has been studied extensively in the alkali halides by Joffe,[23] Theile[24] and Piatti.[25] They found that the values of the breaking stresses in these substances may be raised to closely reproducible values by moistening the crystals for several minutes before applying the stress. For example, the breaking stress of sodium chloride is raised from values of the order of 0.5 kg/mm² to the reproducible value of 10 kg/mm² by wetting. The accepted explanation of this effect is that the unmoistened specimens contain many fine surface cracks which act as sources of stress magnification and weaken the crystals. The solvent action of water operates to remove or smooth these cracks in such a way that the stress magnification arising from them is lowered to a negligible value. The influence of surface cracks has also been studied in the case of mica by Orowan, who has drawn similar conclusions concerning their weakening influence. It should be added that some salts, such as silver chloride, resemble metals more closely[26] than the alkali halides in that they are nearly insensitive to previous history.

Values of the breaking stresses of a number of substances are given[27] in Table VII. Values for

TABLE VII. *The breaking strengths of single crystals. (The values are given in units of kg/mm².)*

CRYSTAL	PLANE	TEMPERATURE	σ_b
Bismuth	(111)	20°C	0.32
		−185°C	0.32
Antimony	(111)	20°C	0.66
Zinc	Basal	20°C	0.18
		−185°C	0.18
		−255°C	0.18
	(10$\bar{1}$0)	−185°C	1.80
Silver chloride	(100)	20°C	~10
Sodium chloride	(100)	20°C	10

[23] A. Joffe, M. W. Kirpitschewa and M. A. Lewitsky, Zeits. f. Physik **22**, 286 (1924).
[24] W. Theile, Zeits. f. Physik **75**, 763 (1932).
[25] L. Piatti, Zeits. f. Physik **77**, 401 (1932).
[26] A. W. Stepanow, Physik. Zeits. Sowjetunion **8**, 25 (1935).
[27] The values for metals are taken from the book by Schmid and Boas. The values for salts from references 21, 22 and 23.

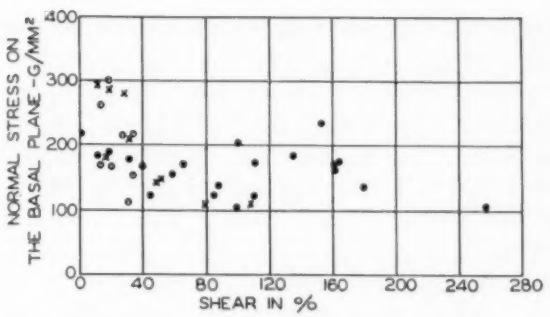

FIG. 49. Dependence of the critical normal stress on the amount of extension for rupture of zinc on the basal plane. (After Fahrenhorst and Schmid.) These results were obtained at −185°C and indicate a slight downward trend.

different crystallographic planes and for different temperatures are given when available. It may be noted that the salts appear to be stronger than the metals.

A theoretical estimate of the breaking stress for an ideal crystal may be made in the following way, suggested by Polanyi.[28] A part of the work expended in breaking a crystal reappears as the energy of the newly formed surface. Thus if we assume that the major part of the attractive forces between the two halves of a breaking specimen operate for distances of the same order of magnitude as the spacing d between neighboring planes, a lower limit to the theoretical breaking stress σ_b may be obtained from the equation

$$\sigma_b d = 2F, \tag{7}$$

where F is the energy required to form one square centimeter of surface and the factor 2 enters in the right-hand side because two surfaces are formed during breaking. Now F cannot be readily measured for solids, but it can be measured for liquids, being just the surface tension. The values of σ_b computed from the measured values of F for metals and salts with the use of Eq. (7) appear in Table VIII. It may be seen that in metals the computed lower limit to σ_b is about 1000 times larger than the observed values. Zwicky[29] has made a more careful estimate of the value for sodium chloride, using the ionic theory of salts, and obtained a theoretical value of 200 kg/mm² in place of the value 84 kg/mm² estimated with the use of Eq. (7). Although this accentuates the discrepancy be-

[28] M. Polanyi, Zeits. f. Physik **7**, 323 (1921).
[29] F. Zwicky, Physik. Zeits. **24**, 131 (1923).

tween the observed and calculated values for an ideal crystal, we may note that the ratio is only 20 for the salt. An upper limit for the critical breaking stress for an ideal crystal may be obtained by use of reasoning analogous to that used in evaluating the critical shearing stress. If we assume that a tension strain of 0.5 is required to produce a deviation from Hooke's law, because the atomic potential well is not parabolic for displacements larger than this, the stress at which breaking should be observed should be of the order of magnitude $0.5E$, where E is Young's modulus. Values of this quantity are given in Table VIII. It may be seen that these values are somewhat higher than those obtained from Eq. (7).

As in the case of the critical shearing stress for slip, we may conclude from this discrepancy between observed and calculated values of σ_b that lattice imperfections have a weakening influence on the tensile strength of crystals. If the theoretical values computed from Eq. (7) are valid, the factor by which the actual value for sodium chloride is lower than the theoretical one is not as great as in the case of slip.

Let us now speculate on the origin of the low values of the breaking stress. We shall discuss three possible sources of weakness presenting first the one that seems most reasonable at present.

(1) In the first place, it is possible that the weakness arises simply from stress magnification associated with weak spots at block boundaries. If this viewpoint is adopted, it is necessary to assume that the weak spots occur in a fairly regular fashion, for, at least in the case of metals, the breaking stress depends upon previous history to within a factor as small as three. Since the total stress magnification factor is of the order of 1000, this implies that the weak spots differ from specimen to specimen of the same material by no more than a percent. It is difficult to imagine that weak spots having this degree of regularity can arise as the result of accidents of growth, as is assumed in Buerger's theory of the formation of mosaic structure. It is possible, however, that measurements, such as those shown in Fig. 49, are made with crystals prepared in so nearly the same way that the accidents of growth are nearly the same in all specimens.

TABLE VIII. *Theoretical value of the breaking stress. (The values are expressed in kg/mm².)*

SUBSTANCE	σ_b (MIN.) EQ. (7)	σ_b (MAX.) (0.5 E)	σ_b (OBS.)
Al	372	3000	
Ag	656	4000	
Au	782	4000	
Bi	247		0.32
Cd	416	3500	
Fe	~1200	10000	
Cu	885	6000	
Ga	267		
Hg	320		
K	165		
Na	122		
Pb	261	800	
Pt	125	8000	
Sb	249		0.66
Se	63		
Sn	357	2000	
Zn	580	5000	0.18
AgCl	93		~10
NaCl	84		~10

One of the great advantages of this picture of the weak spots is that it readily explains the fact that breakdown is practically insensitive to temperature, at least in regions well below the melting point. If the imperfections occur during growth, they should be completely frozen in at a temperature near or lower than room temperature in metals such as zinc and bismuth.

It is interesting to note the following point. Since the stress magnification required to explain the low rupture strength of sodium chloride seems to be only about twenty, whereas that required to explain the low shearing stress on the basis of magnification alone would be nearer one thousand, we have evidence against the theory that the mosaic structure alone accounts for the weakness toward shear. In other words, the type of imperfection required at block boundaries to explain the weakness for breaking seems to be milder than that needed to produce dislocations without the aid of temperature fluctuations, at least in this salt.

(2) In the second place, it is possible that the weakness of crystals is related to temperature fluctuations. We may note that in the case of breaking, unlike that of slip, the crystal will give completely if only a single weak spot is produced during the period of measurement. At most, we should expect a single slip band to occur from one weak spot in the case of slip. For this reason, the rupture strength could seem

to be independent of temperature, even if it required temperature fluctuations, as long as the time between the required fluctuations was small compared with the time required to make a tensile test. If the time between fluctuations were long compared with this time, it would be found that a specimen would rupture for the experimental breaking stress in a static tensile test only after waiting sufficiently long. An effect of this type is not observed, so we may conclude that the time between effective fluctuations must be much less than a second in actual experiments if temperature fluctuations play an important role.

Now let us estimate the time between fluctuations on the basis of a simple model of the rupture process, assuming that the crystal is perfect except for thermal motion. We shall assume that fluctuations produce transient cracks which give rise to a stress magnification of about 100. We shall assume for simplicity that these cracks have the form of an oblate spheroid having major axis a and minor axis b, the larger diameter lying in the rupture plane. If b is taken as one interatomic distance, that is, about 10^{-8} cm, it follows that a must be of the order of $100 \cdot 10^{-8}$ cm since the stress magnification of the spheroidal crack would be of the order of a/b. In a typical case, such as that of rocksalt or zinc, the surface energy of a crack of this type is of the order of magnitude $100 \cdot \pi a^2/4$ ergs, since the surface energy is about 100 ergs/cm^2. This energy is about 100 ev. The probability that such a fluctuation will occur in unit time in a crystal one cubic centimeter in volume is of the form

$$p = \frac{N}{\tau} \exp(-\epsilon/kT),$$

where N is the number of different ways of forming the crack, which we may assume to be approximately equal to the number of atoms in the specimen, namely 10^{22}, ϵ is the activation energy computed above, and τ is the time required to form the crack when the activation energy is available. Since the process of formation requires the cooperative action of many atoms, τ should generally be greater than the atomic oscillational period of 10^{-13} second. However, we shall employ this value in order to estimate p under the most favorable conditions. Since $\epsilon/k = 100 \cdot 11{,}500 \sim 10^6$°K, we obtain

$$p = 10^{35} \exp(-10^6/T),$$

which is 10^{-1000} sec.$^{-1}$ at room temperature. It would be of the order of 1 sec.$^{-1}$ at room temperature only if ϵ were less than 10 ev, and of the same magnitude at liquid-air temperature only if ϵ were less than 1 ev. Since these values of ϵ seem to be unreasonably small, we may exclude the possibility that temperature fluctuations create the cracks responsible for weakness.

(3) It is interesting to ask whether dislocations can play a role in breaking. We may note that the tension stress normal to the slip plane in which the dislocation moves varies as

$$E\lambda/2\pi r, \tag{8}$$

where E is Young's modulus, λ is the slip distance, and r is the radial distance (cf. Section 2), which implies that the tension may be very large near the center of the dislocation. In fact, if we set r equal to λ, the tension given by this expression is $E/2\pi$ which is of the order of magnitude of the theoretical breaking stress. Actually, expression (8) is not valid for distances as small as λ; however, even if it were it is doubtful whether the region of high tension stress would be sufficiently large to play an important role in breaking.

Now the expression (8) should be valid for values of r as large as 50λ, for which it takes the value $E/100\pi$. This is of the same order of magnitude as the observed breaking stress. Thus if the measured breaking stress were characteristic of the perfect lattice each dislocation would be the center of a badly cracked region extending about fifty atom diameters from the center of dislocation. The precise effect such cracking would have is not clear, but it is obvious that we would have to modify many of the applications of dislocations given previously.[30] It seems safe to say that the theory of dislocations presented in earlier sections is consistent with the notion that the regions of weakness for rupture occur at block boundaries (scheme 1 of this section), and is not consistent with the notion that they are generated entirely by thermal fluctuations (scheme 2).

[30] It is interesting to note that if such cracking occurred at elevated temperatures, near the melting point, each dislocation would become the source of holes.

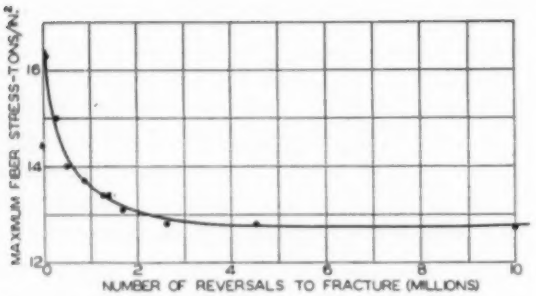

FIG. 50. Typical curve showing the relationship between maximum applied stress during a cyclic load and the number of cycles required to produce rupture. It may be seen that there is a safe range of stress below about 12.8 tons/in.^{2} (1 ton/in.^{2} = 1.55 kg/mm^2). (After Stanton and Pannell.)

We may summarize the discussion of this section by saying that the observed rupture strengths of materials are about a hundred times smaller than reasonable theoretical ones, and that the most likely sources of weakness are imperfections occurring at block boundaries, and not thermal fluctuations. The stress magnification factors that must be assumed at block boundaries do not seem to be so large that they imply that dislocations can be generated by application of stress alone.[31]

6. FATIGUE[32]

Solids break under oscillating stresses whose maximum value is smaller than the critical tensile stress for rupture determined in static tests. This effect, known as fatigue, has been studied primarily in polycrystalline specimens. Figure 50 shows, for example, the relation between the maximum stress and the number of cycles required to produce fracture in a typical polycrystalline case. It may be seen that there is a stress below which the specimen will not break, regardless of the number of cycles. Above this limiting *safe stress*, or *endurance limit*, the number of cycles decreases with increasing load and approaches unity for the static tensile stress. It seems to be a general rule, at least in the case of polycrystals, that the safe stress is about half the limiting static value.

Work on fatigue in single crystals has been carried out principally by Gough[33] and his collaborators. These investigators have shown that fatigue is usually accompanied by evidence of slip and work hardening. This deformation stops early in the history of a specimen in the safe range but continues to the breaking point in the unsafe range.

Orowan[34] has proposed the following picture of the mechanism of fatigue: The specimen contains weak spots which act as sources of stress magnification. These may be assumed to be the same spots that are responsible for the weakness toward rupture in static tests. For stresses larger than the safe limit, the stress near some of these weak spots would rise above the values required for rupture if the material were not plastic. Actually, slip occurs in these regions during the early stages of a fatigue test, and, as result, the stress becomes distributed so that the value for rupture is not exceeded. Work hardening accompanies the flow, however, so that the slip strain decreases monotonically during subsequent cycles. Thus the maximum stress near the weak spot rises with the number of cycles. In the safe range the limiting value of the peak stress is less than the critical stress for rupture, whereas it is larger in the unsafe range.

Using this picture, Orowan has given an excellent semi-quantitative account of the facts surrounding fatigue.

It should be added that fatigue is only one of several phenomena occurring under oscillating stresses. We shall discuss others in the next installment in connection with polycrystals.

[31] In a paper appearing after the foregoing was written, R. Fürth (Proc. Roy. Soc. **177**, 217 (1941)) has suggested that the criterion for breakdown is not that proposed by Polanyi and employed by Zwicky in his work on sodium chloride, but is, instead, that the elastic energy per unit volume be equal to the heat needed to melt the same amount of substance. This postulate leads to theoretical values of the rupture stress that are in much closer agreement with the observed ones than those obtained from Polanyi's equation without the use of the notion of stress magnification. However, Fürth's theory seems to face the following problems: (a) The mechanism for converting elastic energy into heat has not been treated in a convincing quantitative fashion. (b) It is not made clear that the conversion of elastic energy into heat with the consequent melting would actually weaken the crystal for tensile breaking. It is possible that this work will completely revise our notion both of rupture and of plasticity, but considerable extension is needed before this is achieved.

[32] The practical aspects of fatigue are presented in the book *Fatigue of Metals* by H. J. Gough (Scott, Greenwood and Son, 1924).

[33] H. J. Gough, D. Hanson and S. J. Wright, Phil. Trans. Roy. Soc. **226**, 1 (1925); H. J. Gough, Proc. Roy. Soc. **118**, 498 (1928); H. J. Gough and H. L. Cox, Proc. Roy. Soc. **123**, 143 (1928); **127**, 453 (1930); J. Inst. Metals **45**, 71 (1931); **48**, 227 (1932).

[34] E. Orowan, Proc. Roy. Soc. **171**, 79 (1939).

Résumé of Recent Research

Recent Measurement of the Velocity of Light

At about the time Michelson, Pease, and Pearson were compiling the results obtained from their rotating mirror measurements of the velocity of light, Wilmer C. Anderson was attacking the problem at Harvard University with an entirely new process. Preliminary results from this electrical method[1] showed sufficient promise to warrant an attempt for still higher accuracy with an improved apparatus.[2]

Briefly the method consists in splitting a modulated beam of light into two parts by

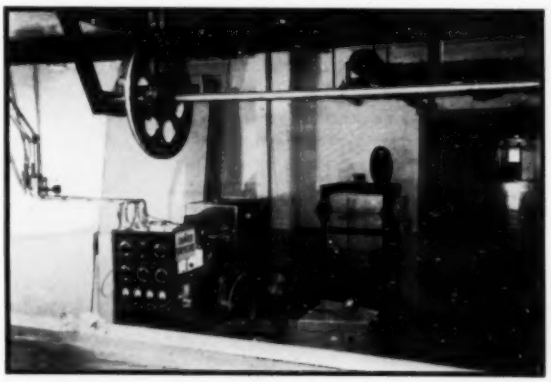

FIG. 1. General view of the velocity of light apparatus from a point directly beneath the concave mirror support, at one end of the long optical path.

means of a half-silvered mirror, and after sending over different optical paths, recombining them on the surface of a photoelectric cell. This cell has a circuit tuned to the frequency of modulation. Across this tuned circuit the two beams will generate a resultant voltage that is dependent upon the phase existing between the two components, this phase in turn depending upon the difference in length of the optical paths traversed by the two beams. Thus, if this path difference amounts to an even number of half wave-lengths, the resultant voltage will be a maximum, but if the path difference amounts to an odd number of half wave-lengths the voltage will be a minimum. With amplification of this resultant voltage, the method becomes extremely sensitive to slight changes in the path length of one of the beams.

In the improved apparatus, the light from a 1000-watt high pressure, water-cooled mercury arc was modulated at a frequency of 19.2 megacycles with a water-cooled Kerr cell, and after passing over the respective paths, was recombined on the surface of an eleven-stage photosensitive electron multiplier tube. The resulting voltage output was further amplified through numerous stages of standard electron tube amplification, and eventually used to drive an automatic photographic recorder.

The frequency of modulation was controlled by the laboratory standard, which was in turn compared frequently with the national broadcast standards. The error was estimated to be less than one part in several million. The base line was measured with an Invar steel tape, calibrated at the National Bureau of Standards with an estimated error of less than one part in 210,000.

The average of 2895 readings gave the value of 299,776 km/sec. for the velocity of light in vacuum. This includes a group velocity correction not considered in previous results. The accuracy was limited by an electron transit

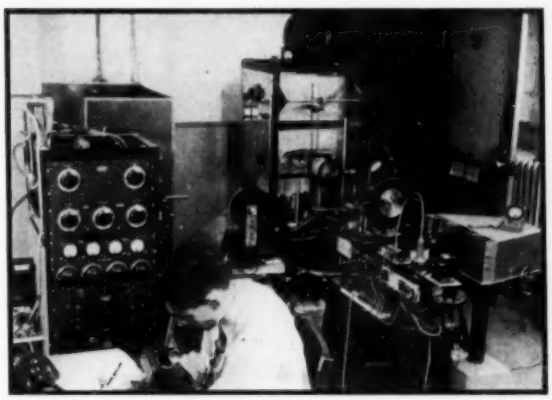

FIG. 2. General view of apparatus showing the light source and modulator at the left, the receiving apparatus in the center, and the recording apparatus in the right foreground. Mr. Plass, an assistant, is shown measuring some of the records with a comparator.

time phenomenon showing up as a result of the type of construction used in the multiplier tube, and due to a discrepancy in the coincidence of the two light beam components. The average daily deviation was ± 9 km/sec., but the average deviation from the final mean value was ± 14 km/sec. This was easily accounted for on the basis of the phenomenon mentioned above. The

conclusion was drawn that insofar as the accuracy of the present measurements permitted, the value for the velocity of light was a constant, and not subject to variations as supposed by some.

[1] W. C. Anderson, Rev. Sci. Inst. **8**, 239 (1937); J. Opt. Soc. Am. **31**, 187 (1941).
[2] Made possible by grants from the Carnegie Corporation of New York.

Here and There

Spectroscopy Conference

Those who plan to attend the Ninth Summer Conference on Spectroscopy and Its Applications to be held at the Massachusetts Institute of Technology on July 21, 22 and 23, should signify their intention in advance, according to an announcement recently received. No fees are charged for attendance at the Conference, but attendance will be limited to 200.

This Conference will repeat to a considerable extent the type of program presented at the conferences held during the past eight summers. The early sessions will be devoted principally to applications of spectroscopy to the analysis of materials. Other topics to be considered are absorption spectrophotometry, photographic photometry, biological and chemical effects of spectral radiation, industrial applications of spectroscopy, analysis of spectra and the measurement of wave-lengths. The more technical and theoretical papers will be reserved for the later sessions.

Requests for copies of the program, for reservations, or for further information, should be addressed to Professor G. R. Harrison, Massachusetts Institute of Technology, Cambridge, Massachusetts.

★

Olivet College Awards Honorary Degree

Ferry C. Houghten, Director of the Research Laboratory of the American Society of Heating and Ventilating Engineers at Pittsburgh, Pennsylvania, was awarded an honorary degree of Doctor of Science by Olivet College, Olivet, Michigan, at its annual Founders' Day convocation on February 24, 1941. Dr. Houghten was graduated from Olivet College in 1913 with an A.B. degree. He received his M.S. degree at the University of Washington in 1915.

★

Ohio Section American Physical Society Meets

Fifty-five members and guests were present at a luncheon and business meeting following the morning program of the fourth meeting of the Ohio Section of the American Physical Society, held at Muskingum College, New Concord, Ohio, on Saturday, March 29.

Mathematical Tables Project Progresses

The Project for the Computation of Mathematical Tables, under the Federal Works Agency, Work Projects Administration, has now published the following tables, according to an announcement by the Technical Director, Dr. Arnold N. Lowan:

1. Table of the First Ten Powers of the Integers from 1 to 1000, 80 pp. (1939).
2. Tables of the Exponential Functions e^x, 535 pp. (1939).
3. Tables of Sines and Cosines for Radian Arguments, 275 pp. (1940).
4. Tables of Circular and Hyperbolic Sines and Cosines for Radian Arguments, 405 pp. (1940).
5. Tables of Planck's Radiation and Photon Functions. Published in J. Opt. Soc. Am. **30**, 70–81 (1940).
6. Tables of the Sine, Cosine, and Exponential Integrals for the range from 0 to 2 at intervals of 0.0001 to 9 decimal places.
7. Tables of the Sine, Cosine, and Exponential Integrals for the range from 0 to 10 at intervals of 0.001 to 9 or 10 significant digits.
8. Table of Grid Coordinates (American Polyconic Projection) at 5 minute intervals of latitude and longitude for latitudes from 7° to 28°.

Work is going forward on a number of other tables, and the Project states that it would welcome suggestions for the computation of tables of interest in pure and applied mathematics, as well as information regarding computational work in progress elsewhere. Communications should be addressed to Oliver A. Gottschalk, Acting Administrator, Work Projects Administration, 70 Columbus Avenue, New York City.

Requests for copies of published tables should be addressed to Dr. Lyman J. Briggs, Director, National Bureau of Standards, Washington, D. C.

★

Meteorology Department Formed

Dr. Sverre Petterssen has been appointed Head of the Department of Meteorology of the Massachusetts Institute of Technology for the next academic year. Dr. Petterssen, who was for seven years in charge of the Weather Forecasting Institute in Bergen, Norway, and who since 1939 has been acting head of the long-established course in meteorology, which now becomes a separate department, will succeed Professor Carl G. A. Rossby, who has been on an extended leave of absence as assistant chief of the United States Weather Bureau in charge of research. Professor Rossby will resign to join the faculty of the University of Chicago.

Science

★

American Chemical Society Awards Medal

Dr. Linus Pauling, Head of the Division of Chemistry and Chemical Engineering at the California Institute of Technology, was the recipient of the 1941 William H. Nichols Gold Medal of the New York Section of the American Chemical Society, a news item in *Science* announces. The award, made in recognition of Dr. Pauling's "fundamental inquiry into the nature of the chemical bond," was presented March 7 at a joint meeting of the New York Section of the American Chemical Society and the Society of Chemical Industry.

Coffin Fellowships Awarded

Charles A. Coffin Fellowships have been awarded seven graduates of as many colleges and universities by the General Electric Company, it was announced in April. These Fellowships, granted annually under terms of the Charles A. Coffin Foundation, enable outstanding graduates to continue or undertake research work in educational institutions, either in this country or abroad. The fields in which awards are made include electricity, physics and physical chemistry. This year 21 applications for the Fellowships were made.

The seven men receiving the award, their schools and the schools in which they will pursue additional studies are: William J. Barclay, Oregon State, to study at Stanford University; Willard H. Fenn, University of California, to study at same school; Henry M. Foley, University of Michigan, to study at same school; John A. Hornbeck, Oberlin College, to study at Massachusetts Institute of Technology; Paul M. Marcus, Columbia University, to study at Harvard University; Theodore Moreno, Stanford University, to study at same school; and Robert L. Sproull, Cornell University, to study at same school.

★

Call for Meteorologists

Applicants who have experience in meteorological research or experience in practical work in forecasting or in performing other meteorological duties, such as, for example, might be obtained with the airlines, are desired for the recently announced Civil Service examinations (unassembled) for the following positions: Principal Meteorologist, Senior Meteorologist, Meteorologist, Associate Meteorologist, and Assistant Meteorologist. Specialized branches for each of the above positions include: radiometeorography, synoptic meteorology, climatology, dynamic meteorology, statistical meteorology, or any other well-defined branch of the subject. The duties of the positions are "to plan, supervise, conduct, or assist in conducting investigations or research work in the special branch in which appointment is made, the degree of responsibility and importance of the duties varying in accordance with the grade of the position."

Applications will be rated as received at the United States Civil Service Commission, Washington, D. C., until December 31, 1941, unless sufficient eligibles are obtained and notice of an earlier closing date is given.

For July

***The Physical Aspects of Boundary Lubrication*, by OTTO BEECK**

***Frictional Phenomena*, by ANDREW GEMANT**

***Electron Theory of Thermoelectric Effects*, by W. V. HOUSTON**

***Theory of the Plastic Properties of Solids. IV*, by FREDERICK SEITZ AND T. A. READ**

Also contributed original research papers

Award in Biological Chemistry

For his "brilliant work on isotopes as tracers in chemical reactions," Dr. David Rittenberg of the School of Medicine of Columbia University, has been awarded the sixth annual Lilly Award in biological chemistry, presented by the American Chemical Society, *Science* reports. The Lilly Medal, with a prize of $1000, which goes to investigators of thirty-five years of age or under, was established in 1934 by Eli Lilly and Company of Indianapolis to "promote interest in fundamental research in biological chemistry and to recognize young men and women in a way which should mean much to the progress of this field in the United States." Dr. Rittenberg has worked with Professor Schoenheimer of the School of Medicine of Columbia, using atoms of heavy hydrogen and heavy nitrogen produced in the laboratory of Professor Harold C. Urey, *Science* points out.

★

Summer Courses in Applied Mathematics

During a summer program extending from June 12 to August 6, New York University is offering a group of courses in applied mathematics under the Engineering Defense Training Program of the United States Office of Education. These courses, available to research workers in industry and to students who may become useful in relevant industrial research, include: Advanced Methods in Applied Mathematics, Fluid Dynamics and Applications, Bending and Buckling of Elastic Plates, Transient Analysis of Electrical Networks, and Seminar on Vibrations.

Calendar of Meetings

June

12–20 American Society of Mechanical Engineers, Kansas City, Missouri
16–20 American Institute of Electrical Engineers, Toronto, Ontario
16–19 American Society of Heating and Ventilating Engineers, San Francisco, California
17–18 American Association of Physics Teachers, Pasadena, California
18–20 American Physical Society, Pasadena, California
19–21 National Colloid Symposium, Ithaca, New York
20–21 American Physical Society, Providence, Rhode Island
23–27 American Association for the Advancement of Science, Durham, New Hampshire

July

23–25 American Society of Civil Engineers, San Diego, California

August

27–29 American Institute of Electrical Engineers, Yellowstone National Park

September

8–12 American Chemical Society, Atlantic City, New Jersey
8–10 American Astronomical Society, Williams Bay, Wisconsin
22–26 American Association for the Advancement of Science, Chicago, Illinois
25–26 Society of Automotive Engineers, Milwaukee, Wisconsin

October

6–10 National Safety Council, Chicago, Illinois
12–15 American Society of Mechanical Engineers, Louisville, Kentucky
13–16 Society of Motion Picture Engineers, New York, New York
15–17 American Society of Civil Engineers, Chicago, Illinois
20–24 American Society for Metals, Philadelphia, Pennsylvania
20–24 American Welding Society, Philadelphia, Pennsylvania

Honors Recently Announced

The American Academy of Arts and Sciences has awarded the Rumford gold and silver medals for 1941 to Dr. Vladimir Kosma Zworykin, Director of the Research Laboratory of the Radio Corporation of America, in recognition of his work on photo-cells and their application, the development of television and of the electron microscope.

Science

Peter Kapitza, Russian scientist known for his work on magnetism and low temperature, has been awarded one of forty-eight Joseph Stalin prizes "for outstanding achievements by Soviet Russian research workers," according to *Science*.

★

Continuation of his study with the cyclotron of the properties of atomic nuclei and the interaction of neutrons is planned by Dr. John R. Dunning, recipient of the Ernest Kempton Adams Research Fellowship, according to a recent note in *Science*. Dr. Dunning is Associate Professor of Physics at Columbia University.

New Book

Temperature Measurement

By Robert L. Weber. Pp. 171+x, Figs. 155, 21.5×27.5 cm. Edwards Brothers, Inc., Ann Arbor, Michigan, 1941. Price $2.50.

The book is divided into three parts. One is concerned with theory (112 pages), the second contains a list of 22 suggested experiments (28 pages), while the third is an appendix (12 pages), containing information pertinent to the field of temperature measurement. The chapter titles for Part I are: Expansion thermometry, Heat transfer, Thermoelectricity, Thermoelectric pyrometry, Radiation, Radiation pyrometry, Resistance thermometry, Recording pyrometry, Temperature control, Calorimetry, Thermal analysis, Elementary thermodynamics, Special methods of temperature measurement, Extreme temperatures, and International temperature scale.

The text covers more ground than is implied in the title but does not treat all topics normally covered in college heat courses. The author's purpose is to provide a text suitable for use by "students in physics, chemistry, engineering, metallurgy, and ceramics." It seems especially well suited for those preparing for industrial positions. The impression given is that the selection of material is excellent and that its treatment is also generally excellent though marred somewhat by a number of errors and instances of loose treatment of units and definitions.

To elaborate the first point, one notes that there are many illustrations and descriptions of modern industrial type instruments, and there are many excellent tables of useful reference data of which Table II, Chapter IV, Thermocouple protection tube materials, is an example chosen at random. Here are given for 31 such materials the maximum safe temperatures, compositions, characteristics, and applications. Frequently circuit diagrams and complete working descriptions are included for such devices as electronic thermoregulators, recording pyrometers, potentiometers, etc. Also one is impressed with the great number of references to a wide variety of journals. The more academic aspect of the subject has not been neglected. The three-dimensional heat flow equation and Planck's radiation law are developed and there is a discussion of the thermodynamics involved in the adiabatic demagnetization cooling process. However in many instances the treatments, though generally accurate, seem too brief to permit easy assimilation by those unfamiliar with it. There are summaries for each chapter and many good problems.

As regards errors and loose uses of units, etc., some examples from the first few chapters will suffice. The list, while not complete, is representative. (1) On page 2 the steam point on the Rankine scale is stated incorrectly, as is the interval between the ice and steam points. (2) On page 3, the equation seems to be incorrect and the "cubic expansion coefficient" of a gas is given as 1/273 with no unit specified. (3) On page 8, Eq. (6), t is used for temperature where previously it has meant time. (4) On page 18, the Peltier coefficient is defined as the "heat transferred when unit quantity of electricity traverses the junction." A more acceptable definition would be, the heat transferred per unit of electricity traversing the junction, where "per" has the implication "divided by." The first definition requires some such incorrect unit as the calory for measurement of a Peltier coefficient, while the second is compatible with a correct unit such as the calory/coulomb. A similar criticism may be made of many of the definitions of radiation terms found on page 39. This type of definition is common throughout this text and indeed, throughout many other texts also. Many authors do not recognize this criticism as just. (5) On page 39, the fact that steradiancy is a radiant energy term while brightness is a light term is not clearly stated. (6) On page 40 it is stated that Planck introduced his quantum hypothesis and from it deduced the radiation law which bears his name. Actually, these two events occurred in reverse order. (7) On page 42, "Kelvin's law" by typographical error has replaced Kirchhoff's law. (8) On page 43, it seems to be implied that brightness temperature and radiation temperature are two terms for the same concept. Actually they differ considerably. For tungsten at 2500°K the latter is more than 400°K less than the former for $\lambda = 0.665\mu$. (9) On page 87, "nucleuses" for the plural of nucleus, although given as a preferred form by Webster, is not in common scientific usage.

To summarize, the reviewers feel that the book is fundamentally sound, well suited for its purpose, and generally well written, but that it needs some revision, particularly in the matter of units and definitions.

A. G. Worthing
David Halliday
University of Pittsburgh

Contributed Articles

Temperature Distribution in Vacuum Tube Coolers with Forced Air Cooling

I. E. Mouromtseff
Lamp Division, Westinghouse Electric and Manufacturing Company, Bloomfield, New Jersey
(Received February 12, 1941)

Section I. Theoretical Derivation of Temperature Distribution

LET us consider a metal cylinder, such as the copper anode of a vacuum tube, or the core of an air cooler, which is heated from within over the midportion AB (Fig. 1). The entire cylinder is cooled by a fluid (water, air) flowing uniformly along its outer surface in the axial direction,—as a rule,—upwards. The ends are not heated, but obviously they contribute to a better cooling due to the heat conduction along the metal wall. The purpose of this discussion is to find the law of temperature distribution along the tube wall, in order to apply it to the establishing of permissible power dissipation under various conditions of heat generation and cooling. Regarding the tube dimensions, we shall assume that the wall has a uniform thickness, small as compared to the cylinder length.

In operation, heat is generated uniformly throughout the middle portion of the tube. It flows partly across the wall to be directly transferred to the cooling medium; partly it reaches the cooling fluid via the cold ends. We can logically anticipate that the temperature of the wall will not be uniform but will gradually decrease toward the ends of the tube; at the same time, with the assumption of complete radial symmetry, all points on the periphery of any cross section will have the same temperature. We can also anticipate that in a state of equilibrium there will be one particular cross section within the boundary of the heated portion, where the temperature will be at a maximum. Analogous to the watershed line between two rivers flowing in opposite directions, the cross section with maximum temperature will divide the tube into two parts with heat flowing in opposite directions toward the cold ends. There is no heat exchange between the two parts on both sides of the dividing line, so that each side will have its own pattern of temperature distribution. In the case of cold ends of equal lengths as assumed in Fig. 1, the temperature dividing line will be located exactly at the middle of the heated part; with unequal cold ends as in Figs. 3, 4 and 5 it will be shifted toward the shorter end. In either of these cases as well as in all the following discussion, unless it is stated to the contrary, under the temperature of the wall we consider its temperature above that of the cooling fluid at the corresponding point. Hence, for computation of the temperature above the ambient one must take into consideration the gradual temperature increase of the fluid (in the direction of its flow) effected by the absorbed heat; this is actually done in Figs. 3, 4 and 5.

In the following discussion we shall neglect the temperature drop across the wall; if necessary, it can be introduced later on in the final results.

Let us designate by t_b the boundary temperature at the cross section BD separating the heated portion of the tube and the cold end. In a state of equilibrium the temperature distribution *along the cold end* is given by the expression

$$t_x = t_b \cdot \cosh\,(Q' - qx)/\cosh\,Q'. \qquad (1)$$

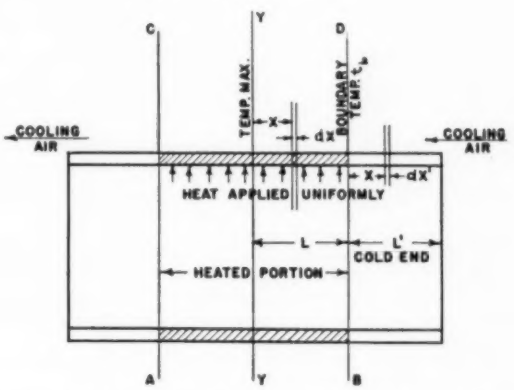

FIG. 1. Metal wall heated on inside cooled on outside.

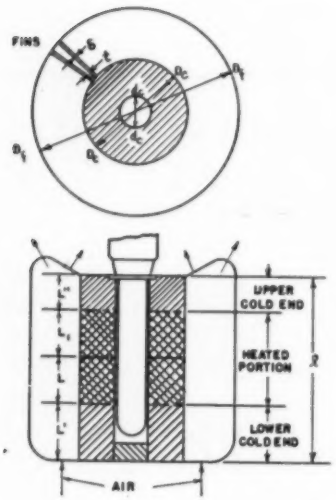

STRUCTURAL DATA

		INCHES	CM
D_f	OUTER FIN DIAMETER	7.5	19.1
D_c	OUTER CORE DIAMETER	3.75	9.52
d_c	INNER CORE DIAMETER	1.63	4.14
	FIN THICKNESS	.0625	.159
t	FIN SPACING AT ROOT	.075	.191
T	FIN SPACING AT FREE END	.150	.381
	FIN SPACING, AVERAGE	.1125	.286
W	FIN WIDTH (RADIAL DIRECTION)	1.88	4.78
R	FIN LENGTH (AXIAL DIRECTION)	9.0	22.8
n	FIN NUMBER	86	
L'	LENGTH OF LOWER COLD END	2.70	6.85
L''	LENGTH OF UPPER COLD END	1.72	4.36
$L+L_1$	TOTAL LENGTH OF HEATED PORTION	4.60	11.5

FIG. 2. Optimum design of 891-R and similar air coolers.

Here $q^2=hp/ak$ and $Q'=qL'$ (2)

with the following meaning of the symbols:*

x is the distance of a point on the cold end from the boundary cross section BD, in cm.

t_x the temperature at the same point, in °C.

h is the heat transfer figure from copper to cooling fluid, referred to the outer surface of the tube, in cal./sec. cm²·1°C. For a given structure of the cooling device and fluid temperature h depends on the physical constants of the fluid and its velocity.[1]

p is the circumference of the tube, in cm.

a is the area of the annular cross section of the tube, in cm².

k is the heat conductivity of copper (or other metal if such is used) in cal./sec. cm·1°C.

L' is the length of the cold end, in cm.

The expression (1) is a solution of a differential equation

$$ak\partial^2t/\partial x^2\cdot dx-pht\cdot dx=0, \qquad (3)$$

where t stands for wall temperature at any point. This equation is similar to one discussed elsewhere.[2] In the present case, its first member represents the heat obtained by an annular element of an infinitesimal length, dx, due to heat conduction within the wall; the second member corresponds to the heat lost by the same element to the cooling fluid.

In order to determine the actual value of the boundary temperature, t_b, and also, to derive an expression for temperature distribution along *the heated portion* of the tube we can start with a differential equation obtained from Eq. (3) by simply supplementing it with a member expressing heat generation. In this case $x=0$ lies at the cross section YY with the maximum temperature. If heat is generated at the rate M cal./sec. cm², one can write

$$ak\cdot\partial^2t/\partial x^2\cdot dx+(Mp-hpt)dx=0 \qquad (4)$$

or

$$\partial^2t/\partial x^2-q^2t=q^2\cdot m/e, \qquad (5)$$

where by m we designate the product Mp, that is, the rate of heat generation per unit length of the tube and by e the heat transfer figure referred to the same axial length and the entire perimeter of the tube; i.e., $e=hp$. The solution of Eq. (5) is

$$t_x=A\epsilon^{qx}-B\epsilon^{-qx}+m/e. \qquad (6)$$

The boundary conditions are:

For $x=0$ one has $\partial t/\partial x=0$

$x=L$ one has $t=t_b$ and $qx=Q$. (7)

Hence

$$t_b=A\epsilon^{Q}-B\epsilon^{-Q}+m/e$$

$$0=A+B \qquad (8)$$

and finally:

$$t_x=m/e-(m/e-t_b)(\cosh qx)/\cosh Q. \qquad (9)$$

* *Note.*—Quantities marked here and in the following by (′) or (″) pertain to the cold ends, while simple letters designate quantities belonging to the heated portion of the tube or those in common to all parts.

Quantities Q, Q' and Q'' are dimensionless; they depend on the physical constants involved in the heat transfer mechanism and on structural parameters of the wall. With all other constants equal these quantities are proportional to the respective lengths of the cold ends of the heated portions.

[1] W. H. McAdams, *Heat Transmission* (McGraw-Hill, New York and London, 1933) p. 165, Eq. (19).

[2] I. E. Mouromtseff, "The influence of the grid focusing effect," Communications p. 9 (December, 1938).

By L we designate here the distance between the cross section with the temperature a maximum and the beginning of the cold part. By setting

$$x=0, \quad t_x=T_{\max} \tag{10}$$

we obtain

$$T_{\max}=m/e-(m/e-t_b)/\cosh Q. \tag{11}$$

The average temperature over the heated length, L, will be found by integrating Eq. (9):

$$T_{Av}=1/L\cdot\int_0^L t_x dx=m/e-(m/e-t_b)(\tanh Q)/Q. \tag{12}$$

In order to calculate the numerical value of t_b entering into the expressions for temperature distribution both along the heated and cold portions of the tube, one can reason in the following manner: Heat generated in the hot portion L cm long is mL. Heat lost to the cooling medium by the same heated portion is eLT_{Av} and by the cold end, $-eL't_{Av}$. Therefore, the relation must exist

$$mL=eLT_{Av}+eL't_{Av}. \tag{13}$$

From the paper referred to above[2] (or by the integration of Eq. (1)) we have:

$$t_{Av}=t_b\cdot(\tanh Q')/Q'. \tag{14}$$

Combining Eqs. (12), (13) and (14) we obtain

$$t_b=m/e\cdot 1/(1+\tanh Q'/\tanh Q). \tag{15}$$

All quantities in this expression are operational constants (m, e, q), or structural parameters $(Q=qL$ and $Q'=qL')$; therefore, t_b can be calculated. With the numerical value of t_b available one can further calculate numerical values for $T_{\max}$, T_{Av} and t_{av}, using expressions (11), (12) and (14). It is obvious from the foregoing discussion that the boundary temperature t_b is, generally speaking, different for the two cold ends as they are generally of unequal lengths; it is also obvious that the maximum temperature, $T_{\max}$, can be calculated independently, using the data of the side either to the right or to the left of the $T_{\max}$ cross section. However, $T_{\max}$ can have only one value. If this is not the case in the calculation, the location of the temperature-dividing line has been assumed incorrectly.

It may be of interest to note that the temperature distribution curve along either part of the heated portion (on the two sides of the temperature maximum) as expressed by Eq. (9) is an image of that of the adjacent cold end (Eq. (1)) with the initial ordinate, $(m/e-t_b)$ substituted for t_b, and Q for Q'.

It may also be noted that the physical meaning of the quantity, m/e, appearing in all the above expressions is the temperature of the hot part of the tube, *if there is no heat conduction* in the longitudinal direction. This can actually occur either in the absence of cold ends, or in the case of an air cooler composed of a stack of disks with imperfect thermal contact between them.

Section II. Numerical Example

In order to illustrate the theoretical results of the foregoing section by a numerical example, we shall apply the derived relations to a practical case of a vacuum tube with an external copper anode, operated in an air cooler schematically shown in Fig. 2. The cooler consists of a heavy walled core with a number of radial fins. The tube is soldered in the central bore of the core; the length of the latter is such that there are "cold ends" extending below and above the heated portion of the anode. The length of the directly heated part of the anode and, hence, of the core is determined by the internal tube structure, namely, by the extension of its filament. Air is forced through the ducts between the fins in an axial direction at a rate of 220 l/sec. (480 c.f.m., the latter symbol standing for "cubic feet per minute"), which corresponds to the linear velocity, 1180 cm/sec. All important dimensions necessary for the following calculations are given on the drawing. We assume, further, that anode dissipation is 500 watts per centimeter length of its hot portion, that is,

$$m=500 \text{ watts}\equiv 120 \text{ cal./sec.} \tag{16}$$

Heat generated in this portion flows radially through a thin layer of solder and through the core to the fins by which it is transferred to the moving air. In the absence of "cold ends" there would be no longitudinal heat flow in the core; this we shall first assume to be the case.

In order to determine the core and, hence, the anode temperature it is generally convenient to replace the total cooling effect of the fins by the direct heat transfer from the outer core surface to the air. This can be done by the following

reasoning. Let us single out a horizontal slice of the cooler limited by two planes perpendicular to the tube axis 1 centimeter apart. Then, designating by h_f the rate of heat transfer from the fins to the air per 1 cm² of fin surface and 1°C temperature difference and by S_f the total cooling fin area of the segregated zone, one can obtain the total heat transfer rate per unit temperature difference for the entire zone:

$$e_f = h_f S_f \text{ cal./sec.1°C.} \tag{17}$$

Dividing e_f into the figure of heat generated within the same zone one will obtain the average fin temperature:

$$T_{f\text{Av}} = m/e_f. \tag{18}$$

Further, the relation between the average and the maximum fin temperature at their roots—the latter being the same as the core temperature, T_c—is given by an expression similar to that of Eq. (14):

$$T_{f\text{Av}} = T_c(\tanh Q_f)/Q_f. \tag{19}$$

Finally, the condition of continuity of heat flow requires that

$$e_c T_c = e_f T_f. \tag{20}$$

Hence,
$$e_c = e_f(\tanh Q_f)/Q_f. \tag{21}$$

Here, e_c is the desired total rate of heat transfer per unit length zone, referred to the outer core surface and per unit temperature difference, and Q_f is a dimensionless quantity similar to Q' of Eq. (2), obtained by application of Eq. (1) to the radial heat flow through the fins. In this particular case

$$Q_f = q_f L_f \quad \text{and} \quad q_f = (2h/\delta k)^{\frac{1}{2}} \text{ cm}^{-1}, \tag{22}$$

because the cooling perimeter, p, of each fin within the zone is 2 centimeters and its cross section is $1 \times \delta$ cm, if by δ we designate the fin thickness. L_f represents the radial length of the fin. As to the basic figure of heat transfer, h_f, it is a function of the physical constants of the air, its velocity and of the dimensions and shape of the air ducts. The following expression for calculation of h_f is given in *Heat Transmission*.[1]

$$\frac{hD}{k} = 0.024\left(\frac{D\rho V}{\eta}\right)^{0.8}\left(\frac{\eta C_p}{k}\right)^{0.4}, \tag{23}$$

where ρ, η, k and C_p are, respectively, density, viscosity, thermal conductivity, and specific heat of air, V is air velocity; and D is "equivalent diameter" of the individual air ducts. Using the numerical data given in Fig. 2 and assuming for evaluation of the physical constants, the ambient temperature 45°C, one will find:

$$\begin{aligned} h_f &= 0.00143 \text{ cal./sec. cm}^2 \cdot 1°\text{C.} \\ e_f &= 0.85 \text{ cal./sec. } 1°\text{C.} \\ e_c &= 0.705 \text{ cal./sec. } 1°\text{C.} \end{aligned} \tag{24}$$

Once m and e_c are known, one can determine the core temperature, T_c, in the absence of longitudinal heat flow, from the condition of thermal equilibrium within each zone:

$$m = e_c T_c.$$

In our case

$$T_c = m/e_c = 120/0.705 = 170.5°\text{C.} \tag{25}$$

As mentioned before, m/e_c is an important quantity as it appears in all final equations determining various temperatures on the core. In addition, in order to proceed with further calculation we must determine two other parameters Q and Q', both dimensionless, entering in various formulae directly, or under signs of hyperbolic functions. Both quantities depend on q as given by:

$$q = (e_c/ak)^{\frac{1}{2}}, \tag{26}$$

where e_c is substituted for hp as in Eq. (2). The cross-sectional area of the core is:

$$a = \pi/4 \times (6.67^2 - 4.15^2) = 21.5 \text{ cm}^2. \tag{27}$$

Heat conductivity of copper, k, is taken 0.9 cal./sec. cm·1°C. Hence:

$$\begin{aligned} q &= (0.705/21.5 \times 0.9)^{\frac{1}{2}} \\ &\quad \times (0.0354)^{\frac{1}{2}} = 0.188 \text{ cm}^{-1}. \end{aligned} \tag{28}$$

Then we obtain:

$$\begin{aligned} Q &= qL = 0.188 \times 5.75 = 1.82, \\ Q' &= qL' = 0.188 \times 6.85 = 1.29, \\ Q'' &= qL'' = 0.188 \times 4.38 = 0.825. \end{aligned} \tag{29}$$

Q' and Q'' refer to the lower and upper cold ends of the core, respectively. L is the distance between the assumed location of the temperature maximum and the beginning of the cold end; this maximum is assumed thus far to be exactly at the middle of the hot portion.

Further, from mathematical tables we find:

$$\begin{aligned} &\tanh Q = 0.765 \quad \text{and} \quad \cosh Q = 1.54, \\ &\tanh Q' = 0.859, \\ &\tanh Q'' = 0.678. \end{aligned} \tag{30}$$

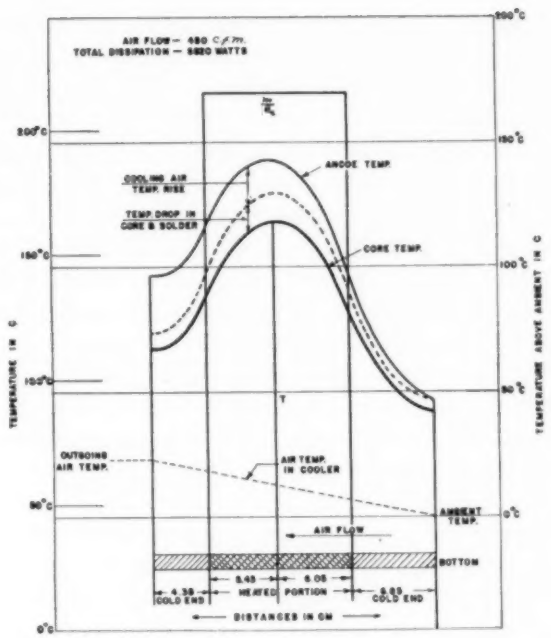

FIG. 3. Calculated temperature distribution in the core of the air cooler.

With the obtained numerical data we shall first calculate from Eq. (15) the boundary temperature for the bottom end:

$$t_b' = m/e \times 1/(1+\tanh Q'/\tanh Q)$$
$$= 170 \times 1/(1+0.859/0.765) = 80.2°\text{C}. \quad (31)$$

For the upper end:

$$t_b'' = 170 \times 1/(1+0.678/0.765) = 89.6°\text{C}. \quad (32)$$

Further, from Eq. (11) we shall calculate the maximum temperature which—as we assumed—lies at the middle of the heated portion. Using t_b' we obtain:

$$T'_{\max} = 170 - (170-80.2)/1.544 = 112°\text{C}, \quad (33)$$

while using t_b'' we have

$$T''_{\max} = 170 - (170-89.6)/1.544 = 119.6°\text{C}. \quad (34)$$

The double value for $T_{\max}$ indicates, as mentioned in Section I, that our assumption regarding the location of $T_{\max}$ is incorrect. However, by a systematic trial we can find the exact location of $T_{\max}$ and its correct value. In our case, we find that with $L = 6.05$ cm for the lower end and 5.45 cm for the upper end:

$$\begin{aligned} t_b' &= 83.2°\text{C} \quad \text{and} \quad T'_{\max} = 119.3°\text{C}, \\ t_b'' &= 90.8°\text{C} \qquad\quad T''_{\max} = 119.3°\text{C}. \end{aligned} \quad (35)$$

A complete curve of temperature distribution along the core, as calculated from Eqs. (1) and (9) is plotted in Fig. 3. It pictures clearly the influence of the cold ends as one would logically expect it: The effect results in a general reduction of temperature all over the cooler as compared to the case of no cold ends, when $t_x = \text{const} = m/e_c$°C. By a direct inspection of the mathematical formulae it is not difficult to arrive at a conclusion that the numerical value of the maximum temperature depends on the relative lengths of cold ends and of the adjacent heated portions of the tube drained of heat by the respective cold ends. It is also obvious that the location of the maximum is displaced from the middle of the heated portion toward the shorter cold end.

By simple reasoning one can assume that at any cross section of the core the radial heat flow is proportional to the temperature at this particular point above the ambient as shown by the temperature distribution curve. Therefore, in our case the radial heat flow at the point with the maximum temperature is:

$$F_{\max} = m \times T_{\max}/(m/e_c) = T_{\max} \times e_c$$
$$= 119.3 \times 0.705 = 84 \text{ cal./sec.} \quad (36)$$

Hence, the temperature drop across the core of this cross section can be computed from the expression

$$\Delta t_c = F_{\max} \times 1/2\pi k_c \times \ln D_c/d_c = 84 \times 0.177$$
$$\times \ln 2.63/1.63 = 7.1°\text{C}. \quad (37)$$

For the calculation of the temperature drop across the solder wall (1 mm to 1.5 mm thick) it is more appropriate to neglect longitudinal heat flow in the thin anode wall and in the layer of solder. Accordingly,

$$\Delta t_s = 120 \times 0.1/\pi \cdot d_c a_{\text{tin}} = 120/10 \times \pi \times 4.15$$
$$\times 0.15 = 6.3°\text{C}. \quad (38)$$

Finally, we must consider the ambient temperature and the average increase in temperature of the cooling air passing through the cooler. The ambient temperature is usually assumed to be 45°C, and the average temperature increase of the air under the assumed operating conditions is

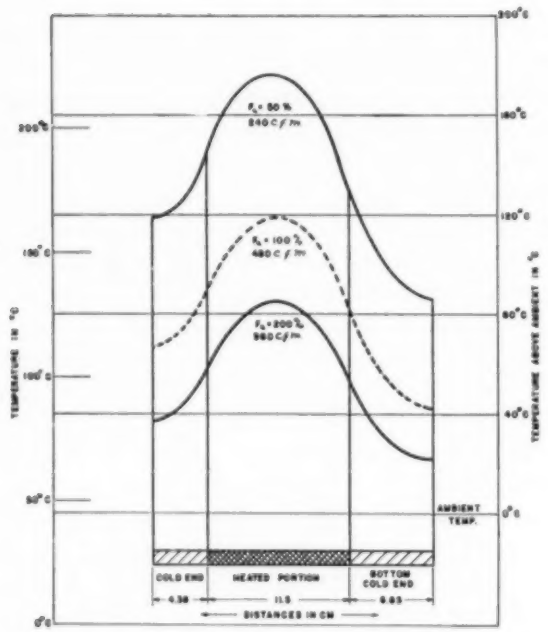

FIG. 4. Temperature distribution in the core for "normal" air flow, 50 percent of the "normal," and 200 percent of the "normal."

11°C (calculated from the rate of air flow, air density, specific heat and total heat dissipation.)

By summing up all individual temperature drops we shall find the maximum anode temperature:

$$T_{a\,\max} = t_{amb} + t_{a\,air} + T_{c\,\max} + \Delta t_c + \Delta t_s$$
$$= 45 + 11 + 119.6 + 7.1 + 6.3 = 189°C. \quad (39)$$

The results of this last calculation are reproduced graphically in Fig. 3. In addition to the heavy line curve of the calculated temperature distribution in the core above the temperature of the cooling air, the thin-line curve represents the anode temperature by adding the temperature drop in various parts of the cooler. The horizontal line in the upper part of the drawing corresponds to m/e_c, the core temperature calculated for uniform heating and cooling as it would be in the absence of the cold ends. One may note that strictly speaking the temperature of the cooling air is to be represented in Fig. 3 by a curve, the ordinates of which at each point are proportional to the area under the heavy lined temperature distribution curve between the inlet and any chosen point. However, for practical purposes it is sufficient to draw a straight line between the initial and the final air temperatures, the latter being calculated from the known rate of air flow and the rate of the total heat transfer from the cooler to the air; this straight line is shown in Fig. 3.

Once the calculated maximum anode temperature is known, the permissible anode dissipation limit can be determined by proportional increase or reduction of the dissipation figure assumed in the calculation (500 watts per 1 centimeter length) so that the calculated temperature does not exceed the permissible anode temperature. The latter depends on the material of the anode, the melting point of the solder used, degree of outgassing tube parts, etc. Ordinarily this temperature is established experimentally.

Thus, the fact of non-uniform temperature distribution along the core must be considered in establishing the tube dissipation ratings, as permissible dissipation is governed by the maximum temperature at any one place rather than by the average temperature. If the effect of the cold ends is entirely neglected, or a uniform temperature distribution throughout the core is assumed, the calculated temperature becomes either too high or too low; correspondingly, the calculated permissible dissipation becomes too low or too high. Thus in our numerical example the difference would amount either to −42 percent or +25 percent of the correct figure.

SECTION III. HEAT DISSIPATION LIMIT AS FUNCTION OF AIR FLOW RATE

One of the important problems in air cooling is: how does the maximum core temperature vary

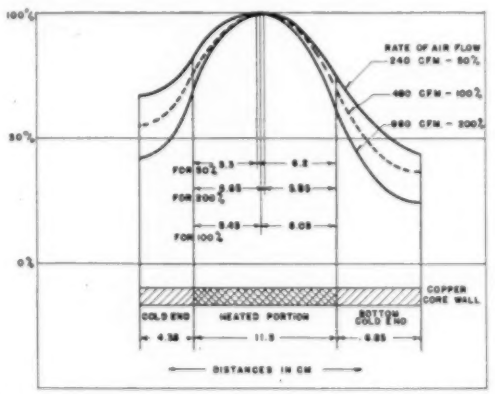

FIG. 5. Relative temperature distribution in the core of the cooler for the "normal" air flow, 50 percent of the "normal," and 200 percent of the "normal." Total dissipation, 5820 watts.

with the rate of air flow, if the power dissipated in the anode remains constant. We shall not present the details of the entire calculation and shall only examine its final results. In fact, one does not need to repeat all the steps outlined above for each individual air velocity. Indeed, with a complete set of data obtained for the "normal" velocity one can more easily arrive at similar data for any other velocity by using proper ratios. The results of such transformations actually carried out for the velocity twice the "normal" and one-half of the normal are shown in Fig. 4. The same curves are replotted in Fig. 5 to a relative scale taking in each case the maximum temperature as 100 percent. From Fig. 4 it follows that the higher the air velocity, the lower is the maximum temperature (also the temperature at all other points). However, Fig. 5 shows that with higher velocities the temperature is less uniform along the anode. Figure 6 gives permissible dissipation calculated from the maximum temperature as a function of rate of air flow. It is interesting to note that the slope of this curve is 0.54 while the rate of heat transfer is proportional to $V^{0.8}$ (see Eq. (23)). This is obviously due to the influence of quantities Q_f, Q and Q' appearing in the expression for e_c and $T_{\max}$ both directly and under the signs of hyperbolic functions. In other words, the slope depends not only on air velocity but also on structural parameters of the cooler.

A closer analysis of the quantity Q', which is characteristic of the effect of the cold ends, reveals that its role in bringing down the maximum temperature ceases when Q' approaches the value of 3. Indeed, tanh Q' appearing in Eqs. (15) and (31), then practically equals unity, and cannot increase any further no matter how large Q' is. In fact even with $Q'=1.8$, tanh Q' is equal to 90 percent of its maximum value. This shows that for given radial dimensions of the core there is a limiting length for cold ends beyond which their extension does not contribute anything to the cooling of the tube. From an examination of the expression

$$Q'=aL'=L'(e_c/ak)^{\frac{1}{2}}, \tag{40}$$

one can easily arrive at a further conclusion that the higher the air velocity, that is, the greater e_c, the shorter is the limiting length of the cold ends.

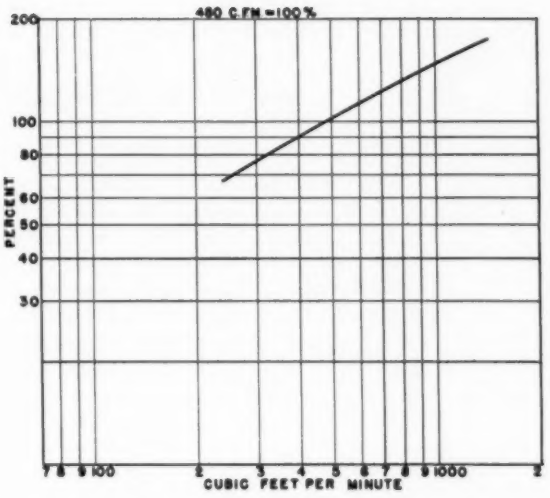

FIG. 6. Relative dissipation limit *vs.* air flow rate.

Indeed, from Eq. (40) one has

$$L'=Q'/q=3/q \quad \text{for} \quad \tanh Q'=1; \tag{41}$$

or $$L'=1.8/q \quad \text{for} \quad \tanh Q'=0.9.$$

In our numerical example we shall find: for "normal" velocity, $q=0.188$ cm^{-1} and $L'_{\max}=16$ cm for 100 percent and $L'_{\max}=9.6$ for 90 percent effect. For 50 percent "normal" velocity, $q=0.148$ cm^{-1} and $L'_{\max}=20$ cm for 100 percent and $L'_{\max}=12$ for 90 percent effect. For 200 percent "normal" velocity, $q=0.234$ cm^{-1} and $L'_{\max}=13.5$ for 100 percent and $L'_{\max}=7.7$ for 90 percent effect.

On the other hand, one can show in a quite similar manner that with the cold ends of the maximum length (tanh $Q'=1$) their role is decreasing as the length of the heated portion of the anode increases; it almost completely disappears when $Q=qL$ approaches the value 4.6. This follows from Eq. (11) if one substitutes for t_b its value from Eq. (15).

If we assume tanh $Q'=1$, the maximum temperature becomes

$$T_{\max}=\frac{m}{e_c}(1-\epsilon^{-Q}). \tag{42}$$

With increasing Q the exponential term decreases, and at the indicated value of $Q=4.6$ becomes 1/100 so that, practically, the maximum temperature at the hottest point, $T_{\max}$ is the same as m/e_c which is the uniform temperature in the absence of the cold ends.

A Method of Measuring the Thermal Conductivity of Rock Cores

J. B. Hersey
Department of Physics, Lehigh University, Bethlehem, Pennsylvania
(Received March 7, 1941)

A method of measuring the thermal conductivity of long rock core samples is described. It is an adaptation of Bidwell's method of measuring the thermal conductivity of metals. The core is packed in Silocel in a cylindrical container. Heat is supplied by a flat electric heater on one end of the core sample, and measurements of temperature are made along the core and at several radial distances in the insulator. Isothermal surfaces in the insulator are determined and found to be conical surfaces within several centimeters of the core. These are parallel for some distance along the core. Using this fact the conductivity of the core is computed relative to that of the Silocel. A value 5.92×10^{-3} cal./cm deg. sec. was obtained for a sample of Norite and 2.59×10^{-3} for a Pyrex rod at room temperature.

THE method of measuring thermal conductivity described in this report was developed in the course of some work on the thermal properties of rocks. It is an adaptation of a method used by Bidwell[1] in his work on metals. In his method a long cylindrical sample of the metal to be measured is heated at one end and surrounded by a good insulator of known conductivity. Measurements of temperature are made along the sample and at chosen radial distances in the insulator. Over the central portion of his sample Bidwell found that the heat loss from the side of the sample could be considered as flowing radially into the insulator. Using this conclusion the conductivity of the sample was computed from the temperature data and the known conductivity of the insulator. It has been found for the case of poor conductors, that is, of the order of ten times the conductivity of the insulator, that this heat loss can no longer be considered radial, but that by determining the shape of the isotherms in the insulator the conductivity of the sample can be computed.

Experimental Procedure

A core sample of Norite sixteen inches long and approximately $1\frac{1}{8}$ inches in diameter is mounted along the axis of a cylindrical container ten inches in diameter and twenty inches long. A flat electric heater is attached to the top of the sample and thermocouples are pasted onto the rock at intervals of 4 cm near the bottom and 2 cm near the top. The sample is packed in Silocel and small glass tubes are mounted in the insulator at three distances from the axis of the apparatus. The tubes are so arranged as to be separated from each other as far as possible.

All temperature measurements are made with thermocouples of Driver-Harris Advance and Nichrome V wire 0.0031 inch in diameter. In the range from 0 to 100 deg. C, these were calibrated at the boiling points of water and of ethyl alcohol. The quadratic relation between degrees centigrade (T) and microvolts (E) is

$$E=43.3T+0.00365T^2.$$

It was found that by using wire of such materials and of such a size there was no significant heat conduction away from the point of measurement along the wires themselves.

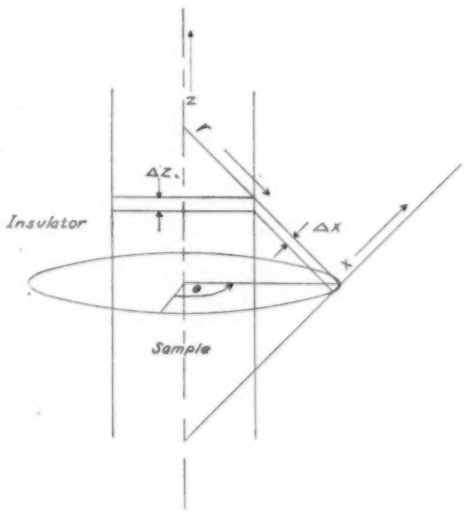

Fig. 1.

[1] C. C. Bidwell, Phys. Rev. **56**, 594–597 (1939).

In preparation for a run the heater is turned on twenty-four hours before the measurements are to be made, and test measurements at a few points in the apparatus are made for at least two hours before the run to make sure of equilibrium conditions. In the run itself temperature measurements are made by the couples pasted onto the rock sample and by a single couple inserted in turn into the various glass tubes. In the final tabulation of temperature distribution at any given radial distance, the figures are the average of determinations in at least two tubes at that distance in different azimuths. Temperature is plotted as a function of distance from the bottom of the apparatus. The temperature curve along the sample is analyzed to obtain the second derivative of temperature with respect to distance. All four curves are used to plot a cross section showing the isotherms in the insulator. It was found that the isotherms are conical surfaces and, further, that for some distance along the middle of the sample these surfaces are parallel.

The parallel conical isothermal surfaces suggest the following treatment of the data. Let z be the coordinate along the axis of the cylinder. The heat loss in a length Δz of the sample is

$$H=\pi a^2 K_x \frac{d^2T}{dz^2}\Delta z, \tag{1}$$

where K_x = conductivity of sample a = radius of sample. This quantity of heat flows perpendicular to the isothermal surfaces in the insulator and is confined to a conical sheet of thickness Δx. If θ is the angle between the element of an isothermal cone and the axis then

$$\Delta x=\Delta z\cos\theta. \tag{2}$$

Let r be the distance from the axis, measured parallel to a flow line, to any given isotherm. It is seen that r forms an orthogonal coordinate system with the distance x along the element of the cone and an azimuthal angle (see Fig. 1). Since the heat flow is independent of this angle the equation of flow may be integrated with respect to r and the temperature, just as in the case of radial flow in a cylinder, except that a factor $\cos\theta$ is introduced by the cone, and the resulting equation is

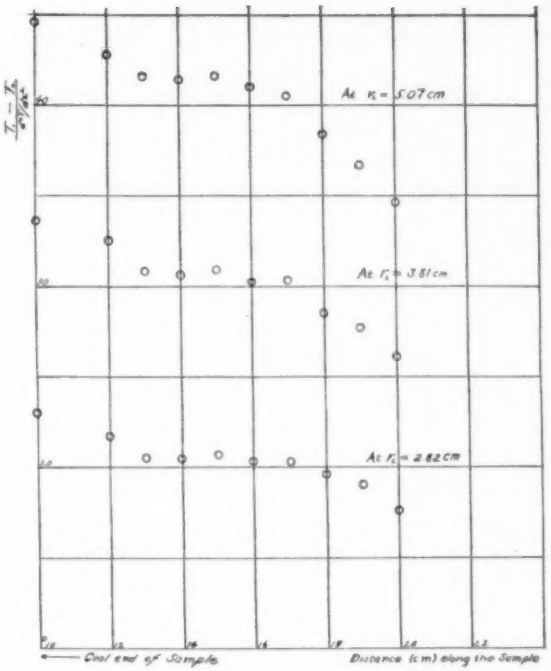

FIG. 2. Variation of the ratio $(T_1-T_2)/(d^2T/dz^2)$ along the sample.

$$H=2\pi\frac{K_s(T_1-T_2)}{\log_e(r_2/r_1)}\cos\theta\Delta x, \tag{3}$$

where T_1 = temperature at the sample, T_2 = temperature taken on the same flow line as T_1 at the desired distance in the insulator, r_1 and r_2 are the r distances corresponding to T_1 and T_2, K_s = conductivity of the insulator (Silocel). H, the quantity of heat flowing in the conical sheet of thickness Δx, is equal to the heat loss in length Δz of the sample so that

$$a^2K_x\frac{d^2T}{dz^2}\frac{\Delta x}{\cos\theta}=\frac{2K_s(T_1-T_2)}{\log_e(r_2/r_1)}\cos\theta\Delta x. \tag{4}$$

Finally, the unknown conductivity K_x is given by

$$K_x=\frac{2K_s}{a^2\log_e(r_2/r_1)}\cos^2\theta\frac{T_1-T_2}{d^2T/dz^2}. \tag{5}$$

It is seen that in this equation the quantities T_1-T_2 and d^2T/dz^2 are to be determined directly from the temperature data. $\cos\theta$ is measured from the cross section diagram of the isotherms. T_1-T_2 is read from the temperature-distance

TABLE I. *Conductivity of Norite.*

	r_2 (CM)	K_n (GCAL. $CM^{-1}°C^{-1}$ SEC.$^{-1}$)
Run *A*	2.82	5.68×10^{-3}
	3.81	5.84×10^{-3}
	5.07	6.15×10^{-3}
Run *B*	2.82	6.00×10^{-3}
	5.07	5.90×10^{-3}

graphs and d^2T/dz^2 from analysis of the temperature curve along the sample. If the ratio $(T_1-T_2)/(d^2T/dz^2)$ be plotted against distance from the bottom of the apparatus it is found to have a nearly constant value coinciding exactly with the region where the isothermal cones are parallel. The region of constant value of this ratio decreases in size for increasing values of r_2. In Fig. 2, $(T_1-T_2)/(d^2T/dz^2)$ is plotted as a function of distance for a typical run. The three sets of values are for the three different radial distances used. Corresponding values of r_2 are indicated on the graph. In the lowest set the region of constant ratio is roughly five centimeters of the sample. For the upper two curves it is seen to be slightly less, and the deviation from constancy outside the region is markedly greater. The constant value of the ratio is used in Eq. (5) with corresponding r values to compute the unknown conductivity.

In any separate run there are independent sets of values of T_1-T_2 corresponding to the several distances into the insulator for which separate values of the conductivity may be calculated. In Table I are shown values taken from two separate runs. In the first temperatures were measured at all three distances, and in the second at only two.

The insulator used was Silocel, which is crushed diatomaceous earth. The question whether its conductivity varies greatly with different degrees of packing is important when considering its use as a standard for such relative measurements. This problem was studied in a separate series of experiments and the conclusion was reached that while the conductivity certainly does vary slightly with packing, it is quite possible to reproduce set-ups using Silocel in which the differences of conductivity in bulk are certainly less than 5 percent. The conductivity of the Silocel as used in these experiments with rock cores and Pyrex is 2.70×10^{-4} gcal. $cm^{-1}°C^{-1}$ sec.$^{-1}$.

Between runs *A* and *B* of Table I the apparatus was completely dismounted so that the two were obtained relative to different "packings" of the Silocel. Greater precision may be attained with closer control of the Silocel packing, but these results corroborate the measurements on the Silocel itself in indicating that set-ups having very nearly the same conductivity in bulk can be reproduced without precise control. In these experiments the only control was in using the same material each time and packing according to the same general procedure.

One run has been made on a Pyrex rod 1" in diameter and 16" long. The heat supply for this run was so low that temperature differences in the apparatus were too small to produce the same accuracy as for the measurements on Norite. Rough values obtained for the three distances r_2 are

2.56×10^{-3} gcal. cm^{-1} $°C^{-1}$ sec.$^{-1}$.
2.70×10^{-3}
2.50×10^{-3}

These are to be compared with the value 2.82×10^{-3} computed for the approximate temperature of the rod (about 70°F) from data on the thermal conductivity of Pyrex furnished by the Corning Glass Works.

The possibilities of this method have not been explored as yet beyond the results mentioned above. It has an advantage over some other methods that have been used in that it does not depend directly on an electrical or calorimetric measurement of total heat flow.[2] Also no guard ring manipulation is required. Furthermore, it does not have the interface problem such as encountered in the divided bar method used by Benfield[3] and Bullard,[4] and the method of Birch and Clark.[2] On the other hand the limitation imposed by the use of Silocel as a standard will keep the accuracy of results at three to four percent at best.

Although no difficulty has been encountered with the specimens studied so far in this respect, well lithified, uniform cores should be required. This may well mean that many sedimentary

[2] C. D. Niven, Can. J. Research **A11**, 249–253 (1934); F. Birch and H. Clark, Am. J. Sci. **238**, 529–558 (1940).
[3] A. E. Benfield, Proc. Roy. Soc. **A173**, 428–449 (1939).
[4] E. C. Bullard, Proc. Roy. Soc. **A173**, 474–502 (1939).

specimens cannot be measured by this method, though dense limestones and many uniform sandstones and shales should present no difficulty.

It is believed that the average value determined from a run is accurate to better than 10 percent, but probably not better than 5 percent. This order of precision is quite adequate for certain geophysical studies, and because of the fact that rocks to be studied are frequently available in the form of core samples of about the dimensions of the Norite used, this method may prove of use in such studies.

The writer is indebted to Professor C. C. Bidwell, Professor Maurice Ewing and other members of the Lehigh University Physics Department for advice and encouragement in the course of this work, and to the Corning Glass Works for furnishing the Pyrex rod.

A Preliminary X-Ray Study of Binary Alloys of Platinum with Cobalt, Molybdenum and Tungsten

RALPH HULTGREN AND ROBERT I. JAFFEE
Graduate School of Engineering, Harvard University, Cambridge, Massachusetts

(Received February 6, 1941)

At the composition PtCo there exists a tetragonal superlattice with the AuCu structure. It is stable at 600°C, but forms a face-centered-cubic disordered phase at 1000°C. It is the incipient formation of this superlattice which is responsible for the superlative remanence and coercivity reported by Jellinghaus. At 400°C a body-centered-cubic phase begins to form. More than 50 atomic percent molybdenum and more than 35 atomic percent tungsten are soluble in platinum at 1000°C.

SMALL samples of high melting alloys convenient for x-ray diffraction study may be readily prepared in an electron bombardment furnace.[1] Some preliminary studies of alloys of platinum prepared in this way are described in the following pages.

Jellinghaus[2] has reported superlative properties for use as a permanent magnet for a 50 atomic percent platinum-cobalt alloy. After being annealed three hours at 650°C, it had a remanence of 3000 gauss and a coercive force of 4000 oersteds. The product of these quantities, which is often taken as a measure of suitability of a material for use as a permanent magnet, is 12×10^6, more than three times as great as Mishima steel and twice that of Honda's K.S. steel.

Jellinghaus studied the alloy by x-ray diffraction. He found that a sample quenched from 1200°C was face-centered cubic with $a_0=3.75$A, while a cast sample contained this phase along with a second, body-centered-cubic phase with $a_0=2.85$A. He concluded the magnetic properties were due to the incipient formation of the body-centered phase. He noted that the decrease in atomic volume was 14 percent, which he thought might be due to an ordering in the body-centered phase, although no superlattice lines were observed.

Previous microscopic work has indicated that face-centered-cubic cobalt is miscible in all proportions with platinum.[3] The hardness, however, reaches a maximum at 50 atomic percent.[4]

Not much is known of the platinum-molybdenum and platinum-tungsten systems.[3] Dreibholz[5] believes that about 16 weight percent of molybdenum may be soluble at the eutectic temperature, decreasing to less than 2 percent at room temperature. Müller[6] reports that at least 50 weight percent tungsten is soluble in platinum.

EXPERIMENTAL WORK

The metals used were as pure as could easily be obtained, but no elaborate precautions were

[1] Ralph Hultgren and M. H. Pakkala, J. App. Phys. **11**, 643 (1940).
[2] Werner Jellinghaus, Zeits. f. tech. Physik **17**, 33 (1936).
[3] M. Hansen, *Der Aufbau der Zweistofflegierungen* (Julius Springer, Berlin, 1936).
[4] W. A. Nemilow, Zeits. f. anorg. Chemie **213**, 283 (1933).
[5] Dreibholz, Zeits. f. physik. Chemie **108**, 5 (1924).
[6] L. Müller, Ann. d. Physik **7**, 9 (1930).

undertaken to insure purity, since the work was intended to be preliminary. Platinum was filed from pure sheet purchased from the American Platinum Works. Cobalt was obtained as pellets from the Central Scientific Company, and the tungsten and molybdenum were the purest which the A. D. Mackay Company had in stock.

Platinum and cobalt filings were mixed in a very small crucible in a proportion to give 51 atomic percent cobalt. The crucible was composed of pure aluminum oxide and was heated in a tantalum cup in the electron bombardment furnace.[1] The ingot weighed about $1\frac{1}{2}$ grams and had lost about 1.7 percent in weight during melting. The loss was thought to be mainly cobalt, which is slightly volatile, so the ingot should contain nearly 50 atomic percent of each constituent.

Similar technique was used with the platinum-molybdenum and platinum-tungsten alloys except that smaller zirconia crucibles were used and the ingots weighed approximately $\frac{1}{2}$ gram. All ingots were given a homogenizing anneal of one week at 1000°C, first sealing them in evacuated Vitreosil tubes. Filings were then made, annealed and quenched according to the usual technique of this laboratory.[7]

Platinum-Cobalt

Only one alloy of this system was prepared, containing about 50 atomic percent cobalt. Annealed for 119 hours at 1000°C and quenched, it consisted of a single, face-centered-cubic phase with $a_0=3.761$A. Annealed for 192 hours at 600°C, a tetragonal superlattice similar to AuCu was formed. Line positions and intensities checked this structure very closely. The lattice parameters were $a_0=3.818$A, $c_0=3.639$, $c_0/a_0=0.953$. The decrease of atomic volume on ordering was 0.3 percent.

A sample annealed for 384 hours at 800°C contained a mixture of the ordered and disordered states described above. Annealed at 400°C for 504 hours, the sample contained the ordered tetragonal phase and a new, body-centered-cubic phase with $a_0=2.87$A.

These results agree with Jellinghaus in that the high temperature phase is face-centered cubic, but show that the magnetic hardness produced by annealing at 650°C must be due to ordering within the face-centered phase, rather than the body-centered-cubic phase reported by Jellinghaus, which forms only at lower temperatures.

The small atomic volume in the body-centered-cubic phase can hardly be due to ordering, as Jellinghaus supposes. Ordering produces changes of atomic volume of the magnitude of one percent. The 14 percent smaller atomic volume probably indicates the body-centered phase to be richer in cobalt, but conclusions can hardly be drawn without further study.

Alloys of platinum with 10, 20, 25, 30, 40 and 50 atomic percent molybdenum were prepared, homogenized, and then annealed at 1000°C for about six days. All samples gave x-ray patterns showing a single, face-centered-cubic phase with lattice constants near that of platinum. This indicates that in all cases the molybdenum was soluble in the platinum lattice. Similar results were obtained at 800°C.

Alloys of platinum with 5, 10, 15, 30 and 35 atomic percent tungsten treated in the same way gave similar results at 1000°C.

Summary

Platinum and cobalt of 50 atomic percent composition are miscible at 1000°C, forming a face-centered-cubic phase with $a_0=3.761$A. At 600°C, they form a tetragonal superlattice similar to AuCu with $a_0=3.818$, $c_0=3.639$, $c_0/a_0=0.953$. It is this superlattice which is responsible for the superlative magnetic hardness discovered by Jellinghaus. A body-centered-cubic lattice beginning to form at 400°C needs further investigation.

More than 50 atomic percent molybdenum and more than 35 atomic percent tungsten are soluble in platinum at 1000°C.

[7] A. S. Coffinberry and R. Hultgren, Trans. A. I. M. E. **128**, 249 (1938).

Further Study of the Flow of Air Through Porous Media

R. R. Sullivan
The University of Tennessee Agricultural Experiment Station, Knoxville, Tennessee
(Received January 30, 1941)

The streamline flow of air through highly porous wads of textile fibers is studied. The rate of flow is found to be twice as great for fibers parallel to flow as for fibers perpendicular to flow. Shape factors for the channels through which the flow takes place are determined and compared with those for the ideal case of Emersleben. The problem of measuring specific surface of high porosity wads is discussed.

Introduction

THE increasing use of fluid flow measurements for the determination of specific surfaces of porous media, such as sands, wads of textile fibers and the like, has raised questions concerning the conditions under which the approximate solution given by Kozeny[1] may be expected to remain valid. Carman,[2] and Hatch[3] have successfully applied Kozeny's equation to sands covering a wide range of particle size. Fowler and Hertel,[4] Sullivan and Hertel,[5] Wiggins, Campbell and Maass[6] have applied the equation to compact wads of textile fibers. In the application to textile fibers, two features were more readily controlled than in the case of sands; namely, fiber or particle orientation with respect to flow, and the value of porosity of the wad of fibers. The equation as derived by Fowler and Hertel[4] indicated that the macroscopic rate of streamline flow should be proportional to the average value of the square of sine ϕ, where ϕ is the angle between the direction of macroscopic flow and the normal to an element of surface exposed to the flow. This indicates that, other factors being the same, the macroscopic flow through a bed of parallel cylinders whose axes are in the direction of flow should be one and one-half times as rapid as that through a bed of spheres, and twice as rapid as that through a bed of circular cylinders whose axes are perpendicular to the direction of flow. The values for $\langle \sin^2 \phi \rangle_{Av}$ in these cases are 1, $\frac{2}{3}$, $\frac{1}{2}$, respectively. Sullivan and Hertel[7] compared the flow through compact bundles of glass fibers with that through a bed of glass spheres and obtained results in agreement with these predictions.

It is the purpose of the present study to investigate the flow of air through more highly porous media than those hitherto studied. Wads of loosely compressed textile fibers are used for the media.

Theory

Although the general case of flow through a porous medium is too complicated to admit of a complete analytical solution, the special case of laminar flow of an incompressible fluid through a bed of periodically spaced circular cylinders of equal size whose axes were parallel to the flow has been treated by Emersleben.[8] Figure 1 is a

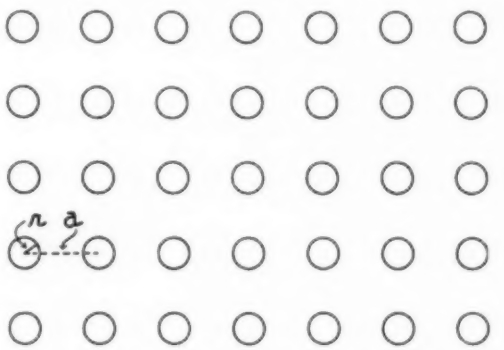

FIG. 1. Cross section of bed of circular cylinders. All cylinder shave radius = r. Distance from center to center of adjacent cylinders = a.

[1] I. J. Kozeny, Wasserkraft und Wasserwirtschaft **22**, 67 (1927).
[2] P. C. Carman, Trans. Inst. Chem. Eng. **16**, 168–188 (1938).
[3] L. P. Hatch, J. App. Mech. **7**, A-109 (1940).
[4] J. L. Fowler and K. L. Hertel, J. App. Phys. **11**, 496 (1940).
[5] R. R. Sullivan and K. L. Hertel, Textile Research **11**, 30–38 (1940).
[6] E. J. Wiggins, W. B. Campbell and O. Maass, Can. J. Research **17**, 318 (1940).
[7] R. R. Sullivan and K. L. Hertel, J. App. Phys. **11**, 761–765 (1940).
[8] O. Emersleben, Physik. Zeits. **26**, 601 (1925).

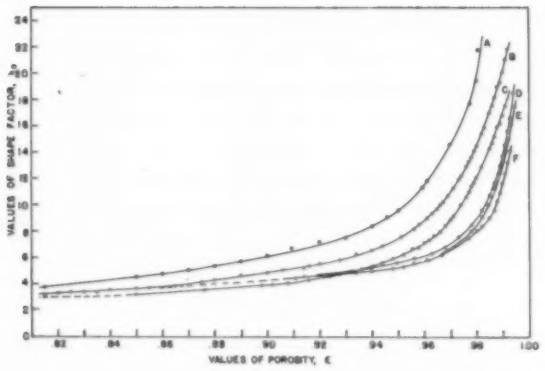

FIG. 2. Shape factors are shown for different values of porosity. Curve *A* is for the theoretical case treated by Emersleben. Curves *B*, *C*, *D*, *E* and *F* are experimental curves for Welsh wool, fine noil wool, B-38-$\frac{3}{8}$″ cotton, B-38-1$\frac{3}{16}$″ cotton, and Sea Island C-38 cotton, respectively.

diagrammatic cross section of the bed of cylinders. Emersleben solved the hydrodynamical equation for a case similar to that of Fig. 1, where, however, the cylinders were not quite circular but represented contours of a constant value, $Z_0(r/a)$, of the Epstein zeta-function[9]

$$Z\begin{vmatrix} 0 & 0 \\ \underline{x} & \underline{y} \\ a & a \end{vmatrix}(2)_\delta.$$

By taking the contours which most nearly fit the circular cylinders of given radius, the solution was then an approximate one for the case of Fig. 1. The approximation, while poor for large values of $\rho = r/a$, becomes successively better as ρ becomes smaller. For $\rho = 0.25$ (corresponding to $\epsilon = 0.804$) it was impossible on an actual plot ($a = 12$ cm, $r = 3$ cm) to distinguish between the contour for $Z_0(3/12)$ and a circle of radius 3 cm.

Emersleben's solution is,

$$V = \frac{\Delta p}{L\mu}\left(\frac{a}{2\pi}\right)^2 \iint_{Z \le Z_0} \left\{ Z_0\left(\frac{r}{a}\right) - Z\begin{vmatrix} 0 & 0 \\ \underline{x} & \underline{y} \\ a & a \end{vmatrix}(2)_\delta \right\} \frac{dxdy}{a^2}, \quad (1)$$

where V = macroscopic velocity of flow in cm/sec., $\Delta p/L$ = pressure gradient in dynes/cm^3, a = grating spacing of arrangement in cm, r = radius of cylinder in cm, μ = coefficient of viscosity in poises, and x and y are rectangular coordinates. Setting $dxdy/a^2 = d\epsilon$, where ϵ = porosity = interstitial cross-sectional area/total cross-sectional area, he obtained

$$V = \frac{\Delta p}{L\mu}\left(\frac{a}{2\pi}\right)^2 \left\{ \iint_{Z \le Z_0} Z_0(\rho)d\epsilon - \iint_{Z \le Z_0} Z(\epsilon)d\epsilon \right\}. \quad (2)$$

Curves were given which allowed easy evaluation of the surface integrals of Eq. (2) in any given case.

The general law of streamline flow through a straight channel of constant cross section[10] is

$$v = (m^2/k_0\mu)\Delta p/L, \quad (3)$$

where v = the average velocity of flow, m = mean hydraulic radius = cross-sectional area open to flow/cross-sectional perimeter exposed to flow, and k_0 = a dimensionless quantity called a shape factor, which has the same value for all cross sections of the same shape. In the case of a channel comprising the space between parallel cylinders (not necessarily equal or circular), $m = \epsilon/S_0(1-\epsilon)$ where S_0 = average specific surface of cylinders = surface of cylinders/volume of cylinders. Also Q = macroscopic rate of volume flow in cc/sec. = $A\epsilon v$ where A = total area of cross section. Thus, for such a channel,

$$Q = (A\Delta P/k_0\mu L S_0^2)\epsilon^3/(1-\epsilon)^2. \quad (4)$$

[9] The Epstein zeta-function is a special case of the general zeta-function.

$$^{(p)}Z\begin{vmatrix} g \\ h \end{vmatrix}(S) = Z\begin{vmatrix} g_1, & \cdots & g_p \\ h_1, & \cdots & h_p \end{vmatrix}(S)_\varphi$$

$$= \sum_{k_1=-\infty}^{\infty} \cdots \sum_{k_p=-\infty}^{\infty} \frac{\exp\left[2\pi i \sum_{\lambda=1}^{p} (h_\lambda k_\lambda)\right]}{[\varphi(k+g)]^{S/2}},$$

where

$$\varphi(k+g) = \sum_{\eta=1}^{p} \sum_{\lambda=1}^{p} a_{\eta\lambda}(k+g)_\eta(k+g)_\lambda; \quad a_{\eta\lambda} = a_{\lambda\eta}$$

$a_{\eta\lambda}$ is a real coefficient; $D = |a_{\eta\lambda}| > 0$; g and h are real; S may be complex; k_j is an integer. Thus,

$$Z\begin{vmatrix} 0 & 0 \\ \underline{x} & \underline{y} \\ a & a \end{vmatrix}(2)_\delta = \sum_{k_1=-\infty}^{\infty} \sum_{k_2=-\infty}^{\infty} \frac{\cos 2\pi(k_1 x/a + k_2 x/a)}{k_1^2 + k_2^2},$$

the δ in this notation meaning that $a_{\eta\lambda} = \delta_{\eta\lambda} = 0$ if $\eta \neq \lambda$ or $a_{\eta\lambda} = \delta_{\eta\lambda} = 1$ if $\eta = \lambda$. The symbol $Z_0(r/a)$ is used to signify the value of

$$Z\begin{vmatrix} 0 & 0 \\ \underline{x} & \underline{y} \\ a & a \end{vmatrix}(2)_\delta$$

along the constant-valued contour which most nearly approximates the circle $x^2 + y^2 = r^2$. For a discussion of the Epstein zeta-function see O. Emersleben, Physik. Zeits. **24**, 73–80 (1923).

[10] P. C. Carman, Trans. Inst. Chem. Eng. **15**, 150–166 (1937).

Equation (4) is equivalent to that of Kozeny. The applicability of such an equation to porous media is usually ascribed to the fact that the shape factors for the forms of the openings supposed to exist in a cross section of the medium are nearly the same. Shape factors are offered ranging from values of 3 for parallel plates of infinite extent to 1.2 for pipes with eccentric cores.[2]

The fact that shape factors for multiply connected channels need not always lie in the above specified range is brought out, however, when such factors are calculated for the case treated by Emersleben Equation (2) may be changed into the form of Eq. (4) by use of the relations, $Q=AV$, $S_0=2/r$, $\epsilon=1-\pi r^2/a^2$. The value of k_0 for the Emersleben case then becomes

$$k_0=\frac{\epsilon^2}{\pi(1-\epsilon)}\Big/\left\{\int\int_{Z\leq Z_0} Z_0(\rho)d\epsilon-\int\int_{Z\leq Z_0} Z(\epsilon)d\epsilon\right\}. \quad (5)$$

Values of k_0 for different values of ϵ have been calculated and are shown graphically by curve A in Fig. 2. It is seen that as the periodic arrangement becomes increasingly porous, the shape factor reaches large values. Thus large factors might be expected to occur in actual cases of porous media where the porosity is high.

Although a porous medium does not in general consist of straight channels of constant cross section, a bundle of textile fibers combed parallel to the direction of flow does approximate such an arrangement. Furthermore, in view of the previous discussion of the effect of particle orientation supplemented by additional data to be presented in this paper, it is believed that differences between a porous medium and a straight channel of proper shape factor may largely be taken care of by an orientation factor $\zeta=\langle\sin^2\phi\rangle_{Av}$. Hence the following equation* will be considered:

$$Q=\frac{\zeta A}{k_0\mu}\frac{\Delta P}{L}\frac{1}{S_0^2}\frac{\epsilon^3}{(1-\epsilon)^2}. \quad (6)$$

For a given mass of fiber placed in a tube and compressed to various porosities by means of a piston, Eq. (6) takes the form,

$$(L^2Q)^{\frac{1}{3}}=\left(\frac{\zeta}{k_0}\frac{\Delta P}{\mu M^2\delta}\frac{1}{S_0^2}\right)^{\frac{1}{3}}(\delta AL-M), \quad (7)$$

where M = mass in grams, δ = density of fiber in g/cc, and L = length of wad of fiber. Where the pressure drop ΔP is kept constant, a plot of $(L^2Q)^{\frac{1}{3}}$ *vs.* L should yield a straight line if a given fiber orientation is maintained and the shape factor does not change.

Experimental

The porous media consisted of wads of cotton or of wool fibers. The flow data were taken in a manner similar to that described for the bed of glass spheres.[7] In the present case, however, copper tubes of suitable length and diameter were equipped with perforated pistons for compressing the wads of fiber to different porosities. The pressure drop across the tube was so small in all cases that the air was not appreciably compressed. When the pressure drop lost by the restraining ends of the tube was measurable it was subtracted from the total drop to give that across the wad of fibers.

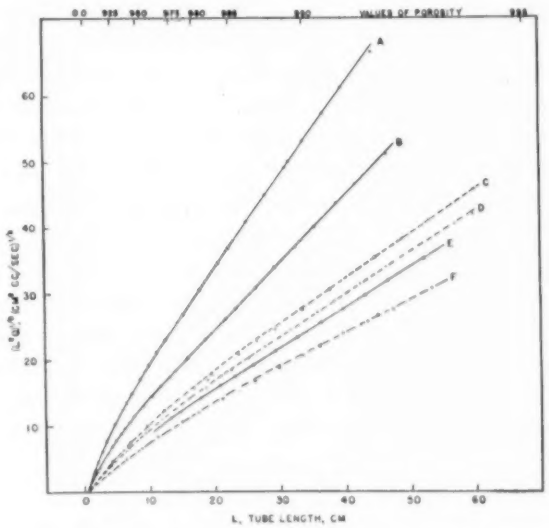

Fig. 3. Air flow data plotted in the manner indicated by Eq. (7). Curves *A*, *B*, *C*, *D*, *E* and *F* are for Welsh wool, fine noil wool, B-38-$\frac{7}{8}$" cotton, B-38-1$\frac{3}{16}$" cotton, Pima cotton, and Sea Island C-38 cotton, respectively. Fibers in all cases were oriented as nearly perpendicular to the flow as possible. Cross-sectional area of tube = 11.83 cm². Pressure drop = 398.67 dynes/cm², and 4.0 cc of fiber were used.

* The ζ as here defined is equivalent to $3/k$ of reference 7. Thus the shape factors for the spheres, glass wool parallel to, and glass wool perpendicular to flow (in reference 7) will be $k_0=3$ in each case.

TABLE I. *Comparison of air flow measurements through tubes of different areas. Pressure drop across wad in all cases = 398.67 dynes/cm²; cross-sectional areas: large tube, 11.83 cm²; small tube 3.12 cm².*

	B-38-¾" Cotton			B-38-1⅝" Cotton			S.I.-C-38 Cotton		
Wad Length L, cm	Porosity (ϵ)	Flow Ratio	Area Ratio	Porosity (ϵ)	Flow Ratio	Area Ratio	Porosity (ϵ)	Flow Ratio	Area Ratio
10	0.9682	3.57	3.79	0.9660	3.87	3.79	0.9643	3.28	3.79
18	0.9823	3.78	3.79	0.9811	3.88	3.79	0.9802	3.59	3.79
26	0.9878	3.69	3.79	0.9869	3.81	3.79	0.9863	3.68	3.79
32	0.9901	3.67	3.79	0.9894	3.74	3.79	0.9888	3.71	3.79
40	0.9921	3.74	3.79	0.9915	3.87	3.79	0.9911	3.83	3.79
50	0.9937	3.76	3.79						
53.5				0.9936	3.85	3.79			
53.75							0.9936	3.78	3.79
57.0	0.9943	3.99	3.79						
61.0				0.9943	4.1	3.79			
63.54							0.9943	3.92	3.79

The specific surfaces of the fibers were determined from microscopic measurements in the manner described in the paper by Fowler and Hertel.[4] Densities of the fibers were obtained by the flow method as described in the same paper.

Two different methods of placing the fibers in the tubes were used. When the cotton fiber axes were to be parallel to the axis of the tube, thin sheets of parallel cotton fibers (ribbon lap) were worked into rolls of varying degrees of porosity and urged into the tube. The measurements were made at the same tube length and later reduced to various tube lengths to compare with other cases. Likewise for wool fibers parallel to the tube axis, loose nontwisted bundles of fiber were urged into the tube. Only those plugs of apparently homogeneous cross sections were used. When the fibers were to be perpendicular to the tube axis they were carded on a rotary card which aligned the fibers in one direction and rolled them into loose bundles whose axes were perpendicular to this direction. These bundles were then placed in a copper tube and compressed in the direction of the tube axis until the proper porosity was reached. Because of friction with the tube walls there was a tendency for the portion of a bundle lying nearest the piston to be more strongly compressed than the remainder of the bundle. For this reason the wad of fiber was composed not of one bundle, but of 26 separate bundles, each of which was compressed separately to the initially desired porosity. For subsequent values of porosity, the 26 bundles comprising the wad were compressed simultaneously in some experiments and separately in others. Comparison of the results obtained by the two methods of compression is made in Fig. 3. The dotted lines of curves *C*, *D*, and *F* represent results of compressing each bundle separately to the desired porosity. The circles of curves *C*, *D* and *F* represent results of compressing the 26 bundles simultaneously by a motion of the piston of the copper flow-tube. The agreement is sufficiently close that only simultaneous compression was used for the sets of 26 bundles giving curves *A*, *B* and *E*.

For a portion of the wool data, a stack of thin sheets of the fiber was punched with a sharp tube and the resulting plugs were then compressed in the copper tube to the desired porosity. In none of the attempts were the desired orientations completely realized.

TABLE II. *Comparison of rates of flow for fibers parallel and fibers perpendicular to the direction of flow. Pressure drop = 398.67 dynes/cm²; Tube area = 3.12 cm². Cotton used = B–38–1 3/16".*

Wad Length L, cm	Porosity	Fibers Parallel $Q_{\parallel}$, cc/sec.	Fibers Perpendicular $Q_{\perp}$, cc/sec.	Ratio $Q_{\parallel}/Q_{\perp}$
7.96	0.9941	75.3	38.5	1.96
7.45	0.9937	73.2	37.2	1.97
6.70	0.9930	69.9	35.6	1.96
5.95	0.9921	66.6	33.7	1.97
5.21	0.9910	62.8	31.7	1.98
4.46	0.9895	59.9	30.0	1.99
3.72	0.9874	55.3	27.4	2.01
2.98	0.9843	51.0	24.6	2.07
2.235	0.9791	45.0	21.2	2.12
1.49	0.9686	35.8	17.4	2.06
1.117	0.9581	30.2	15.5	1.95
0.745	0.9372	21.9	12.2	1.80
0.372	0.8741	12.48	6.24	2.00

Results

Data were obtained which showed a linear relationship between rate of flow and pressure gradient for the highly porous wads over the range of pressures used. Data also showed that the medium was sufficiently homogeneous for an inverse ratio to exist between the rate of flow and the length of plug, other factors being held constant. Table I compares the flow through plugs of different areas of cross section and shows that within the limits of experimental error the flow is proportional to the cross-sectional area, indicating that a wall effect, if present, is small. Thus the flow through highly porous wads of textile fibers follows Darcy's law.

Figure 3 shows flow data for various types of fiber plotted in the manner indicated by Eq. (7). Fowler and Hertel,[4] using rather highly compressed wads, $(0.55 < \epsilon < 0.86)$ found plots of this type to be straight lines which, when extrapolated, passed through the point of zero porosity. Since the orientation of the fibers for Fig. 3 had been controlled (fibers perpendicular to flow), the lack of linearity for the present curves is tentatively attributed to a change of shape factor k_0. Using an orientation factor of $\zeta = \frac{1}{2}$, shape factors were calculated from the data of Fig. 3 and are compared in Fig. 2 with those for the ideal case of Emersleben. It is noted that as the porosity decreases, the experimental shape factors approach the value of 3.0 as found for spheres and for glass wool. That the factors are smaller in the experimental than in the ideal case agrees with expectation. A smaller shape factor indicates a larger flow. Where the distribution of free area in a cross section follows a uniform pattern as in the case of Emersleben, a lower rate of flow would be expected for a given porosity than in the actual case where non-uniformity of distribution is contributed to by the various types of packing and by the lack of uniformity of fiber size and shape. It is interesting that the shape factor k_0 for large textile fibers packed to a given high porosity is greater than the shape factor for small fibers packed to the same high porosity. The reason for this is obscure, though the difference in

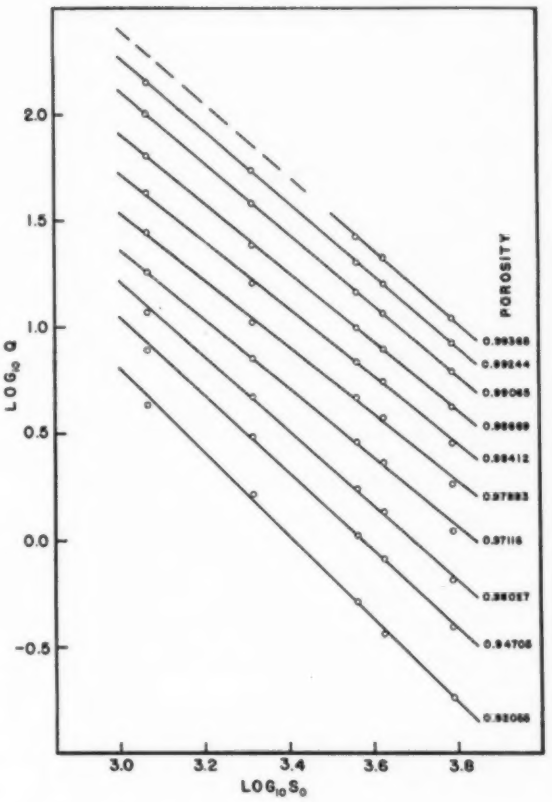

FIG. 5. $\log_{10} Q$ *vs.* $\log_{10} S_0$ at different values of porosity. Q = flow in cc/sec. through fiber wad of 11.83 cm² cross-sectional area and 50 cm long when subjected to a pressure drop of 398.67 dynes/cm². S_0 = specific surface of fiber composing the wad. The fibers used were Welsh wool, fine noil wool, B-38-$\frac{7}{8}$" cotton, B-38-1$\frac{3}{16}$" cotton, and Sea Island-C-38 cotton.

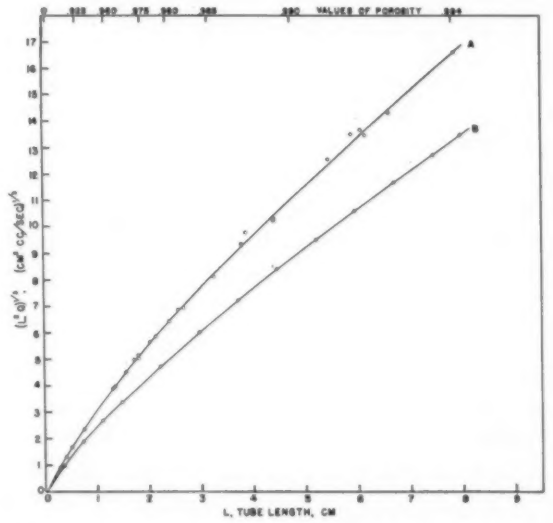

FIG. 4. Air flow data for B-38-1$\frac{3}{16}$" cotton plotted in the manner indicated by Eq. (7). Curve *A* is for fibers parallel to the flow. Curve *B* is for fibers perpendicular to the flow. Area of tube = 3.12 cm². Pressure drop across tube = 398.67 dynes/cm². 0.146 cc of fiber was used.

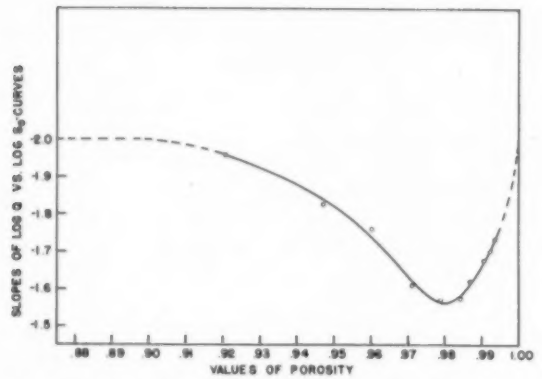

FIG. 6. The slopes of the curves of Fig. 5 have been plotted as a function of porosity. Thus, if the slope is designated as ψ, the ratio of the flows for two different types of fiber at a given porosity is $Q_1/Q_2=(S_{0,1}/S_{0,2})^{\psi}$.

k_0 may be due to different distributions of fiber packing caused by some property such as stiffness of fiber. In the Emersleben case the shape factors would be the same. Figure 4 compares flow data for cotton fibers parallel to the direction of flow with data for the same fibers perpendicular to the direction of flow. Similar comparisons were made with wool fibers. Table II gives ratios for the data of Fig. 4. Within limits of error the ratio $Q_{\parallel}/Q_{\perp}$ is 2.0 over the complete range of porosities studied, thus providing further evidence of the validity of the expression $\zeta=\langle\sin^2\phi\rangle_{Av}$. The value of the orientation factor ζ is therefore taken to be $\frac{1}{2}$ for fibers perpendicular to the direction of flow.

For the measurements of specific surface, Eq. (6) indicates that, other factors remaining constant, the rate of flow Q should vary inversely as the square of the specific surface. In fact it was found for low porosity wads of fibers,[4] and for sand grains,[2,3] that at a given porosity, a given pressure drop, and a given size of wad, the rates of flow for the different fibers or grains were inversely proportional to their specific surfaces squared. A study of Fig. 2 suggests, however, that in view of the changing shape factor this would not be the case for higher porosities. When the data of Fig. 3 are plotted in the manner shown by Fig. 5, it is found, for the fibers studied, that the rates of flow for a given porosity, a given pressure drop, and given wad size, vary not as the inverse square but inversely as a lower power of their specific surfaces. The slopes of the curves of Fig. 5 were determined and Fig. 6 shows how they change with porosity. The curve of Fig. 6 has been extrapolated in both directions. It is known that an inverse square (-2) relationship holds for low porosities; it would appear that if the fibers were completely free from each other ($\epsilon\sim1.0$) the distribution of free space would tend to be uniform, in the sense of an Emersleben arrangement being uniform, and the relationship would again be an inverse square. That the relative values of specific surface for cotton or for wool fibers may be accurately determined from flow data for highly porous wads was shown by Sullivan and Hertel.[5] Analyses indicated as high a consistency for the determination when $\epsilon=0.988$ as when $\epsilon=0.7$.

SUMMARY

It has been found that over a very wide range of porosity the resistance of a wad of textile fibers to the streamline flow of air is twice as much at a given porosity when the fibers are perpendicular to the direction of flow as when they are parallel to the direction of flow. The flow through a bundle of fibers whose axes are parallel to the direction of flow has been likened to that through a straight channel. Shape factors for the channels under various conditions have been determined and compared with those for the ideal case of Emersleben. For high porosities where the shape factors are different for wads of different fiber, the flow at a given porosity may not be considered proportional to the inverse square of the specific surface, but may for the fibers studied be reasonably well represented as proportional to an inverse power lower than the square. Therefore measurements of specific surface of textile fibers may, with proper calibration of apparatus, be made at any porosity, though the problem is simpler if porosities used are less than about 0.87 or 0.88.

It is a pleasure to acknowledge the helpful discussions with Professor K. L. Hertel during the course of the work, and to acknowledge the aid of Miss Louise McCamy and Miss Elizabeth Cotter, who took many of the data used for determination of the shape factors.

Innovations in Instruments

Electronic Vacuum Camera

The crystalline structure of substances millionths of an inch thick can be photographed by means of an electronic vacuum camera, built by Dr. Ralph P. Johnson of the General Electric Research Laboratory in Schenectady.

Supplementing x-ray apparatus which permits study of the interior of substances of greater thickness, the electronic vacuum camera is being used to study deposits on the surfaces of metals; e.g., tarnish, polish, lubricants such as grease and oil, and the first stages of corrosion. The camera consists of a brass tube about three and one-half feet long, and a focusing magnet. A 40,000-volt electronic beam enters one end of the tube, is focused by means of the magnet upon the material suspended in the middle of the tube, diffracts, and produces a picture upon a lantern slide at the other end of the tube. Similar cameras have been built by the Bell Telephone Laboratories and others.

Fused Electrical Instruments

Portable electrical instruments, protected from accidental burn-out by having each range of every instrument fused, are featured by The Winslow Company, Inc., 9 Liberty Street, Newark, New Jersey. These instruments include Types P-11, covering direct-current measurements from a few microamperes to 1000 amperes in single range, multi-range, and volt-ammeter models; P-12, instrument for alternating-current measurements in single current ranges and in single and multi-range voltmeters; P-13 for alternating-current measurements where the current drain of the instrument must be small; and P-14 for high frequency measurements.

Fluorimeter and Microphotometer

Adam Hilger, Ltd., announces two new instruments, the Spekker Photoelectric Fluorimeter and the Hilger Non-Recording X-Ray Microphotometer.

A useful means of chemical analysis consists of the measurement of the intensity of the fluorescence produced in a solution under controlled conditions of illumination. The Spekker Fluorimeter illuminates the solution to be tested with ultraviolet light and measures the resultant fluorescent light by photoelectric means, thus eliminating the personal element from the measurements. It requires only connection to a.c. mains and is self-compensating for variations of line voltage.

The Hilger X-Ray Microphotometer is especially designed to overcome the difficulties generally encountered in density measurements on x-ray film negatives where the lines are relatively diffuse and the grain large. In addition to its normal functions of measuring blackening, it is capable of linear measurement over a range of 15 cm to an accuracy of 0.01 mm.

Advertising literature concerning these two products has been distributed by Adam Hilger, Ltd., 98 St. Pancras Way, London, N.W. 1.

Electro-Metal Spraying Process

A new electro-metal spraying process has been devised and developed by Dr. M. U. Schoop of Switzerland, according to an announcement of his representative, Herman A. Holz, 116–118 West 14 Street, New York, New York. The Schoop process consists essentially of short-circuiting two conducting wires, atomizing the resulting drop of molten metal, and projecting the atomized metal by means of compressed air onto the surface to be metallized. A small luminous arc is formed at the breaking point and insures the continued melting of the wires which are constantly being fed forward by means of a turbine.

Research Reports Available

Utilities Coordinated Research, Inc., of which the late Dr. C. F. Hirschfeld of Detroit was president, announces the availability of a few copies of each of the following reports: Report of the Project Committee on Metallurgical Applications of Electricity, and Report of the Project Committee on Low Curie Point Alloys. Results of work done at Battelle Memorial Institute for Utilities Coordinated Research, Inc., are set forth in these reports, which sell for $1.00 per copy. Applications for copies should be directed to: Preston S. Millar, Secretary, Utilities Coordinated Research, Inc., 2 East End Avenue, New York, New York.

Industrial Instruments

The Brabender Corporation, Rochelle Park, New Jersey, manufacturers of recording apparatus for industrial measuring and control, have announced the following instruments available:

The viscograph, a recording viscosimeter, capable of increasing at a constant rate the temperature of the suspension under test from 20°C to 150°C.

Brabender semi-automatic moisture tester, combination of a modern drying oven and an analytical balance. After drying, the samples under test are weighed inside the oven and the moisture loss is read off a scale graduated in percentages.

The hardness tester, which mills a small sample of material and measures hardness, milling resistance and friability by the resistance offered to grinding.

Adjustable electric contact thermometer with a temperature range from 85°C to 175°C.

The plastograph, a sensitive instrument for use in measuring and recording in graph form the plasticity of materials from light viscous substances to unvulcanized rubber.

Ektra, Miniature Camera

A distinct departure in miniature cameras, the Kodak Ektra, put on the market this year by the Eastman Kodak Company of Rochester, is the first to provide both interchangeable lenses and interchangeable magazine backs for 35-mm film. The magazine backs enable the Ektra owner to switch from one type of film to another in the middle of a roll, quickly and without loss of a single frame.

Gamma-Ray Test for Steel Structure

As a step in speeding up national defense work, parts of steam turbines, propulsion gears and auxiliary apparatus for United States Navy fighting ships now in production are being tested by radiographic means at the Westinghouse Steam Division Works at Lester, Pennsylvania. To make a test, film is placed on the outside of the metal piece to be examined for flaws. Within or beside the metal a small capsule containing radium sulfate is suspended on a midget rigging. The gamma-rays from the radium sulfate penetrate the metal and create a latent image. When the film is developed after an exposure varying from a few minutes to 48 hours, according to the material under test, the positions of flaws in the metal will appear as dark areas on the developed film.

The quantity of radium sulfate used varies in different cases. The largest amount used, 500 milligrams, will serve to examine 10-inch steel.

★

Scleroscope

The efficiency of the new Shore Scleroscope, pictured in the accompanying photograph, has been improved by

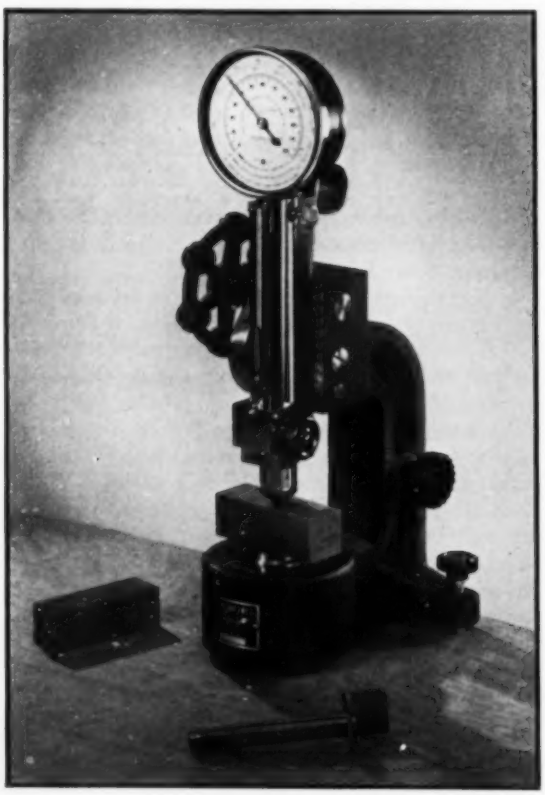

fabricating the head out of molded plastics, according to an announcement of the Bakelite Corporation, 30 East 42 Street, New York, New York. An impact-resistant Bakelite phenolic material was selected by the Shore Instrument and Manufacturing Company, Inc., 9025 Van Wyck Avenue, Jamaica, Long Island, manufacturers of the Scleroscope. The Shore Scleroscope is an instrument used for determining the hardness of plastics, steel, and other materials.

Instrument Booklets

With the publication of the February, 1941, issue, the Rheology Leaflet becomes the *Rheology Bulletin*. The contents of the February issue include: Rheological News, Report on Conference on "Viscosity," Report of Committee on Definitions, Correlated Abstracts, and Contributed Papers.

Recently distributed booklets of particular interest to the physicist include:

The Aerovox Research Worker, November and December issues, with feature articles on "Theory and Operation of Multivibrators" and "Obtaining Precise Audio Frequencies." Published by the Aerovox Corporation, New Bedford, Massachusetts.

The General Radio Experimenter, March, 1941. Carries discussions on "Transmitter Maintenance in the Modern Broadcasting Station" and "Calibrating Three-Phase Power-Factor Meters with the Variac." Published by General Radio Company, 30 State Street, Cambridge, Massachusetts.

Central Scientific Company's *Cenco News Chats*, Number Thirty-two. The scientist featured in this issue is Hans Christian Oersted, discoverer of electromagnetism. It is in his honor that the American Association of Physics Teachers awards the Oersted medal "for notable contributions to the teaching of physics."

A 16-page booklet, "RCA Transmitting and Special Purpose Tubes." Available for 10 cents to cover handling costs from Commercial Engineering Section, RCA Manufacturing Company, Inc., Harrison, New Jersey.

Useful and very well organized material on "high temperature furnaces with platinum resistors as heating units" is collected in an 11-page booklet of that name distributed by Baker and Company, Inc., 113 Astor Street, Newark, New Jersey. Topics discussed in this booklet include resistor, insulation, muffle, power consumption, resistor size, typical furnaces, and melting furnaces.

Various types and models of Rex slide contact rheostats are illustrated and described in Catalog R, recently published by the Rex Rheostat Company, 37 West 20th Street, New York, New York. Protective housing of perforated sheet metal is available for these rheostats.

Jagabi rheostats for the control of electric current in shop, laboratory and research work, with fine adjustment over a wide range, form the subject of Bulletin 1680 of the James G. Biddle Company, 1211–13 Arch Street, Philadelphia, Pennsylvania.

Improved... EASTMAN ALPHA-PARTICLE PLATE

The Eastman Alpha-Particle Plate has recently been improved so that it may now be used for recording proton tracks. They are of good length and grain count, and can be obtained with the minimum of grain in the background. The improved plate is, of course, just as satisfactory as the earlier type for the recording of alpha-particle tracks.

For full information concerning the various Eastman plates for special scientific purposes, write for a free copy of the booklet, *Photographic Plates for Use in Spectroscopy and Astronomy.*

EASTMAN KODAK COMPANY

Research Laboratories **Rochester, N. Y.**

TWO SPECIAL PARTS OF THE

PROCEEDINGS OF THE PHYSICAL SOCIETY

Vol. 49, No. 274 (August 1937) 154 pages

and

Vol. 52, No. 289 (January 1940) 178 pages

consist of

REPORTS OF TWO CONFERENCES

held at the

H. H. WILLS PHYSICAL LABORATORY, UNIVERSITY OF BRISTOL

in JULY 1937 and JULY 1939

ON

CONDUCTION OF ELECTRICITY IN SOLIDS

and

INTERNAL STRAINS IN SOLIDS

Price $1.75

Orders, with remittances, should be sent to

The American Institute of Physics, 175 Fifth Avenue, New York, New York

or to

The Physical Society, 1 Lowther Gardens, Exhibition Road, London, S.W.7

THERMOCOUPLES
for special uses

We manufacture many thermocouples with much higher electromotive force than is obtainable with the standard platinum-rhodium vs platinum couple.

A few typical couples are:

COUPLE	E. M. F., microvolts per °C in range 0-100°C.
Pt-Ir vs Au-Pd	47
Chromel P vs Au-Pd	63
Silver vs Bismuth	76
Bismuth-Tin vs Bismuth	126

These are for use at moderate temperatures only and the e.m.f's, cannot be guaranteed. They are supplied in all wire sizes.

Complete information will be furnished on request.

BAKER & CO., INC.
PLATINUM
113 Astor Street Newark, N. J.

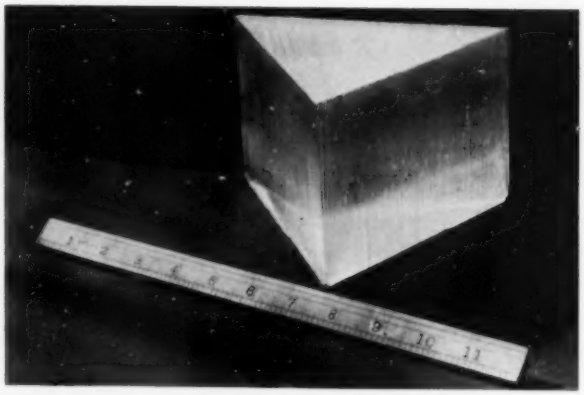

An eight pound rock salt prism blank cut from a twenty-five pound single crystal

SYNTHETIC CRYSTAL OPTICS

For infrared and ultraviolet spectroscopy and for polarizing optics. . . . Single crystals of Lithium Fluoride, Sodium Chloride, Sodium Nitrate, and Potassium Bromide cut to your specifications. . . Write for information.

THE HARSHAW CHEMICAL CO.
SPECIAL PRODUCTS DIVISION CLEVELAND, OHIO

JAGABI "LUBRI-TACT"
LABORATORY RHEOSTATS

Lubricated sliding contact. Four sizes, seventy-six different ratings carried in stock.

Also Compression Carbon Rheostats.

Bulletin 1680-R.

JAMES G. BIDDLE CO.
ELECTRICAL AND SCIENTIFIC INSTRUMENTS
1211-13 ARCH STREET PHILADELPHIA, PA.

Write for REVISED 44 PAGE ENGINEER'S DATA BOOK also new enlarged vapor pressure-temperature chart.

HYDRON

METALLIC BELLOWS

HYDRON Metallic Bellows are used as control elements in temperature-and-pressure-control devices, and for liquid or gas seals of compressors and pumps. We are specialists in the design and production of complete thermostatic and pressure units for temperature and pressure controls. We are, therefore, prepared to extend the fullest co-operation to engineering departments of control manufacturers in the solution of design and engineering problems.

CLIFFORD MANUFACTURING CO.
504 E. FIRST STREET, BOSTON
BOSTON CHICAGO DETROIT LOS ANGELES
PRODUCERS OF BELLOWS EXCLUSIVELY
SERVING AUTOMATIC CONTROL MANUFACTURERS

THREE OUTSTANDING NEW BOOKS

THE THEORY OF GASEOUS CONDUCTION AND ELECTRONICS

By FREDERICK A. MAXFIELD and R. RALPH BENEDICT, University of Wisconsin. In press—ready in June

In this text the authors present a systematic treatment of the fundamental processes involved in gaseous conduction and electronics. The book discusses the production and motions of electrons in high-vacuum, as well as the conditions prevailing in spark, glow, and arc discharges. The principles developed are illustrated by their application to particular tubes and discharges.

INSULATION OF ELECTRICAL APPARATUS

By DOUGLAS F. MINER, Carnegie Institute of Technology. 451 pages, 6 x 9. $5.00

This book contains a discussion of dielectric behavior, followed by a description of the problems encountered in insulating the major forms of electric power equipment, how they are solved, and what tests are of value in determining the performance of insulation.

ELECTRONICS

By JACOB MILLMAN and SAMUEL SEELY, College of the City of New York. In press—ready in June

The authors of this text present a development of basic electronic principles with applications to many problems in electrical engineering and physics. The book includes general considerations of both vacuum and gas filled electronic devices.

Send for copies on approval

McGRAW-HILL BOOK COMPANY, Inc.

330 West 42nd Street **New York, N. Y.**

GAERTNER

INFRA-RED SPECTROGRAPH (Littrow Type)

Range .5461 to 15 microns

with

Bilateral Slits of 40 mm clear aperture and provided with micrometer, reading from 0.01 to 3 mm width of opening.

Rocksalt or Potassium Bromide Prisms of best optical quality.

Mirrors are parabolized 10° off axis, focal length 1 m, figured to high accuracy.

Baffled to eliminate stray light.

Cover is air tight except for the breather tubes. All adjustments of slits, wavelength, etc., are made from outside of case.

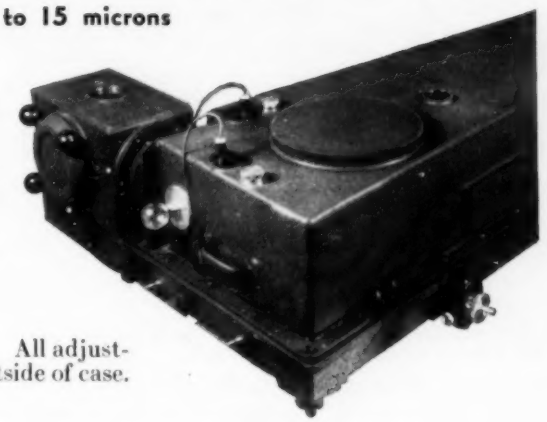

THE GAERTNER SCIENTIFIC CORPORATION

1212 Wrightwood Ave. **Chicago, U.S.A.**

INCREASE EFFICIENCY

UNCOATED COATED

SPECTROSCOPES
MICROSCOPES
OPTICAL INSTRUMENTS

By high vacuum coating with suitable fluoride film* to minimize surface reflection loss shown above in half coated aircraft instrument.

NATIONAL RESEARCH CORPORATION
100 BROOKLINE AVE.
BOSTON, MASS.

*U. S. Pat. 2,207,656

Linde

RARE GASES AND MIXTURES

NEON
ARGON
HELIUM
KRYPTON
XENON
MIXTURES

. . . Spectroscopically Pure
. . . Easily removed from bulb without contamination

Scientific uses for Linde rare gases include—

1. The study of electrical discharges.
2. Work with rectifying and stroboscopic devices.
3. Metallurgical research.
4. Work with inert atmospheres, where heat conduction must be increased or decreased.

Many standard mixtures are available. Special mixtures for experimental purposes can be supplied upon request.

The word "Linde" is a trade-mark of

The Linde Air Products Company
Unit of Union Carbide and Carbon Corporation
30 East 42nd Street UCC Offices in
New York, N. Y. Principal Cities

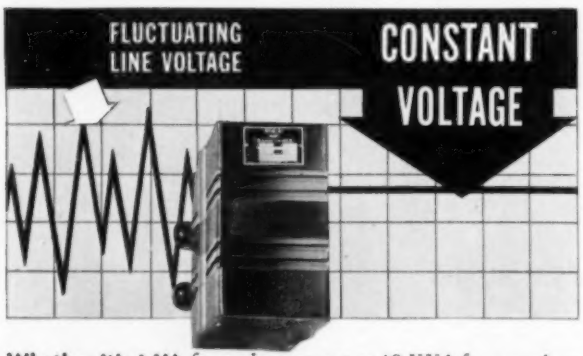

Whether it's 1 VA for an instrument or 10 KVA for a production line—here's constant, stable voltage for you at all times, even though the line voltage varies *as much as thirty percent.*

They are fully automatic and instantaneous in operation—have no moving parts—require no maintenance—and are self-protecting against short circuit.

You can build a SOLA CONSTANT VOLTAGE TRANSFORMER into your product, or incorporate it in your production line or laboratory and know that every test will be made under identical line conditions.

Compact—economical. Standard designs are available, or units can be built to your special specifications.

SOLA ELECTRIC CO. 2525 Clybourn Ave., Chicago, Ill.
Ask for BULLETIN VCV-74
SOLA
Constant Voltage TRANSFORMERS

DO YOU TEACH PHYSICS TO STUDENTS OF ENGINEERING?

If so, you will want to examine

Hammond's PHYSICS

A Text for Science and Engineering Students

Contains 760 pages, 6 by 9 inches, 829 illustrations and 689 problems.

The text may be obtained in single volumes, $4.75, or in two volumes, $2.60 each.

In writing an elementary textbook, there are at least two things the author may have in mind. One is to please the instructor upon a casual reading of the text with the idea of promoting adoptions. The other is to write for the student, who, after all, is vitally concerned, but who has nothing to do with the choosing of the text. The author claims that he had only the student and his needs in mind in the preparation of this text.

Now we have proof. From the University of Pittsburgh, where 214 copies were sold during the year: "It is a book which the students can read. It is really written for the student," and again: "The students like the book very well and find it easy to read."

Comments from other sources: "The book is accurate and the parts are well balanced." And another: "I admire the way you treat the subject matter." From a large state university in the middle west: "I found the book well written."

The treatment of the topics in this text is direct, concise, and complete. Derivations of formulae are given.

Copies for examination may be obtained upon request and a reasonable time will be allowed for examination.

MOUNTAIN STATES PUBLISHING COMPANY
BOX 912
LARAMIE, WYOMING

PORTABLE POTENTIOMETERS

Rubicon portable potentiometers are available in a variety of single and double range models suitable for thermocouple, pH and instrument calibration work. Guaranteed accuracy to .1%.

These sturdy, self-contained instruments are built to give years of satisfactory service under all conditions encountered in the laboratory, shop or field. They are outstanding values in their class.

Ask for Bulletin 270.

RUBICON COMPANY

Electrical Instrument Makers

Ridge Ave. at 35th Street Philadelphia, Pa.

NEW POLAROID* KIT

Adapts lantern-slide projector for polarization demonstrations

With this kit, all the principal demonstrations in the field of polarized light may be shown with a common horizontal lantern slide projector as simply as showing lantern slides. The kit contains 7 specimens, and the projector polariscope which fits into the projector. Two polarizing elements, one rotatable by a convenient plunger control.

Price: Polaroid Projector Kit, complete with projector polariscope specimens, 48-page text and instruction book, No. 450, $19.50.

For new complete catalog write your laboratory supply house, or Division 46

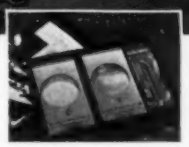

Projector Specimens

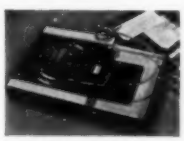

Projector Polariscope

POLAROID CORPORATION

730 Main Street, Cambridge, Mass.

*T. M. Reg. U. S. Pat. Off.

"IS THE STANDARD CELL AN EPPLEY CELL?"

The far-seeing purchasing agent will find it to his advantage to ask this question before making a decision on the purchase of automatic temperature control apparatus because—

For nearly a quarter of a century the leading American manufacturers of such apparatus have used Eppley Standard Cells in their recorders, pyrometers and other instruments utilizing the potentiometric system of measurement.

Today, more than ever before, these manufacturers realize that the standard cell—the heart of the potentiometric system—must be the finest and most reliable cell obtainable.

The technical men responsible for the performance of the instruments know that the Eppley Standard Cell measures up fully to their standards of excellence and reliability.

EPLAB

THE EPPLEY LABORATORY, INC.

SCIENTIFIC INSTRUMENTS

NEWPORT, R.I.

U.S.A.

INDEX TO ADVERTISERS

The following firms have shown their interest in the advancement of physics through their support of the journals and other services of the American Institute of Physics and its Founder Societies. This should entitle them to consideration by physicists whenever possible.

Name — *Page*

BAKER & COMPANY, INC. iv
Platinum, palladium, gold and silver, and their alloys, in wire and sheet form. Laboratory ware and special apparatus.

JAMES G. BIDDLE COMPANY iv
"Jagabi" Rheostats; Adam Hilger and Kipp & Zonen Optical Instruments; "Pointolite" Lamps; Electrical Testing and Speed-measuring Instruments.

CENTRAL SCIENTIFIC COMPANY .....Cover 4
Manufacturers of Cenco Physical Apparatus and Instruments to meet all requirements of University, College and High School Physics Laboratories. Specializing in high vacuum pumps and development of instruments and apparatus for various sciences.

CLIFFORD MFG. COMPANY iv
Hydron metallic bellows for temperature and pressure control devices. Data for engineers.

EASTMAN KODAK COMPANY iii
Purified Organic Chemicals for research purposes; Plates for Photography, Photomicrography, Spectroscopy, Photometry, Astronomy; Wratten Light Filters; Cameras and Films.

THE EPPLEY LABORATORY, INC. vii
Standards of e.m.f. (standard cells). Precision electrical instruments; potentiometers, bridges, temperature bridges, volt boxes. Thermopiles and pyrheliometers.

GAERTNER SCIENTIFIC CORPORATION v
Spectroscopes, Spectrometers, Spectrographs, Spectrophotometers, Heliostats, Measuring Microscopes, Comparators, Cathetometers, Reading Telescopes, Interferometers, Chronographs, Dividing Machines, etc.

GENERAL RADIO COMPANY ii
Manufacturers of electronic measuring instruments; vacuum-tube voltmeters, amplifiers and oscillators; wave analyzers, noise meters and analyzers, stroboscopes; laboratory standards of capacitance, inductance and frequency; impedance bridges, decade resistors and condensers; air condensers and variable inductors; rheostats, Variacs, transformers; other laboratory accessories.

HARSHAW CHEMICAL COMPANY iv
Optical Lithium Fluoride grown in single crystal to predetermined size. Industrial Chemicals.

LEEDS & NORTHRUP COMPANY i
Manufacturers of Galvanometers, Resistors, Bridges, Condensers, Inductances, Potentiometers, Testing Sets; Temperature Measuring, Recording and Controlling Apparatus; Instruments for Measuring and Controlling Conductivity of Electrolytes and Hydrogen Ion Concentrations.

THE LINDE AIR PRODUCTS COMPANY vi
Oxygen, Argon, Helium, Krypton, Neon, Xenon, Rare Gas Mixtures, Nitrogen, Hydrogen, Calcium Carbide, Acetylene, equipment for Oxy-Acetylene welding and cutting.

INDEX—*Continued*

Name — *Page*

MCGRAW-HILL BOOK COMPANY, INC. v

MOUNTAIN STATES PUBLISHING COMPANY vi

NATIONAL RESEARCH CORPORATION vi
Specialists in industrial applications of high vacuum in the fields of physics and chemistry; research, design, consulting; low reflecting glass surfaces, special products produced under low pressure.

PHYSICAL SOCIETY (LONDON) iii

POLAROID CORPORATION ..... vii & Cover 3
Polaroid experimental kit for demonstrating Polarized light. Hand book.

RUBICON COMPANY vii
Galvanometers, electrometers, potentiometers, Wheatstone and Kelvin bridges, resistance boxes, hydrogen ion and conductivity apparatus.

SOLA ELECTRIC COMPANY vi
Constant Voltage Transformers; Fluorescent Lamp Ballasts; Transformers for Power Distribution, Signal and Control Systems and other industrial applications.

UNION CARBIDE & CARBON CORPORATION vi

Back Issues

of these journals are available.

	Single Copy
The Physical Review (from July 1929)..	$ .75
Same (before July 1929).....	1.50
Reviews of Modern Physics.....	1.20
Same April 1936.....	1.75
Journal of the Optical Society.....	.60
The Journal of the Acoustical Society..	1.80
American Journal of Physics (from 1937)	1.00
Same (before 1937).....	1.50
The Review of Scientific Instruments..	.50
The Journal of Chemical Physics.....	1.00
Journal of Applied Physics.....	.70

Special prices for complete back volumes and complete sets.

Orders may be sent to

American Institute of Physics
175 Fifth Avenue
New York, N. Y.